AD-A090 634 AIR FORCE INST OF TECH WRIGHT-PATTERSON AFB OH F/G 8/3
AIRCRAFT DERIVED LOW LEVEL WINDS AND UPWELLING OFF THE PERUVIAN--ETC(U)
AUG 79 G L MOODY
UNCLASSIFIED AFIT-CI-79-195T NL

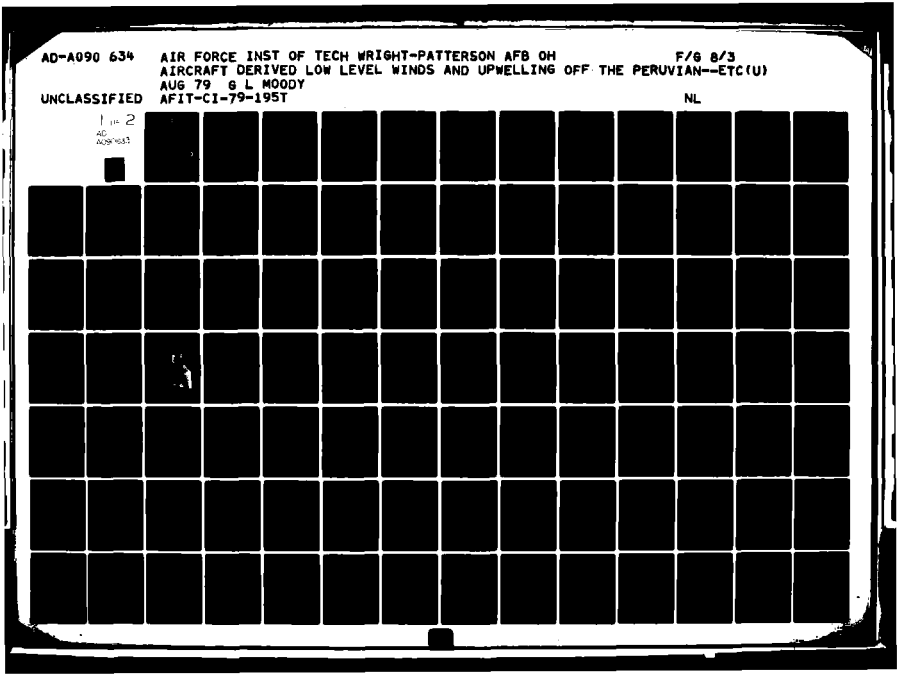

79-195T

LEVEL II 1

AD A090634

DTIC
ELECTE
S OCT 21 1980 D
E

DISTRIBUTION STATEMENT A
Approved for public release;
Distribution Unlimited

80 10 14 163

UNCLASS

SECURITY CLASSIFICATION OF THIS PAGE *(When Data Entered)*

AFIT-TR REPORT DOCUMENTATION PAGE	READ INSTRUCTIONS BEFORE COMPLETING FORM
1. REPORT NUMBER: 79-195T	2. GOVT ACCESSION NO.: AD-A090 634
	3. RECIPIENT'S CATALOG NUMBER: Master's
4. TITLE *(and Subtitle)*: Aircraft Dervied Low Level Winds and Upwelling Off the Peruvian Coast During March, April, and May 1977	5. TYPE OF REPORT & PERIOD COVERED: Thesis
	6. PERFORMING ORG. REPORT NUMBER
7. AUTHOR(s): Glenn Leroy Moody	8. CONTRACT OR GRANT NUMBER(s)
9. PERFORMING ORGANIZATION NAME AND ADDRESS: AFIT Student at: The Florida State University	10. PROGRAM ELEMENT, PROJECT, TASK AREA & WORK UNIT NUMBERS
11. CONTROLLING OFFICE NAME AND ADDRESS: AFIT/NR, WPAFB OH 45433	12. REPORT DATE: August 1979
	13. NUMBER OF PAGES: 110
14. MONITORING AGENCY NAME & ADDRESS *(if different from Controlling Office)*: 12 125	15. SECURITY CLASS. *(of this report)*
	15a. DECLASSIFICATION/DOWNGRADING SCHEDULE

16. DISTRIBUTION STATEMENT *(of this Report)*
Approved for public release; distribution unlimited

17. DISTRIBUTION STATEMENT *(of the abstract entered in Block 20, if different from Report)*
APPROVED FOR PUBLIC RELEASE AFR 190-17.
FREDRIC C. LYNCH, Major, USAF
Director of Public Affairs
23 SEP 1980

18. SUPPLEMENTARY NOTES
Approved for public release: IAW AFR 190-17
Air Force Institute of Technology (ATC)
Wright-Patterson AFB, OH 45433

19. KEY WORDS *(Continue on reverse side if necessary and identify by block number)*

20. ABSTRACT *(Continue on reverse side if necessary and identify by block number)*
Attached

DD FORM 1 JAN 73 1473 EDITION OF 1 NOV 65 IS OBSOLETE

UNCLASS

SECURITY CLASSIFICATION OF THIS PAGE *(When Data Entered)*

THE FLORIDA STATE UNIVERSITY

COLLEGE OF ARTS AND SCIENCES

AIRCRAFT DERIVED LOW LEVEL WINDS AND UPWELLING OFF THE PERUVIAN COAST DURING MARCH, APRIL, AND MAY 1977

by

GLENN LEROY MOODY

A Thesis submitted to the Department of Meteorology in partial fulfillment of the requirements for the degree of Master of Science

Accession For
NTIS GRA&I
DDC TAB
Unannounced
Justification
By
Distribution/
Availability Codes
Dist. | Avail and/or special
A

Approved:

David W. Stuart
Professor Directing Thesis

August, 1979

ABSTRACT

The low-level mesoscale wind field over a major coastal upwelling region off the coast of Peru is investigated. The data were collected as part of the second intensive phase of the JOINT II oceanographic experiment conducted during March, April, and May 1977. The wind and sea surface temperature (SST) data were obtained via a research aircraft flying at 500 feet. Aircraft flights were conducted primarily between 0900 and 1430 LST. Surface data from ships, buoys, and land stations were more extensive in 1977 than in the previous year. The mesoscale data network was also increased.

The mean structure of the 500 ft wind field during this experiment is presented primarily for comparison studies. The most important comparison is the alongshore (tangential) wind component with the SST's. The mean wind and SST fields from the first phase of JOINT II in 1976 are examined for parallels to the corresponding fields in 1977. Four flights on the strongest wind days are contrasted to four flights on the weakest wind days. A study during very light winds is presented to examine upwelling features in the absence of strong wind forcing.

Generally, the mean wind and SST fields for the two phases of JOINT II agree very well. The 1977 wind values are

slightly lower and the SST's warmer than those of 1976, because the 1977 flights were conducted about two hours earlier each day and the winds were lighter on the days of these flights. A reasonable linear relationship was found between the maximum tangential wind value at 500 ft and the coldest SST value for winds greater than 13 m s^{-1}. A direct relationship also exists between the values of the minimum tangential wind component and the warmest SST.

The strength of the wind in this area is related to the pressure gradient between the subtropical high and the lower pressures inland. One example of this occurred when the high was forced closer to the continent lowering the pressure gradient and the resultant winds over the region. During this light wind period other factors such as horizontal advection of surface water, coastal cape effects, and bottom topography were observed to play continuing roles in the upwelling process. The results of all analyses and profiles performed on these data verify that wind forcing is the dominant factor in the broadscale upwelling seen in the survey area. Hydrographic cast and buoy data confirm the importance of the ocean currents to the upwelling process. More extensive data on these currents could reveal the importance of Kelvin waves and flow over bottom topographical features.

ACKNOWLEDGEMENTS

This study is a contribution to the Coastal Upwelling Ecosystems Analysis (CUEA) Program of the International Decade of Ocean Exploration (IDOE), sponsored by the National Science Foundation (NSF).

Sincere appreciation is given to Dr. D. W. Stuart for his advice and guidance throughout the preparation of this thesis; also to Drs. C. L. Jordan and R. C. Staley for their recommendations and consultation.

Gratitude is extended to the National Center for Atmospheric Research (NCAR) Aircraft Facility for both the operation of the Beechcraft Queen Air and the initial processing of the aircraft data tapes.

Special thanks go to W. Peter Wirfel for his modifications to the program that processed the NCAR data tapes to obtain graphical displays of the data.

The Florida State University Computing Center provided a portion of the CDC Cyber 73 and 74 computers and Gould plotter necessary for producing the aircraft tracks and the profile plots, as well as computer time for the statistical calculations.

Special thanks go to Jeff Hawkins, Jack Goodwin, and Phil Rasch for their cooperation and constructive suggestions

during the programming and data reduction necessary for this thesis.

Many thanks are given to Jay Albrecht and to Dewey Rudd for the final drafting on many of the figures.

Deep appreciation goes to Lisa McLendon for typing the first drafts of this thesis and to Mrs. Janina Richards for typing the final manuscript.

TABLE OF CONTENTS

LIST OF TABLES

LIST OF ILLUSTRATIONS

CHAPTER I

INTRODUCTION

Off the west coast of South America are areas of cold sea surface temperatures and exceptional commercial fishing. The winds and ocean currents of this area combine to produce this upwelling of cold, nutrient rich water. The semi-permanent high located west of Chile drives the consistent southerly winds, while the more variable ocean currents provide the colder subsurface water. This report studies the low-level wind structure over an upwelling area off Peru.

This study is part of the second intensive phase of the JOINT II experiment. The first phase was conducted in 1976 at this same location (Fig. 1). Previous experiments of the CUEA (Costal Upwelling Ecosystems Analysis) Program have been CUE I and II in 1972-73 along the Oregon coast and JOINT I in 1974 off the coast of northwest Africa. The purpose of the CUEA program is to study the process called coastal upwelling.

Coastal upwelling is a wind driven ocean circulation. Central to the understanding and study of this process is an accurate description of the wind field. Furthermore, a similar description of the SST field gives an indication of the strength and variability of the upwelling. The meteorological component of JOINT II 1977 was primarily concerned with

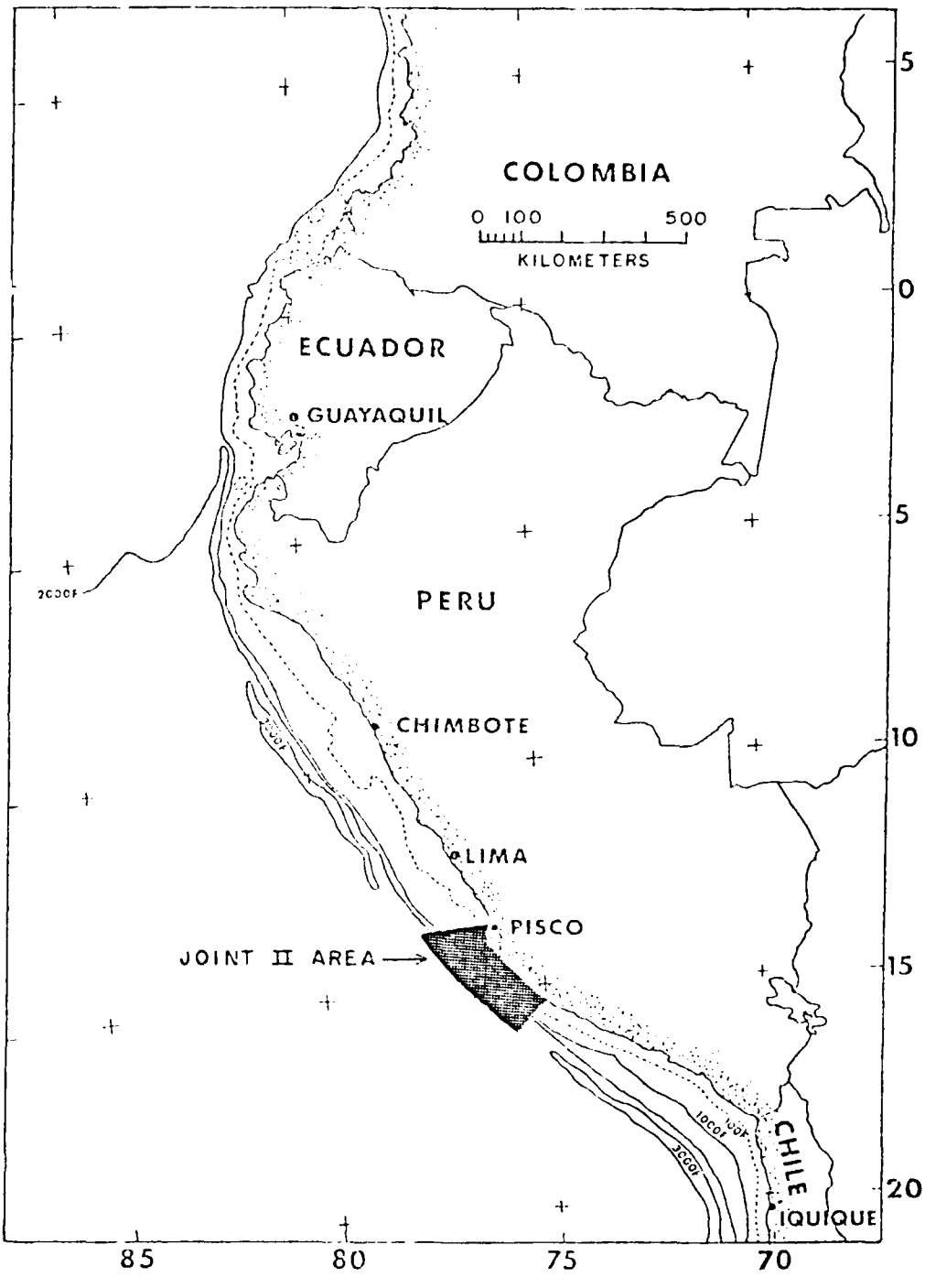

Fig. 1. Map of Peru with location of JOINT II region.

recording the necessary data to accurately describe these fields. This purpose was accomplished via a research aircraft providing an extensive data collection capability over the survey area in a short period of time.

Accuracy is inherently important to any study. Progress in this area during the CUEA Program has advanced primarily through improved navigational systems. Earlier, doppler systems were unreliable over smooth seas and often went into memory during aircraft turns. These difficulties were controlled by the use of the INS (Inertial Navigation System) in JOINT II 1976. Continued progress was made in 1977 by revising the flight track, increasing the data collection density, and by including corrections to the data. A discussion of these corrections is contained in Chapter II.

The principal objective of this thesis is to describe the mesoscale low-level wind field over the upwelling area off the coast of Peru. Profiles, horizontal analyses, and comparison studies of mean and individual flight data are extensively used to accomplish this objective. These data are almost entirely taken at 500 ft (152 m), as that was the altitude of the aircraft. In Chapter III this flight level is shown to be an ideal altitude for this purpose. A presentation of all low-level wind data collected during JOINT II 1977 is being prepared by Stuart and Moody (1979).

Chapter II describes the data collection program of the meteorological component of the JOINT II 1977 experiment.

Emphasis is given to specific collection procedures, reduction techniques, and overcoming problems inherent with the aircraft data.

Chapter III is a presentation and discussion of the low-level wind field in 1977. The orographic features of the JOINT II area are described. A look at climatology verifies that the winds of 1977 are similar to previous years. The mean wind and SST fields in 1977 are contrasted. These same fields are compared to similar analyses of data from JOINT II 1976. Stronger and weaker winds are analyzed using data from four flights of each category. A period of lighter winds containing data from two flights provides a unique opportunity to investigate upwelling factors in the absence of strong wind forcing. This same study is complimented by the increased data network in 1977, which contributed to a closer look at small-scale features. Detailed studies of the surface winds and of the vertical structure over the JOINT II area in 1977 are given by Goodwin (1979), and Wirfel (1979), respectively. Chapter IV contains the summary and conclusions.

Aircraft tracks, wind analyses of the 500 ft level, and SST analyses including streamlines and total isotachs, V_T (component of the wind tangent to the coast), and V_N (component of the wind normal to the coast) for several of the comparisons are found in the Appendix.

CHAPTER II

DATA

This chapter describes the data collection program of the meteorological component of the Coastal Upwelling Ecosystems Analysis (CUEA) program during the JOINT II 1977 experiment. Emphasis is placed on the aircraft-derived 500 ft winds, corrections to these data, surface observations, and limitations of the data. This includes a description of the types of flights, of data gathering and reduction procedures, and of changes from the JOINT II 1976 experiment. A complete listing of meteorological data available from JOINT II 1977 is found in Stuart (1977).

2.1 Aircraft observations

A twin engine Beechcraft Queen Air research aircraft was made available during JOINT II 1977 by the Research Aircraft Facility (RAF) of the National Center for Atmospheric Research (NCAR). During the experiment 45 research flights totaling 184 hours were conducted from 21 March through 7 May 1977. Table 1 shows a listing of all flights including the date, time, and type of pattern. Typical flight tracks are presented in Figs. 2 and 3. The macroscale pattern (Fig. 3) was designed to represent the larger scale features of the survey area. The "MET" flights (Fig. 3)

Table 1

NCAR Queen Air JOINT II 1977 flights

Flight No.	Date	Times (LST)	Pattern
1	Mar. 21	1110-1608	Micro
2	Mar. 22	0906-0947	No data
3	Mar. 22	1353-1740	Macro-South
4	Mar. 23	0858-1415	Micro
5	Mar. 24	0909-1253	Macro-South
6	Mar. 24	1413-1823	Macro-North
7	Mar. 25	0921-1403	Micro
8	Mar. 26	0510-0853	Macro-South
9	Mar. 26	1440-1835	Macro-South
10	Mar. 28	0912-1046	Micro-no map-fog
11	Mar. 29	1038-1444	Macro-South
12	Mar. 30	0909-1403	Micro
13	Mar. 31	0857-1246	Macro-South
14	Apr. 1	0854-1337	Micro-no map-1
15	Apr. 2	0758-1146	Macro-South
16	Apr. 2	1304-1714	Macro-North
	100 Hour Inspection April 3-10		
17	Apr. 11	1017-1240	Micro-no map-2
18	Apr. 12	0905-1159	Macro-South
19	Apr. 12	1313-1717	Macro-North
20	Apr. 13	0900-1351	Micro
21	Apr. 14	0455-0826	MET
22	Apr. 14	0958-1258	MET
23	Apr. 14	1438-1817	MET
24	Apr. 15	0453-0827	MET
25	Apr. 15	1033-1327	MET
26	Apr. 15	1453-1831	MET
27	Apr. 16	0855-1338	Micro
28	Apr. 18	0924-1419	Micro
29	Apr. 19	0758-1152	Macro-South
30	Apr. 19	1257-1718	Macro-North
31	Apr. 20	0941-1505	Micro
32	Apr. 21	0500-0836	MET
33	Apr. 21	0949-1249	MET
34	Apr. 21	1441-1806	MET
35	Apr. 22	0500-0834	MET
36	Apr. 22	1003-1312	MET
37	Apr. 22	1449-1812	MET
38	Apr. 23	0858-1357	Micro

1 - Airspeed sensor failure

2 - Data recording system failure

Table 1 - Continued

Flight No.	Date	Times (LST)	Pattern
	100 Hour Inspection April 24-May 1		
39	May 2	0937-1409	Micro
40	May 3	1350-1733	Macro-South
41	May 4	0847-1336	Micro
42	May 5	0746-1123	Macro-South
43	May 6	0938-1424	Micro
44	May 7	0754-1143	Macro-South
45	May 7	1256-1638	Macro-North

were designed to study the land-sea breeze regime. The microscale (micro) flights were designed to yield synoptic maps of the details of the flight level winds and SST's over the experiment area. Of primary importance to this report are these microscale patterns flown between Punta San Nicolas and Punta Lomitas. There were 15 micro flights flown during 1977 but only 12 produced results usable in this paper. Wind data from flights 10, 14, and 17 (14 had usable sea surface temperature results) were unusable for the reasons given in Table 1. The typical micro pattern (Fig. 2) consisted of 14 parallel legs about 3 nautical miles (nm) apart and extending approximately 28 nm offshore. They were generally flown between 0900 and 1430 LST.

The aircraft was equipped with sensors and an inertial navigational system (INS) to measure time, static and total pressure, pressure altitude and radiometric altitude, temperature, dew point temperature, liquid water content, sea surface temperature, and aircraft position with respect to

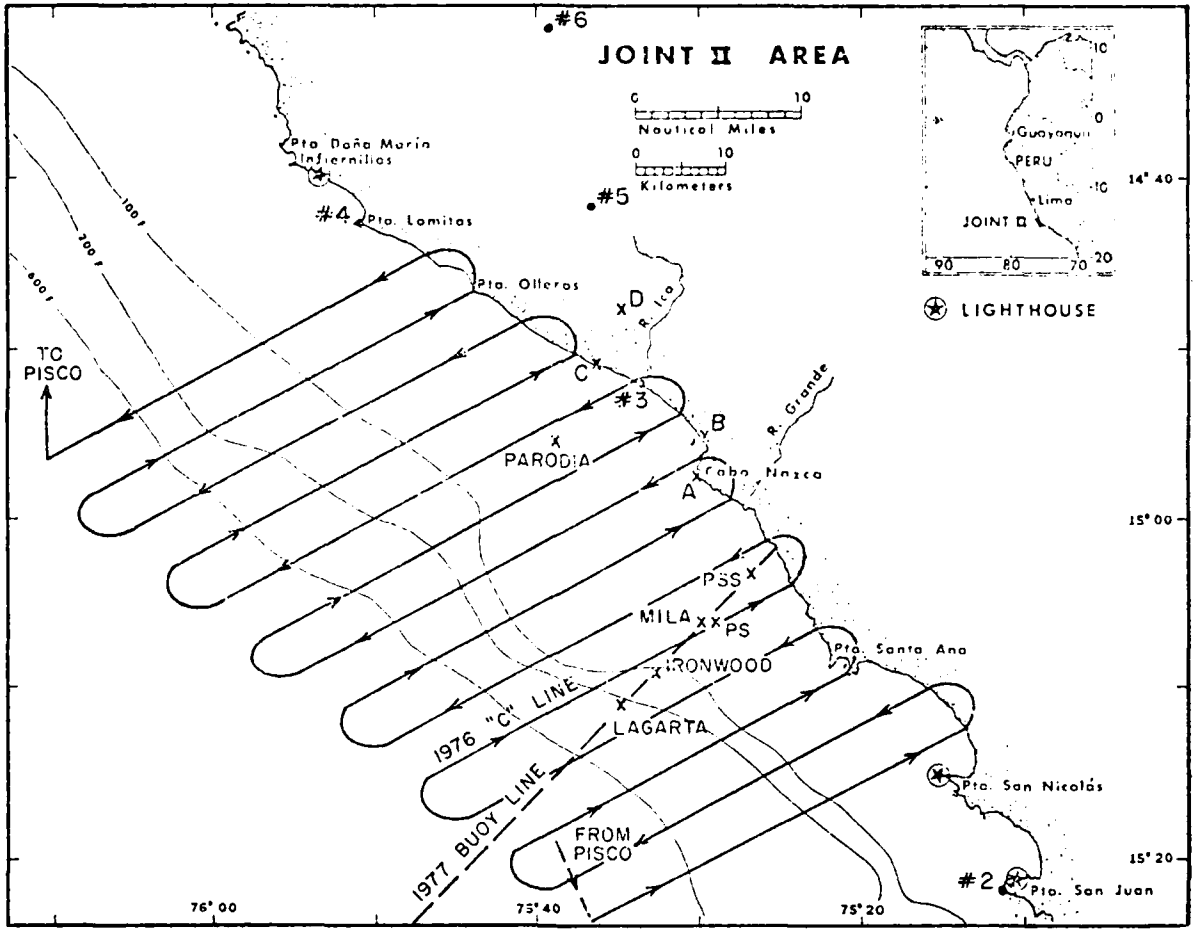

Fig. 2. Map of a portion of the JOINT II region with locations of coastal stations, MET buoys, and typical microscale flight pattern.

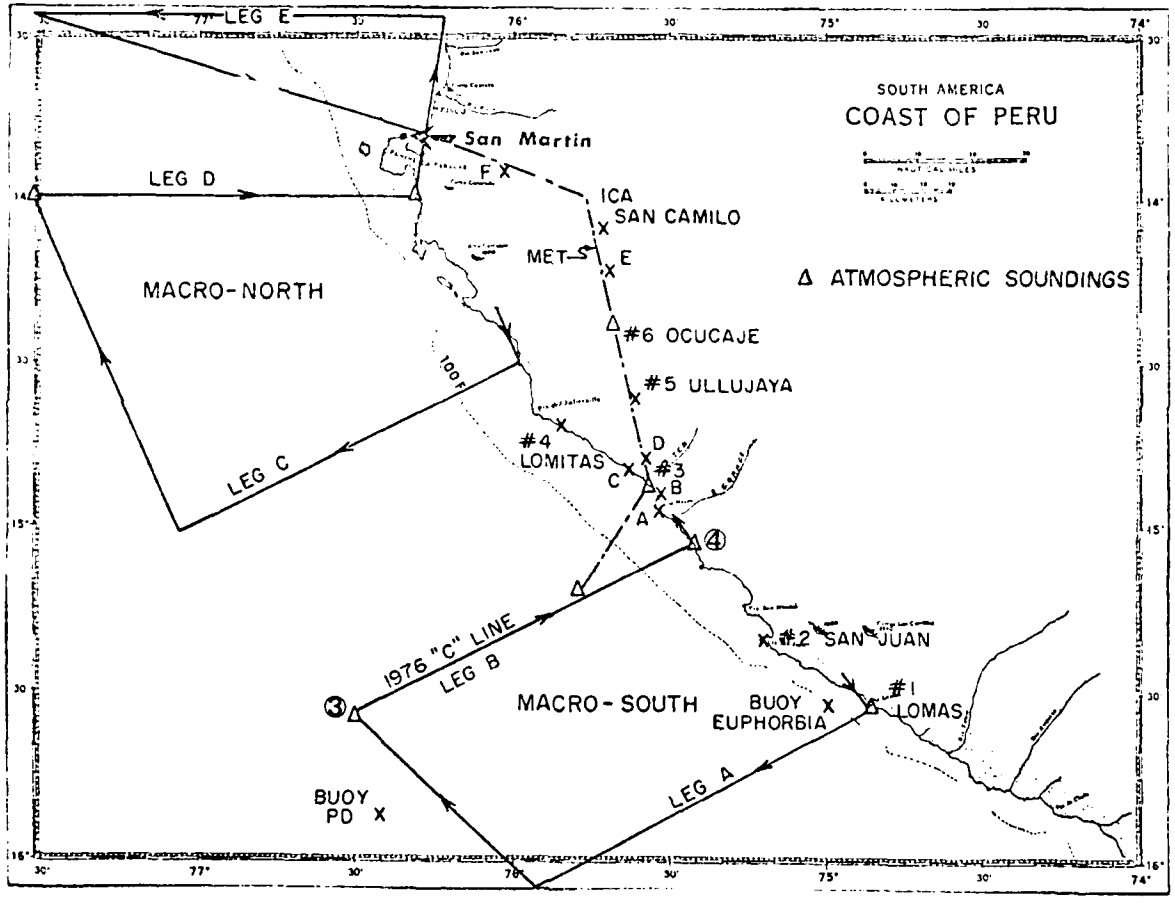

Fig. 3. Map of JOINT II region with locations of coastal stations, typical macroscale and MET flight patterns, and sounding locations.

the earth. Output from these on-board sensors was read at rates from 8-16 times per second by an on-board ARIS III data system and then recorded on magnetic tape.

NCAR further processed the aircraft data tapes by taking one second averages of each quantity and converting the data to a format compatible with the NCAR computers. Necessary corrections and calibrations were applied by an NCAR general processing program. The requested quantities were extracted and placed on magnetic tapes, which were then made available to the investigator.

2.2 Aircraft data reduction

Upon receipt of the data tapes by Florida State University (FSU), the wind data were reduced by using a 30 second average centered on each whole minute. The flight track positions were periodically corrected slightly using known landfall positions and a subsequent best fit with the INS computed positions. The INS computer was not updated inflight.

Corrections obtained from two flight "L" patterns, flown immediately before and after each data run, were used to remove systematic heading and speed errors in the wind data. A more complete description of these flight "L" corrections is given in Section 2.3. Analyses were prepared of the streamlines, total isotachs, and SST's for each of the 12 micro flights from which data were available. The analyses were gridded using a 15×21 array (Fig. 4), and further

processed to compute V_T (wind component parallel to the coast) and V_N (wind component normal to the coast). The components are based on a generalized coastline orientation of 315°-135°. Analyses of these two wind component fields were then prepared. The gridded data were also used to obtain averaged wind fields, averaged SST fields, and profile data.

2.3 Error sources and flight "L" corrections

The position of the research aircraft must be known at all times, if accurate and detailed analyses are to be drawn. The INS (Litton LTN-51) is relied upon for this positional accuracy. The INS measures the velocity and angular orientation of the airplane with respect to the earth. Information from the air sensing probe and the heading indicator determine the speed and direction of the air velocity with respect to the airplane. These variables are all combined to obtain the velocity of the air with respect to the earth. Watson (1978) discusses the INS subsystem and its components. The estimated accuracy of these resolved air velocity measurements is $\pm$ (1.0+0.5t) meters per second (m s^{-1}), when t is in hours. This degree of accuracy was increased in JOINT II 1977 by the periodic adjustment of aircraft track positions based on known landmarks.

Static pressure error associated with the air sensing probe is a source of velocity error. This error can result from sideslip, angle of attack, and the location of the static pressure sensor on the aircraft. Dynamic pressure is found by

subtracting the static pressure from the total pressure. Since dynamic pressure affects any quantity related to aircraft speed, the importance of static pressure error is readily observed. The effect of the error may be seen by examining Fig. 5. The simplified diagrams reveal how an error in the aircraft's true air speed (TAS) will affect the resultant wind direction and speed.

Removal of this static pressure error is a difficult problem, since it involves the difference of two large numbers (the true airspeed and the INS measured groundspeed). Correction is done by tower fly-bys and by flying in opposite directions through a volume of air with the wind speed assumed constant and removing any observed difference in wind speed along the flight path by adjusting the pressure calibration. In JOINT II 1976, the problem was handled by analyzing only the inbound legs of a sawtooth flight pattern. In JOINT II 1977, the flight pattern was changed (Fig. 2) and all the legs were analyzed to enable greater data coverage over the mesoscale survey area. In addition, two flight "L" patterns (Fig. 6) were flown. One at the beginning and the second at the end of each daily data run. These patterns consisted of reciprocal heading, 2-minute legs (upwind and downwind) followed by two reciprocal heading legs flown crosswind. The wind was assumed constant before and after each turn. Table 2 contains average corrections that were applied to the data as a result of these patterns. It is

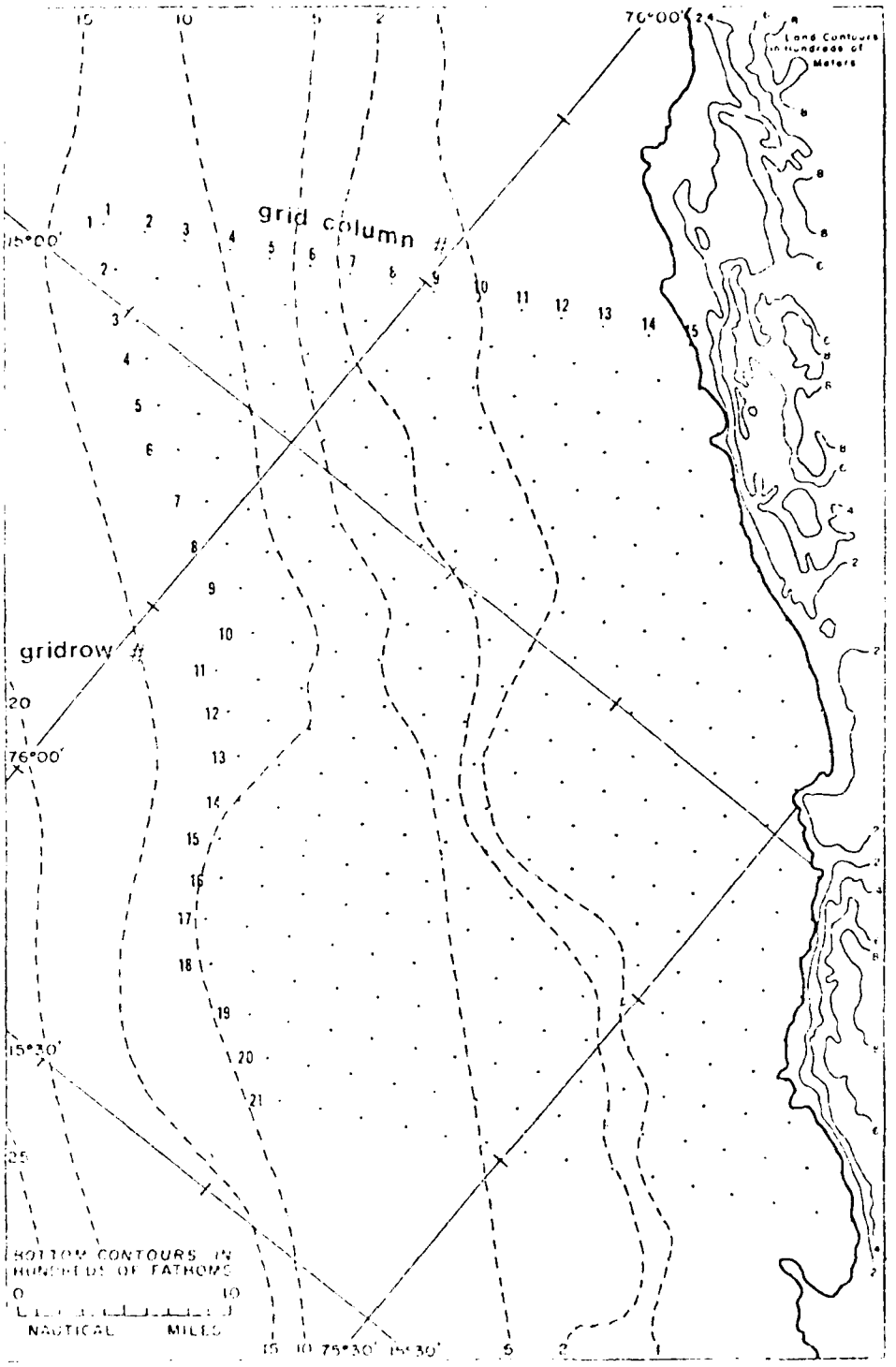

Fig. 4. Grid array adopted for JOINT II region with assigned grid row and grid column numbers.

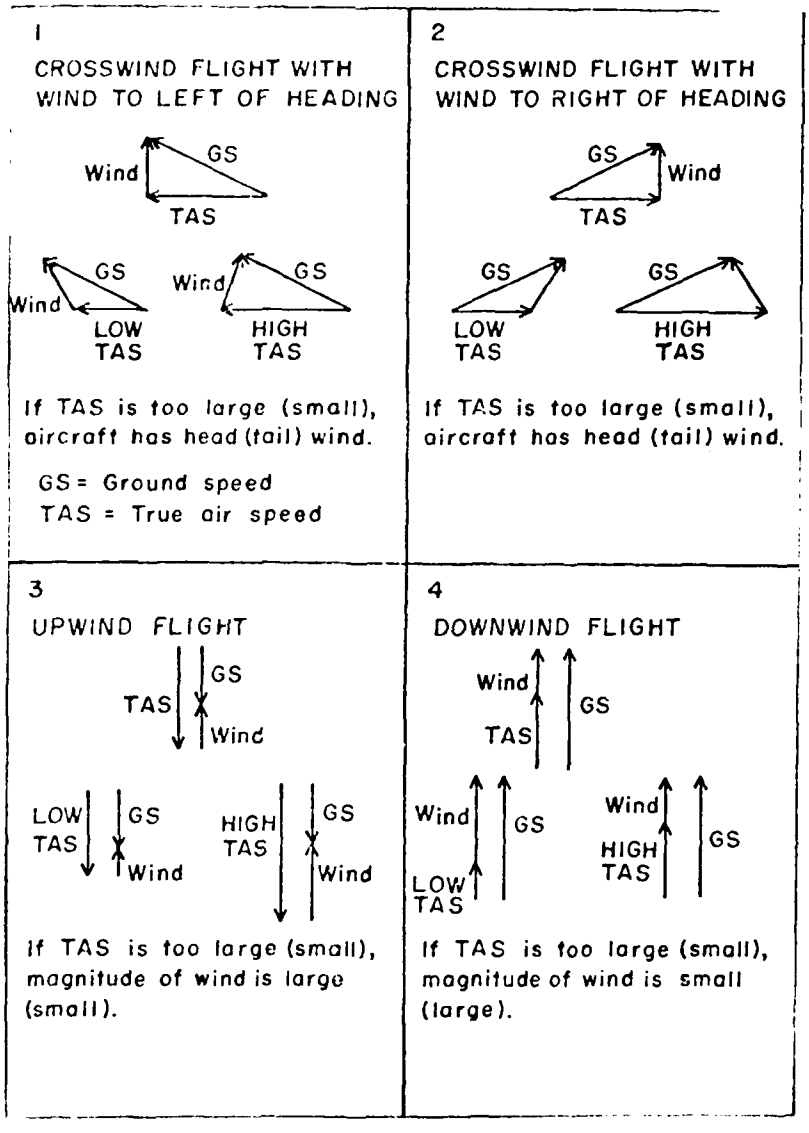

Fig. 5. The effect of true air speed (TAS) errors on the computed wind.

Table 2

Corrections from flight "L" patterns

Flight	Wind direction corrections (degrees)				Wind speed corrections ($m\ s^{-1}$)			
	inbound legs	upwind legs	outbound legs	downwind legs	inbound legs	upwind legs	outbound legs	downwind legs
1	-7	+4	+7	-4	+0.3	+1.6	-0.5	-1.6
4	-6	+1	+6	-1	+0.5	+1.0	-0.5	-1.0
7	-6	+1	+6	-1	0.0	+0.5	0.0	-0.5
12	-9	0	+9	0	+0.7	+1.1	-0.7	-1.1
20	-7	0	+5	0	+1.0	+1.4	-1.0	-1.4
27	-6	+2	+6	-2	0.0	+1.0	0.0	-1.0
28	-7.5	+0.5	+6.5	-0.5	+0.75	+1.2	-0.75	-1.2
31	-38	+6	+25	-2	+0.5	+2.0	-0.5	-1.7
38	-12	0	+8	0	+0.9	+1.3	-0.9	-1.3
39	-7.5	+3	+6	-4	0.0	+1.0	0.0	-1.0
41	-7	+3	+6	-3	0.0	0.0	0.0	0.0
43	-13	+7	+11.5	-6	0.0	+1.5	0.0	-1.5
Avg.*	-8	+1.95	+7.0	-1.95	+0.38	+1.05	-0.4	-1.05

*Data from Flight #31 not included.

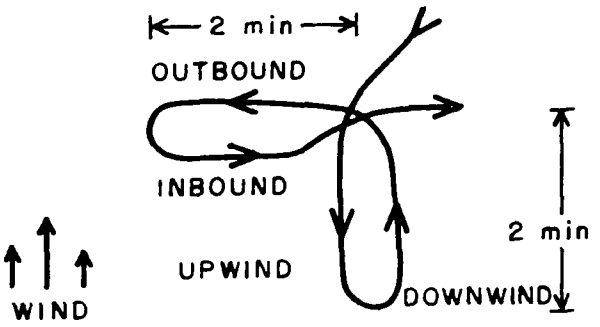

Fig. 6. Drawing of a typical flight "L" correction pattern.

seen that the errors were systematic in that the resultant wind directions were too large (small) and the wind speeds too small (large) for the inbound (outbound) legs. These errors are essentially time independent and are compounded when the wind is light; as seen on flights 31, 38, and 43. A study of Fig. 5 shows that the larger directional error occurs when the TAS is sensed lower than actual. The use of the corrections from the flight L's and the retention of data from both inbound and outbound legs resulted in a more detailed and accurate data network during 1977.

2.4 Surface data

In JOINT II 1977 the number of surface observations was increased. Four ships, taking observations at two hour intervals throughout the day, participated in the experiment (Table 3). Air temperature, wet-bulb temperature, winds, visibility, pressure, clouds, and sea surface temperature (on two ships) were the variables recorded. Five of the six meteorological buoys in the micro area (Fig. 2) provided

continuous overwater observations primarily along a selected buoy line (Parodia buoy was about 25 km north of the line). The sixth buoy, Mila, failed early in the experiment. These buoys recorded winds and air temperature, and three of them also recorded sea surface temperature. Ten specially positioned land meteorological stations (A-E and 1-5 in Figs. 2 and 3) supplemented the normal land station observational network. Wind, air temperature, relative humidity, pressure, and solar radiation were recorded at these stations. Surface data are plotted (in m s^{-1} and °C) on the charts included in this report. These plotted surface data were recorded as close to the time of passage of the aircraft as possible. The ground truth data are plotted when the aircraft passed within a radius of 1.5 nm of a buoy, ship, or land station. The time tolerance for inclusion of the surface data was ±15 minutes for the buoys, ±30 minutes for the land stations, and ±1 hour for the ships. Locations of land stations are given by large circles, of the buoy data by smaller circles, and of the ship data by triangles. A more complete summary of surface observations is found in Stuart (1977). A separate report on the surface winds during JOINT II 1977 is being prepared by Goodwin (1979). Preliminary results indicate a good linear correlation between the total tangential component wind speeds at the surface and the corresponding wind speeds at 500 ft. In his comparisons using buoy winds and aircraft (500 ft) winds, correlation coefficients ranged from 0.82 to 0.87.

Table 3

Ships involved in the JOINT II 1977 experiment and their cruise dates

Ship name	Cruise dates
R/V MELVILLE	March 4, 1977- March 9, 1977
	March 12, 1977- March 30, 1977
	April 9, 1977- April 24, 1977
	May 5, 1977- May 22, 1977
R/V ISELIN	March 16, 1977- March 31, 1977
	April 4, 1977- April 23, 1977
R/V WECOMA	March 16, 1977- March 30, 1977
	April 5, 1977- April 23, 1977
	April 30, 1977- May 16, 1977
R/V CAYUSE	March 17, 1977- March 30, 1977
	April 5, 1977- April 13, 1977
	April 21, 1977- April 27, 1977
	May 5, 1977- May 17, 1977

2.5 Limitations of the data

The advantage of using an aircraft to record the 500 ft winds and SST's is that data may be gathered continuously over a relatively large area. However, there are problems with the use of an aircraft. It takes time to move across the pattern; thus observations are not truly synoptic. In most cases the flight time between completion of the first flight "L" in the southwest corner until initiation of the second flight "L" was about three hours. This sampling is

only representative of atmospheric motions around midday along the Peruvian coast at about 15°S. This temporal limitation is generally less of a problem in the JOINT II area than in previous experiments due to the consistency of the prevailing winds.

The pattern altitude on the micro flights was always 500 ft. This altitude will not always be the height of the maximum wind; however, it is an ideal level to study the horizontal wind field. This subject is addressed later in this report (see Section 3.3).

Due to a reduction in the duration of daily flights during JOINT II 1977, there were no vertical soundings taken on the micro flights. Thus, increased reliance must be placed on the vertical profile data obtained in 1977 from the macroscale flights (flown approximately every other day), as well as the studies and results of JOINT II 1976 (Watson, 1978). The data obtained from the macroscale flights in 1977 are the primary source of a separate report on the atmospheric structure off the coast of Peru (Wirfel, 1979). Keeping these limitations in mind, the next chapter begins the analysis and interpretations of the data.

CHAPTER III

THE WIND FIELD

This chapter examines the wind field at 500 ft. Comparisons of the wind field with the corresponding SST field are made for overall mean values and for weak vs. strong flights. The wind field in JOINT II 1977 is compared with that of 1976. Finally, the SST field is studied during a period of unusually light winds. Due to their bulk, not all of the individual charts and profiles are included in this study. They will be published at a later date as a separate data report.

3.1 Topography

An accurate investigation of the wind field over the survey area requires a familiarity with the orographic features along the coast and over the coastal ocean floor. These features are best seen in Fig. 7. Careful observation will reveal that the bottom contours in this figure differ from those shown on most of the other maps in this paper. The explanation is that the bottom contours shown in Fig. 7 were not available until after the maps were completed for publication. The source of the more recent and accurate bottom contours is Preller (1979).

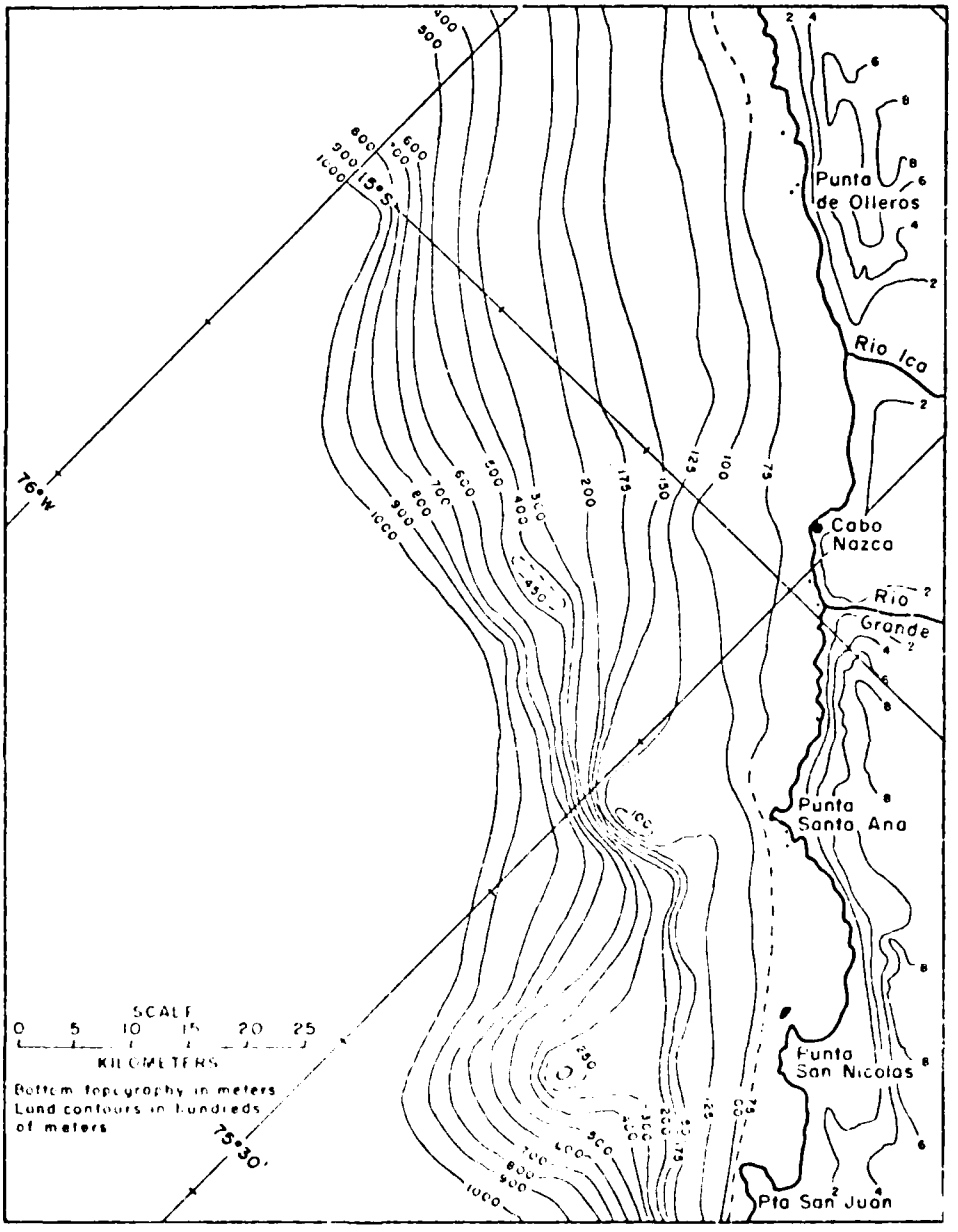

Fig. 7. Map of a portion of the JOINT II region with bottom topography and land contours.

The Peruvian coastal terrain is characterized by steep, rugged mountains broken at intervals by narrow river valleys. The average elevation of these arid coastal ridges is 700 m with some peaks to 900 m. Two river valleys cut through the coastal ranges along the JOINT II area. The Ica River valley with its north-south orientation is an important feature in the understanding of the wind field. Several land meteorological stations were positioned in or near this valley (Fig. 2). The Rio Grande valley forms a steep narrow gorge 20 km southeast of the mouth of the Rio Ica. Three prominent capes of significance are: Cabo Nazca, Punta Santa Ana, and Punta San Nicolas. Cabo Nazca (elevation 350 m) is a high escarpment that extends into the Pacific and separates the two valleys.

The bottom contours in the northern half of the survey area basically parallel the coast as they drop off toward the Peruvian trench, while the southern half features two prominent seamounds. This bathymetry is considered in more detail in the study of the SST field under light wind conditions (Section 3.8).

3.2 Climatology

To show that the measurements of wind and SST taken during JOINT II 1977 are representative, a closer look at climatology is required. The prevailing southeasterly winds along the coast of Peru are primarily driven by the South Pacific subtropical high and its associated counterclockwise

circulation. A lesser feature is the low pressure trough that is typically centered over the lower terrain east of the Andes Mountains and often extends southward along the coast of South America.

The center of this large scale high pressure migrates from 32°S, 90°W in January to 28°S, 88°W in July (Stuart, 1975). Thus, an average position for April is 30°S, 89°W. During the JOINT II 1976 experiment, the average position was 33°S, 91°W; while in 1977 it was 30°S, 87°W.

Figure 8 shows the 0000 GMT, 17 April 1977 National Weather Service surface analysis for South America and the eastern South Pacific. This position of the high is typical of the 1977 survey period. Further, Fig. 8 reveals that the JOINT II area is clearly at a lower latitude (on the equatorward side) of the subtropical high. This positioning accounts for the consistent southeasterly coastal winds along Peru. In response to the seasonal motion of the Hadley High, its maximum north-south momentum transport is in the winter. This corresponds to the maximum upwelling (coldest SST's) in July (Stuart, 1975).

On a smaller scale, the first order manned weather station at San Juan, Peru (CORPAC, Civilian Airport Corporation of Peru) is chosen to study the mean winds. These monthly mean winds were obtained from the National Climatic Center of the National Oceanic and Atmospheric Administration (NOAA). The mean wind speeds and percentage frequency of the two

most prominent directions (SSE-S) are given in Table 4 for 1976, 1977, and the period 1957-1969.

Table 4
Climatological wind data for San Juan, Peru (CORPAC)

Month	Mean wind speed ($m\ s^{-1}$)			Percentage frequency of surface winds (SSE-S)		
	1957-69	1976	1977	1957-69	1976	1977
March	5.0	5.6	5.3	91.9	84.1	46.7
April	5.1	5.3	5.9	89.8	86.8	69.5

The wind speeds in each comparison are very similar with both the 1976 and 1977 values exceeding the climatological mean. The directional figures for 1977 are somewhat misleading in that the average wind direction was about 180° due to an increased southwesterly component. So consistent is the southerly flow at San Juan that only five hourly directions observed during both months were greater than 220° or less than 150°. The anemometer at San Juan is located such that nearly all the observations report a wind direction directly out of the south.

Due to the questionable exposure of the anemometer at the CORPAC San Juan location, a comparison anemometer (Punta San Juan) was used for the JOINT II experiment (Stuart, 1975). The resulting comparisons are seen in Fig. 9. The wind speeds during the respective times of the experiments in 1976 and 1977 agree fairly well. The Punta San Juan wind

speeds are approximately one m s^{-1} greater than the CORPAC winds. The data for this figure were also obtained from the National Climatic Center of NOAA, as well as JOINT II data files.

The general oceanic circulation off Peru is composed of several currents (see Fig. 10, from Idyll, 1973). Two surface currents flowing toward the equator are the Peru Coastal Current (a narrow belt of cold water close to shore) and the deeper and wider Peru Oceanic Current. The Peru Countercurrent flows southward between the two shallow currents and extends to a greater depth. The larger Peru Undercurrent also flows southward and is centered at about 200 m depth. Wyrtki (1966) concluded that the JOINT II area (15°S) is a transitional zone, as to the source of upwelled water. His computations imply that south of 15°S upwelling is supplied by the Peru Coastal Current, and north of 15°S by the Peru Countercurrent. Peru is unique from other upwelling regions in that the mean wind and prevailing current oppose one another except in a shallow surface layer.

Figure 11 depicts the average SST's off Peru for the Autumn season based on the period 1928-1969. These data were taken from Zuta and Urquizo (1972). It agrees very well with the mean SST map of all micro flights (Fig. 16), considered in this report.

The wind and SST data gathered during JOINT II 1977 seems to agree well with observations taken in 1976 and the available climatological data of the area.

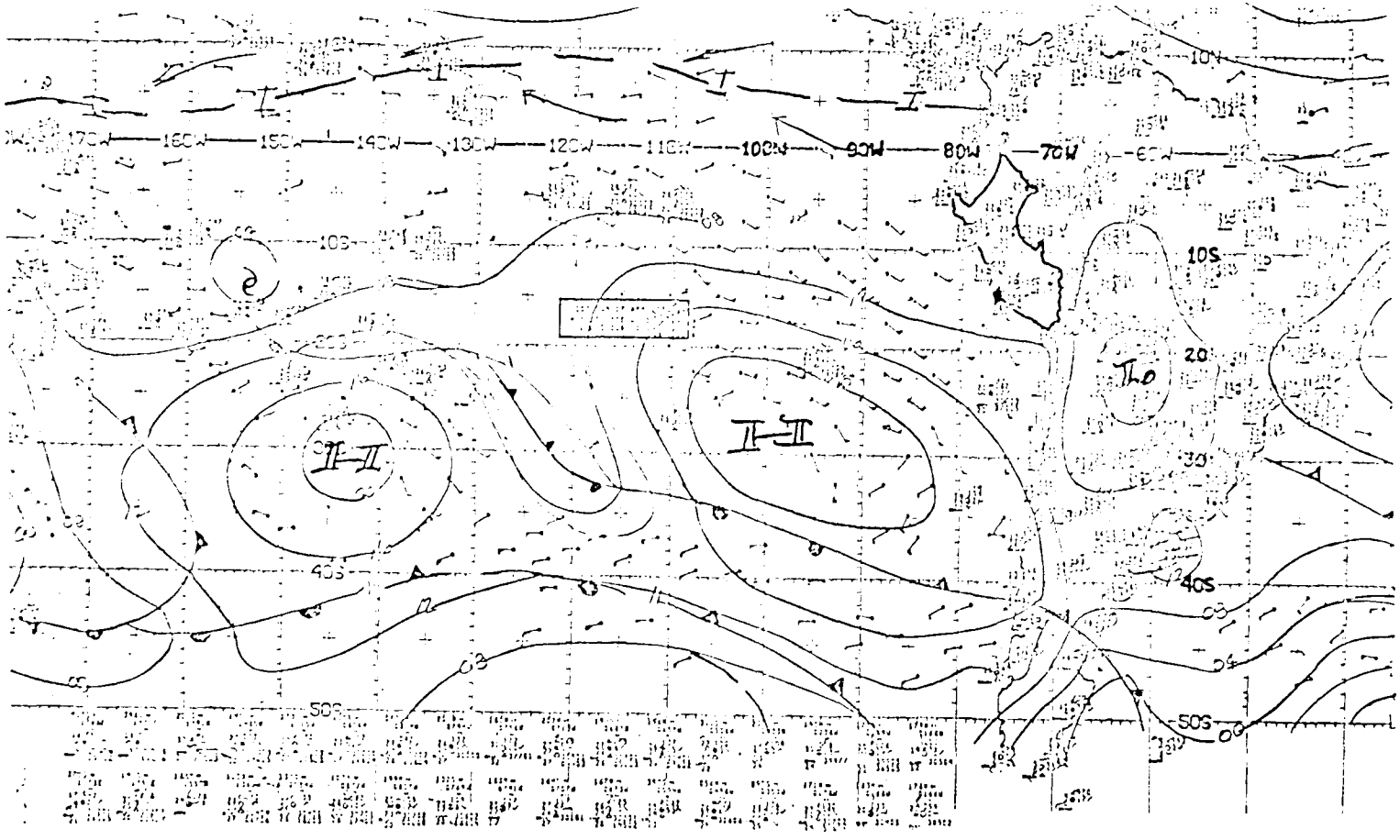

Fig. 8. Sea-level pressure analysis via National Weather Service 0000 GMT 17 April 1977.

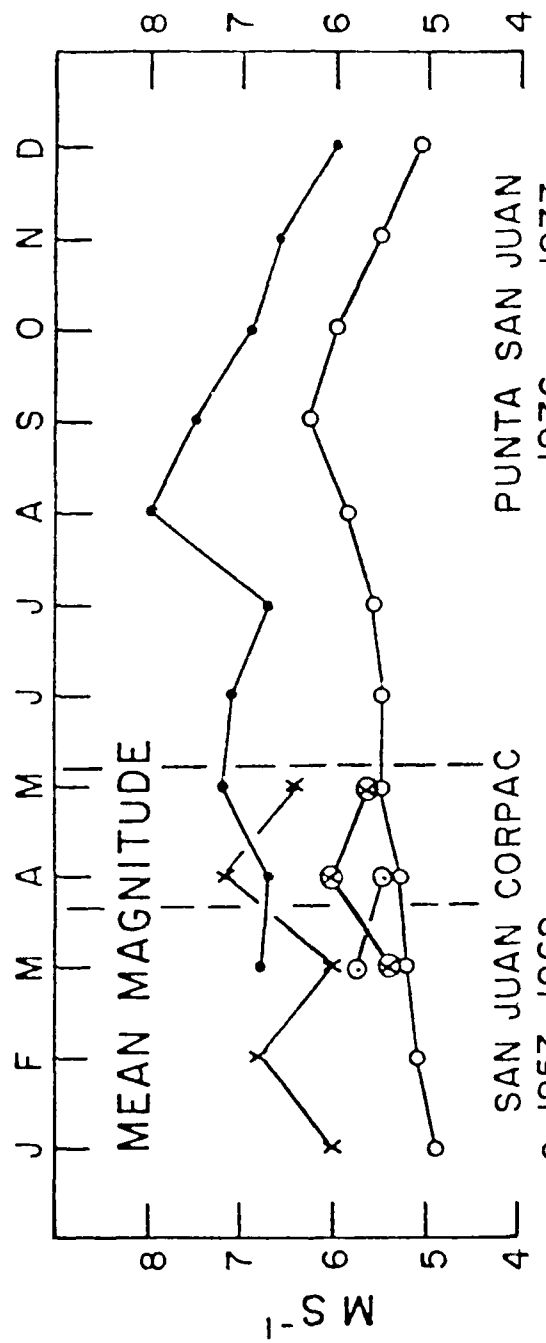

Fig. 9. Chart of climatological comparison results for two anemometer locations in San Juan, Peru.

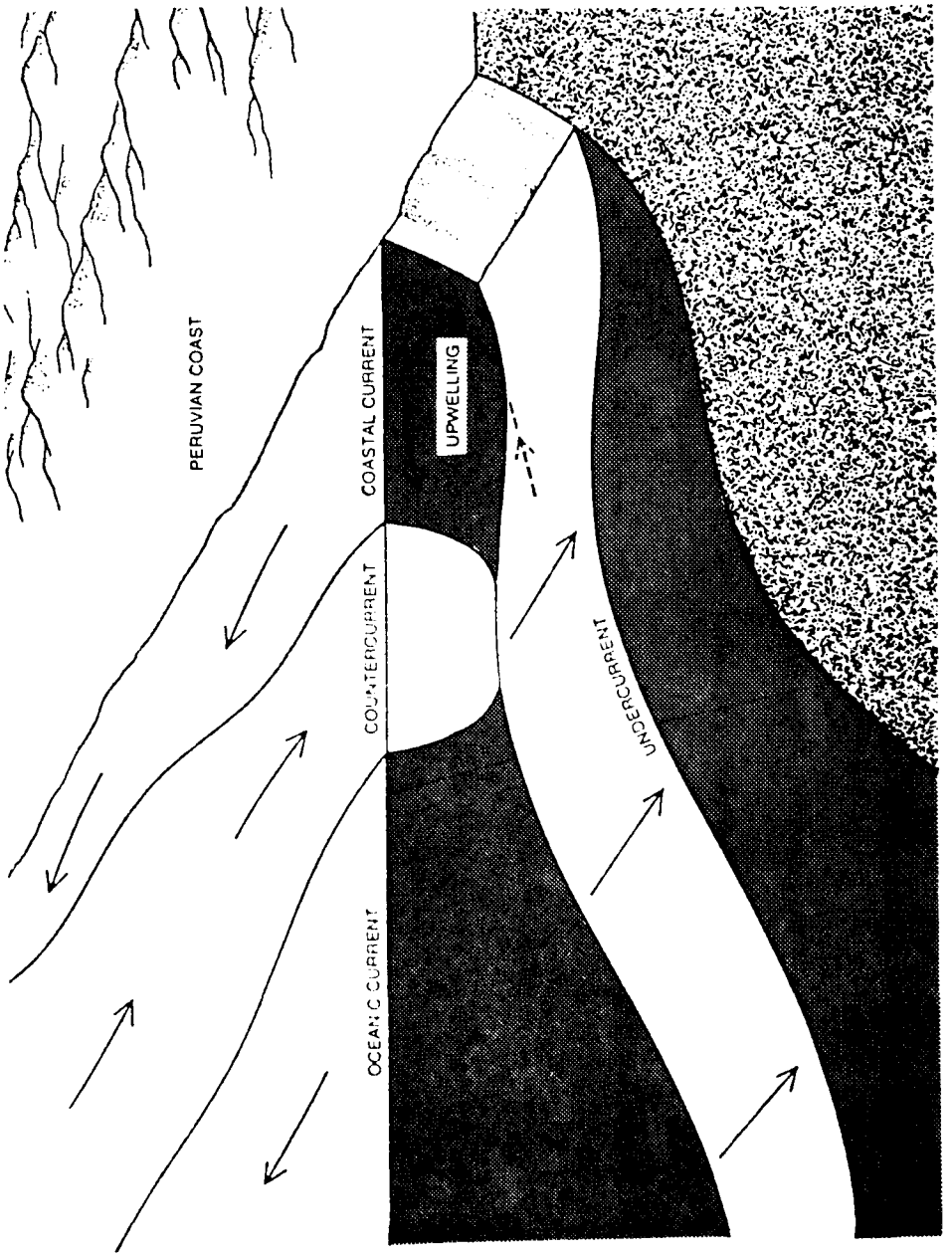

Fig. 10. Map of the ocean currents along the Peruvian coast.

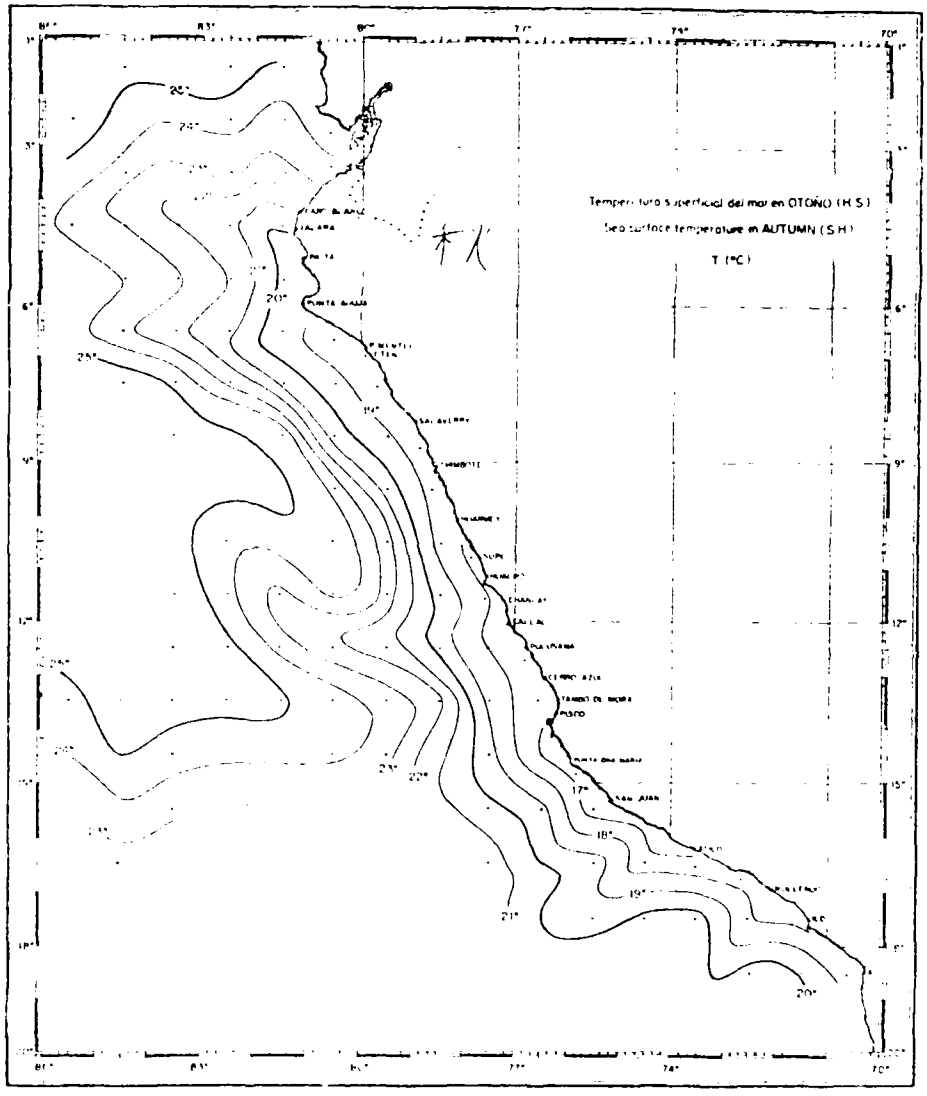

Fig. 11. Map of average sea surface temperatures (SST's) off the coast of Peru during the Autumn season for the climatological period 1928-1969.

3.3 Mean wind field

The mean wind field in 1977 over the JOINT II area is very similar to the pattern found in 1976. Figure 12 is the mean streamline and total isotach pattern at 500 ft during 1977. It is readily seen that the streamlines generally parallel the coast except seaward of the mouth of the Ica River, where the flow is difluent with a component up the valley. The steep coastal terrain seems an effective barrier to onshore flow elsewhere along the coast. This same pattern is repeated on other mean maps and on individual flight maps except when the winds are light. In these cases of weaker winds the streamlines display a more erratic pattern and the onshore flow is increased.

A maximum is present in the total isotach pattern 6 nm southwest of Cabo Nazca. A smaller maximum (located 16 nm offshore from Punta de Olleros) connects a broad belt of stronger winds aligned approximately southeast to northwest. In contrast, an area of minimum wind speeds is present at the coast just north of the Ica River mouth. Generally, all of these isotach features are repeated on the other maps of 1977.

A complete explanation of these features was given by Watson (1978). In short, the air accelerates as it approaches the wide Ica River valley opening due to the sea breeze and its associated local thermal forcing. As a consequence, a deceleration is seen to the north of the valley.

A closer look at Fig. 12 shows a small diagram on the left side with positive unit vectors in the V_T and V_N directions (315° and 045°, respectively). These components refer to the generalized orientation of the coastline in the JOINT II region. The mean V_T-component pattern (Fig. 13) is nearly identical to the pattern of the total isotachs. This is expected since the flow across the survey area is almost parallel to the coast. Individual V_T-component charts display a pattern similar to the mean. The only difference is that as the winds strengthen, the position of the V_T-component maximum southwest of Cabo Nazca moves closer to shore. The exact location of this offshore maximum seems dependent on the frictional effect of the coastal topography.

Figure 14, the V_N-component analysis, shows strong onshore flow near the mouth of the Ica River valley and the mouth of the Rio Grande valley. Somewhat weaker onshore flow is seen along the lower terrain north of Punta San Nicholas. The negative V_N-component values in the lower portion of the analysis are evidence that the winds enter the JOINT II region with an offshore component due to the orientation of the coastline further south (120-300°). A comparison of the individual V_N-component charts with the mean shows that as the wind increases, the onshore flow at the river mouths also increases. Furthermore, offshore flow is seen north of the Ica River.

Figures 15a and 15b are vertical profiles of the mean wind components taken at points ③ and ④ (see Fig. 3). Data

were averaged from 11 macroscale flights with the average times for these soundings being 1140 LST and 1230 LST, respectively. The profile taken at point ④ is more representative of the mesoscale survey area. The level of maximum V_T-component (12.3 m s^{-1}) is around 985 mb at point ④, while it rises to a broader maximum (10.5 m s^{-1}) near 960 mb out at point ③. This difference is directly related to changes in the subtropical inversion (Wirfel, 1979). The lower and more concentrated V_T-component maximum nearer the coast appears to be a significant factor to the intensity and the location of the resultant upwelling patterns below. The V_N-components in Fig. 15b show some onshore flow due to the thermal forcing near the coast. The flow at point ③ is all offshore, since its location is beyond the thermal influence. These figures and the preliminary results of Goodwin (see Section 2.4) confirm the usefulness of 500 ft (or approximately 990 mb) as an excellent flight level for investigating the wind field.

3.4 Mean SST field

The mean SST field for the twelve micro flights considered in the report is shown in Fig. 16. The striking feature of Fig. 16 is the broad cold plume (17°C) extending from the coast between Cabo Nazca and Punta Santa Ana westward. Colder temperatures (18°C) also begin at the coast 12 nm north of the Ica River mouth. Between these two cold areas the SST's rise to a warm maximum (19.5°C) 5 nm north of the

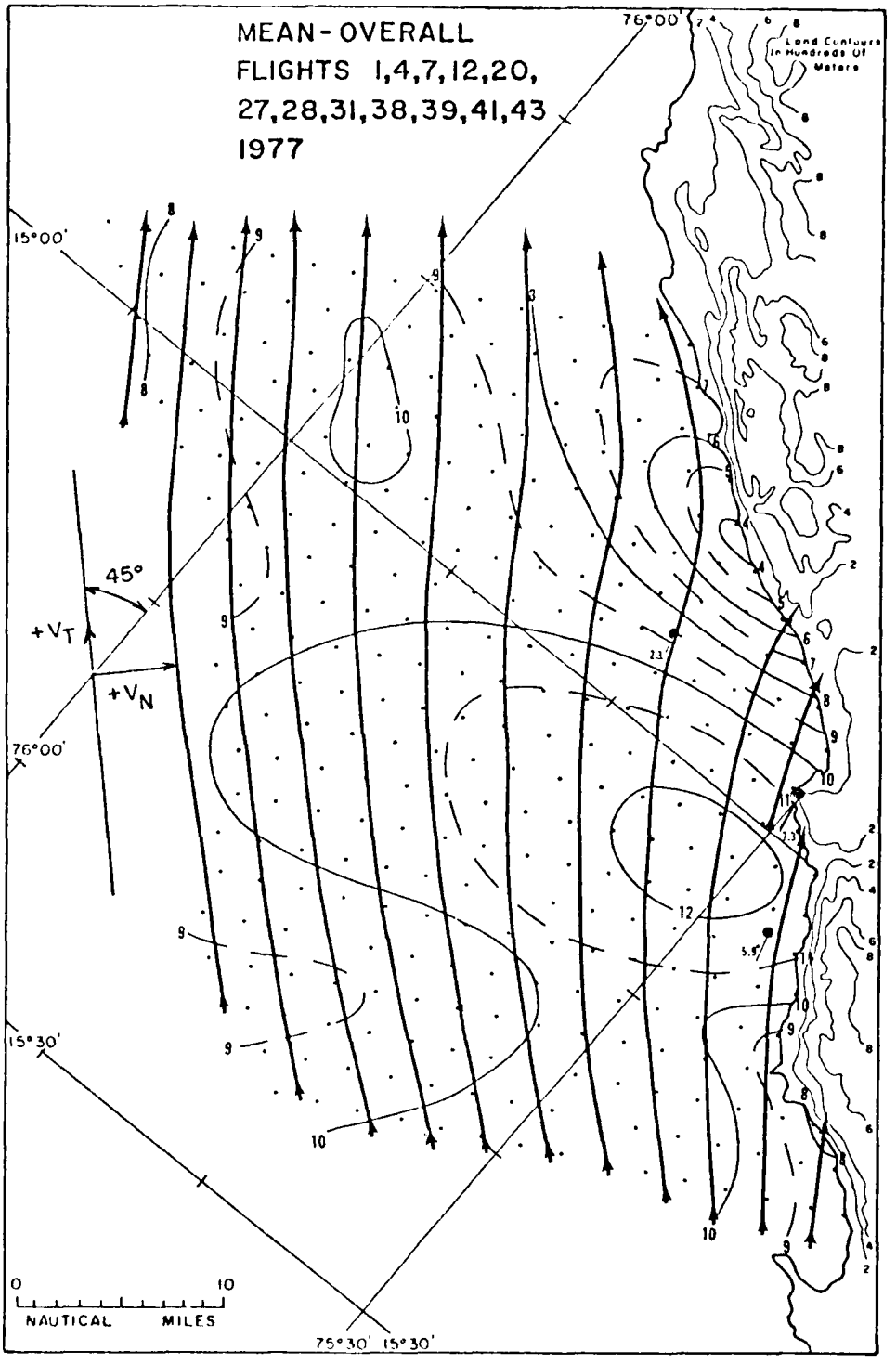

Fig. 12. The mean streamline and total isotach patterns at 500 ft as recorded by an aircraft during March, April, and May 1977.

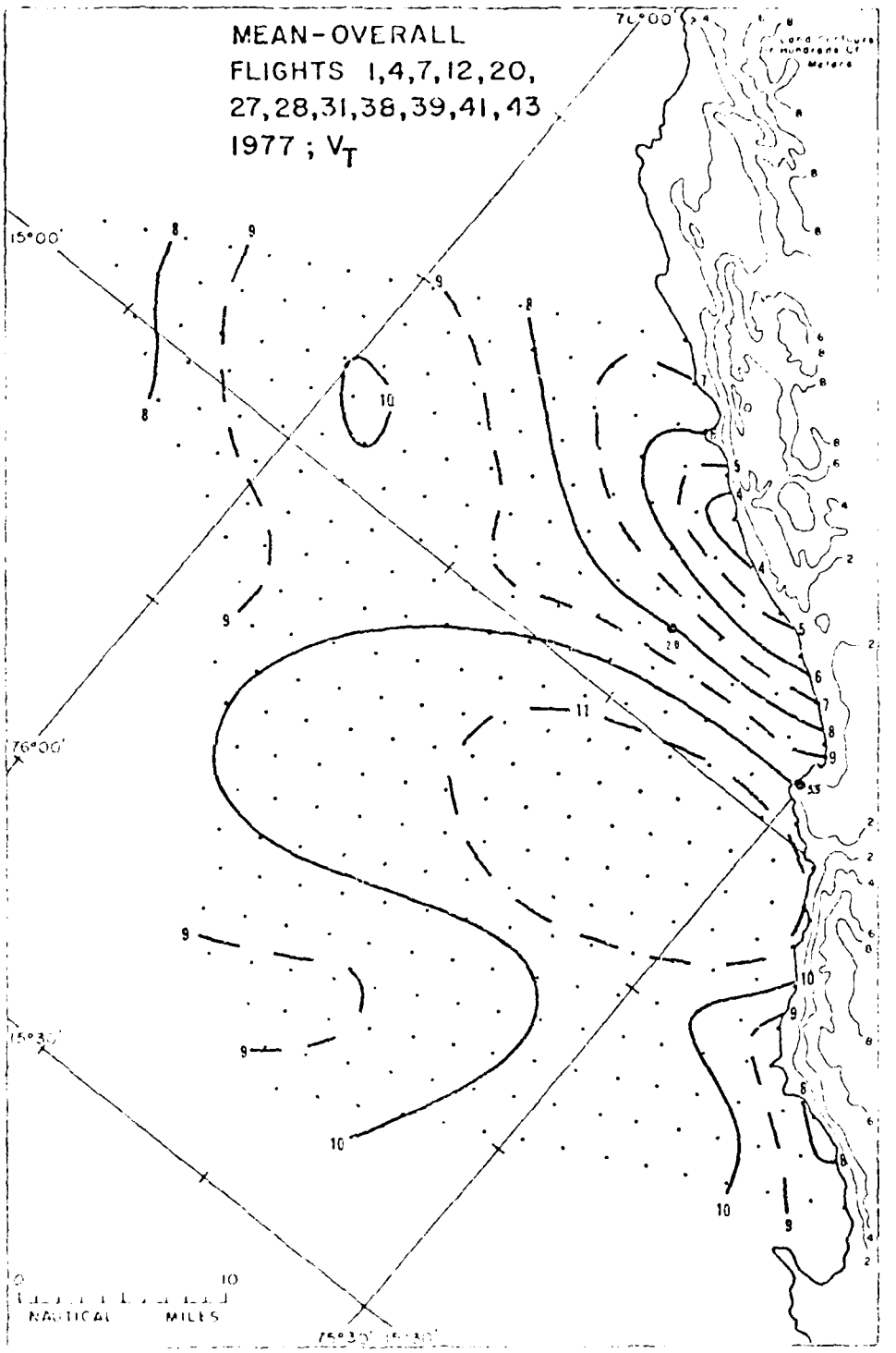

Fig. 15. The mean V_T-component pattern at 500 ft as recorded by an aircraft during March, April, and May 1977.

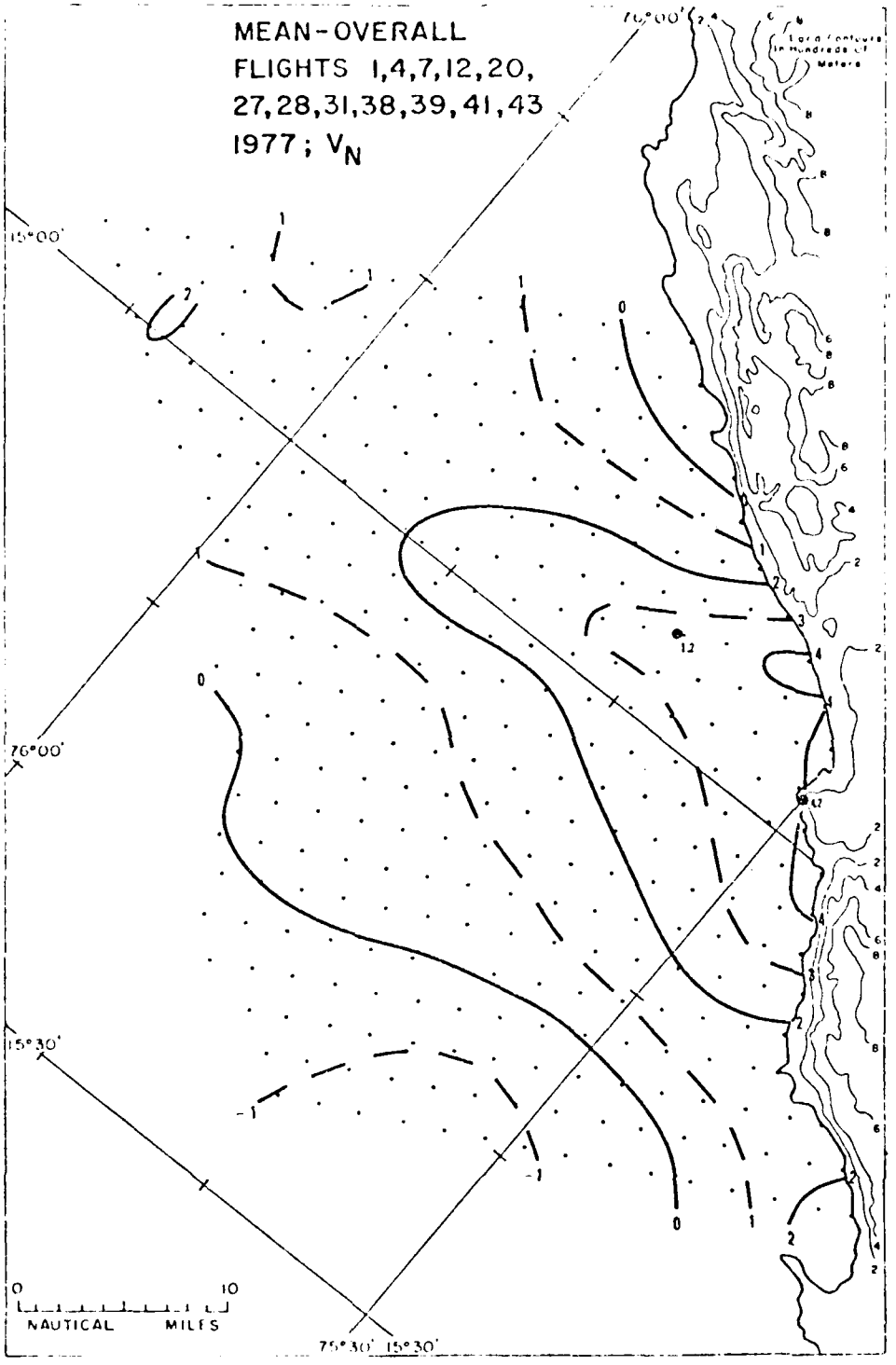

Fig. 14. The mean V_N-component pattern at 500 ft as recorded by an aircraft during March, April, and May 1977.

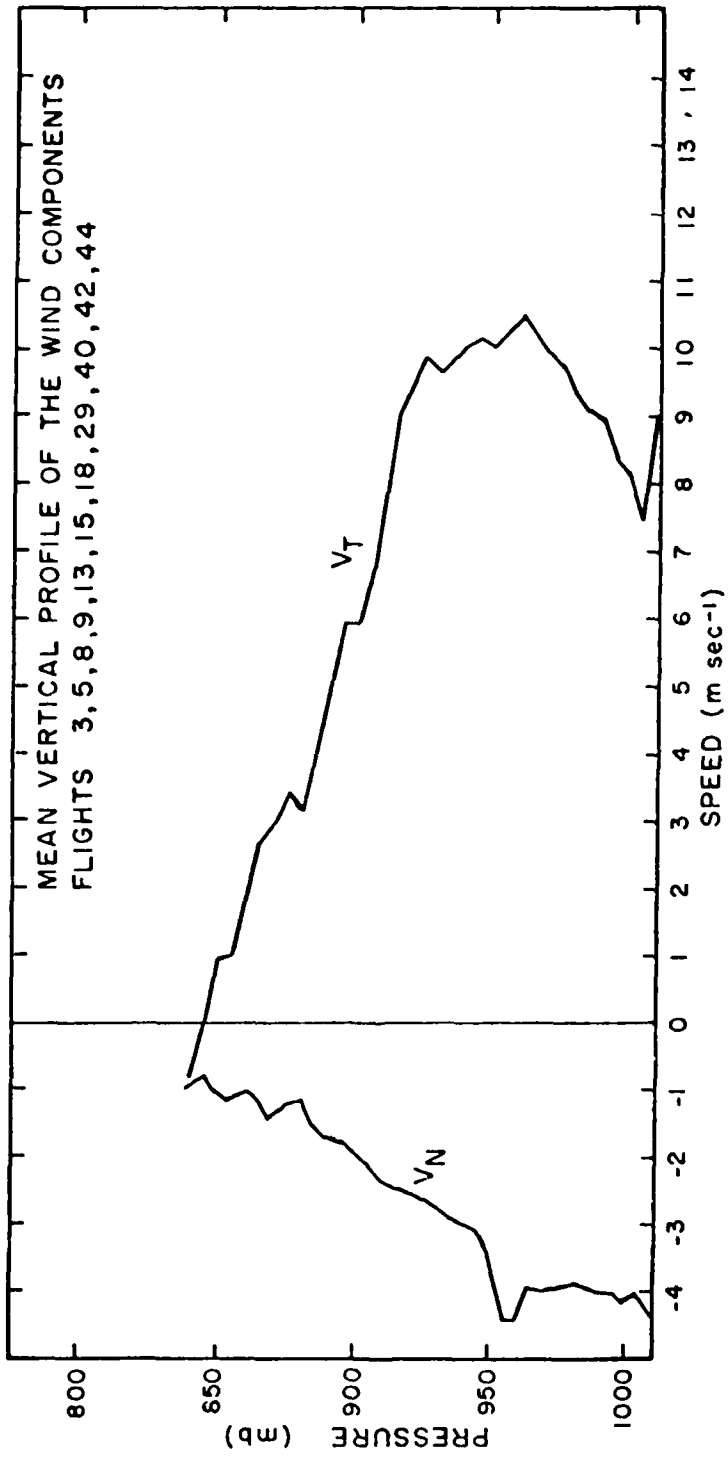

Fig. 15. (a) Vertical profiles of the mean V_T and V_N-components at 70 nm seaward from Cabo Nazca.

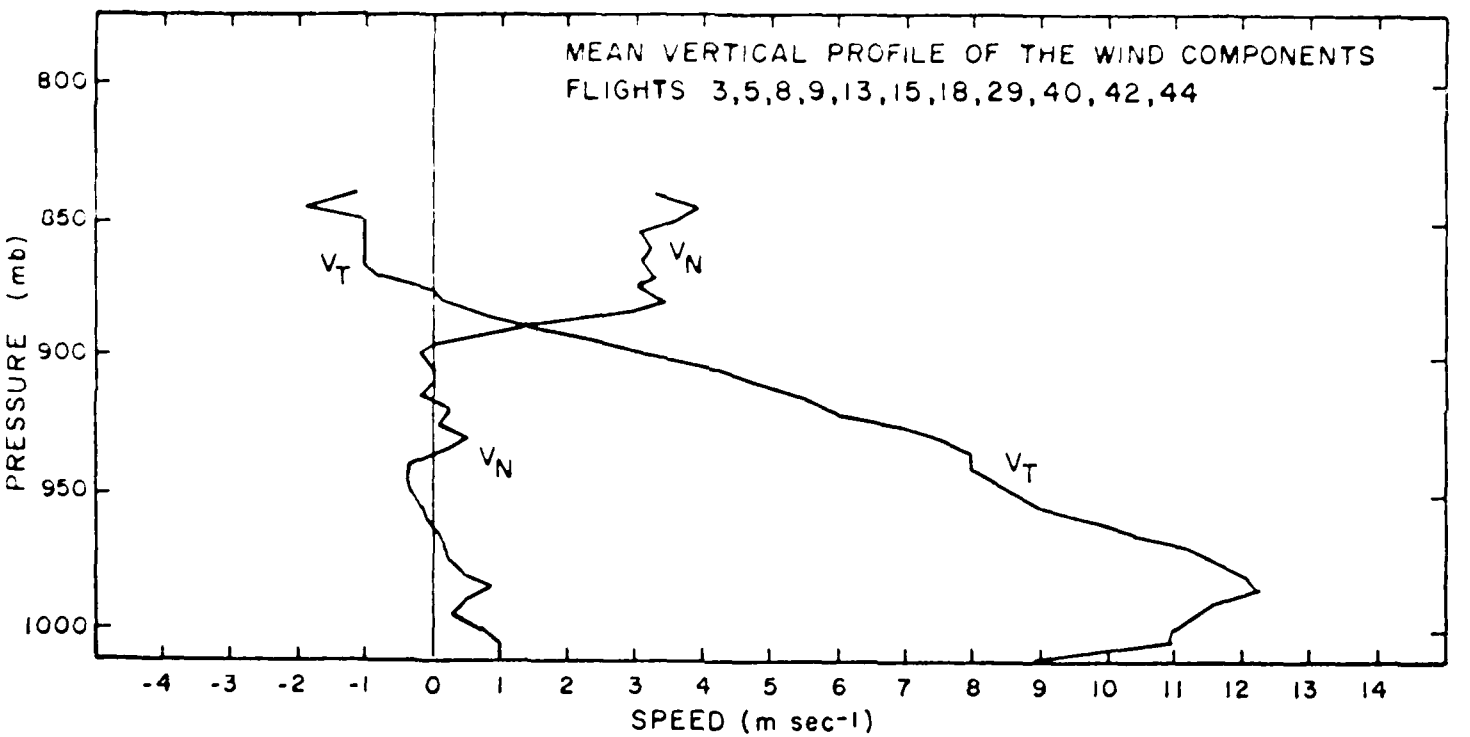

Fig. 15. (b) Vertical profiles of the mean V_T and V_N-components at 10 nm down the coast from Cabo Nazca.

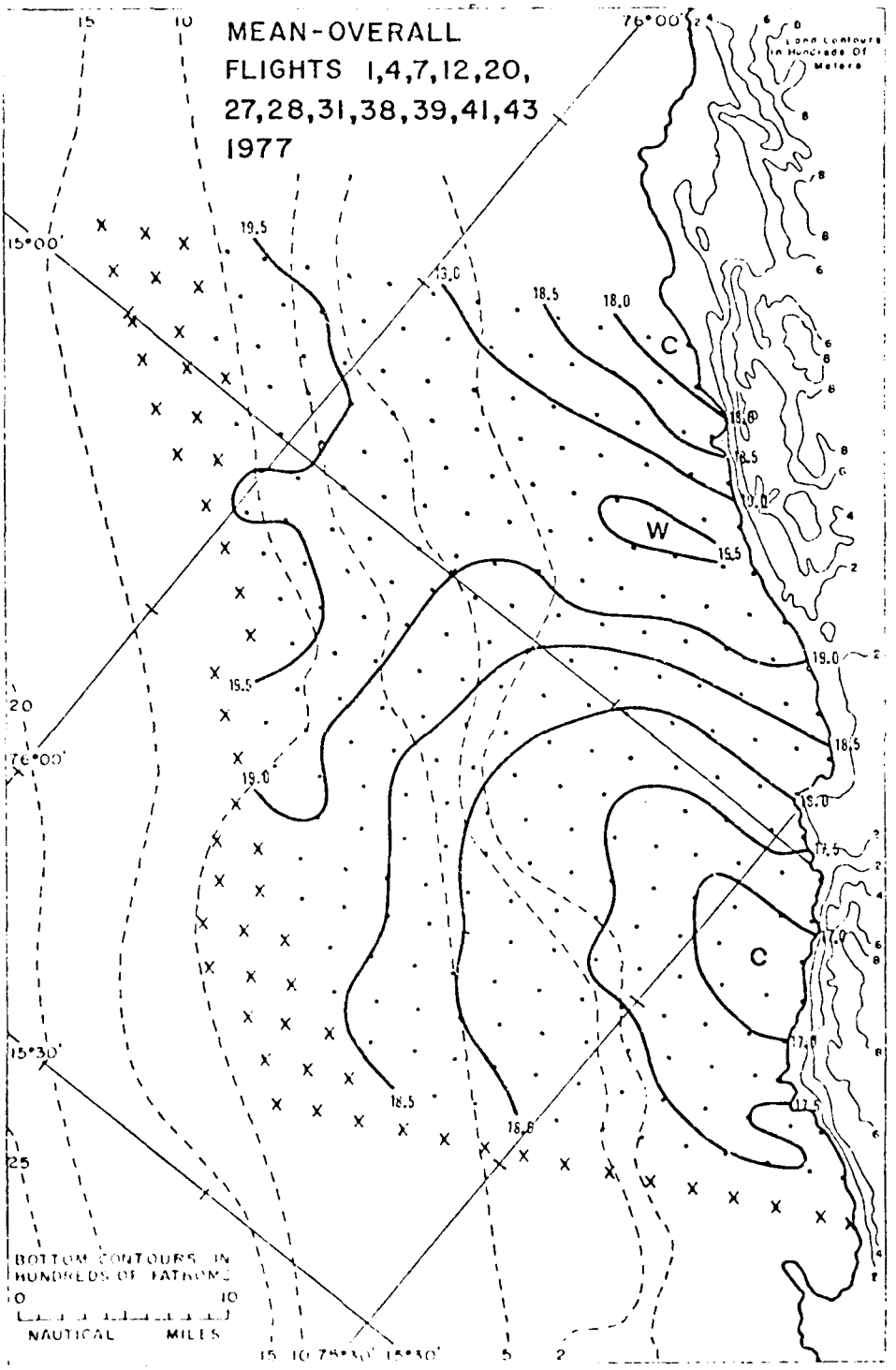

Fig. 16. The mean sea surface temperature (SST) pattern as recorded by an aircraft during March, April, and May 1977.

river valley opening. Warmer temperatures also prevail along the western portion of the grid. Individual flights (see Stuart and Bates, 1977) generally show good agreement with these features except for flights 31 and 38, which are the subject of a separate section of this report (Section 3.8).

Except for the southwest part of the survey area, there does not seem to be a parallel orientation of the mean SST isotherms with the bottom contours. This parallel alignment has been in evidence in previous experiments (Holladay and O'Brien, 1975 and Nanney, 1978). The best explanation seems to be that coastal influences mask the paralleling effect over the majority of the small mesoscale area. A larger scale study would be required to investigate this effect further. In such a study, Gunther (1936) found that surface isotherms generally parallel the coast and that there was little correlation between the mean gradient of the continental shelf and the SST's.

The X's appearing over grid points in Fig. 16 are where there were fewer than 9 of the 12 data values available for analysis. Areas of temperatures colder than 16.5°C are shaded on all the SST analyses.

3.5 A comparison of the mean wind and mean SST fields

Since coastal upwelling is a wind driven ocean circulation, a comparison of the wind and SST fields seems a logical method of studying the upwelling phenomenon.

Upwelling theory suggests where colder temperatures should be expected. Ekman's theory (1905) states that the net transport of water due to wind stress is directed 90° to the left of the wind in the Southern Hemisphere. This is due to the effect of the earth's rotation (Coriolis) and to frictional forces. The amount of water mass displaced by this Ekman transport is proportional to the tangential wind component (V_T). The coast prevents replacement of the displaced water, except by upwelled colder water below. The result of this theory should be increasingly colder SST's from the coast out to the maximum V_T-component. The SST's should then begin to increase seaward of this V_T-component maximum due to convergence in the surface layer resulting in downwelling. It should also be understood that because of the response time of upwelling to a wind impulse it is difficult to relate a particular SST feature to a wind feature seen at the same time.

In comparing Figs. 13 and 16, the observer sees that the V_T maximum (11 m s^{-1}) seems to correspond with the SST minimum value (17°C). However, they do not align exactly as theory predicted. Showing better agreement is the V_T-component minimum (4 m s^{-1}) and the SST maximum (19.5°C), while the closed tangential isotach value of 10 m s^{-1} in the northwest portion of the grid has no SST minimum counterpart.

The upwind position of the SST minimum from the location of the strongest forcing, agrees with existing theories. Yoshida (1967) concluded that the region of maximum upwelling

is displaced poleward from the region of maximum wind along the eastern boundary of an ocean due to the response of the wind stress to the alongshore pressure gradient. Yoshida states:

> "... a simple physical explanation is that the upwelling-producing wind along the eastern boundary creates a region of divergence in the wind stress field poleward of the wind maximum region, and one of convergence equatorward."

Arthur (1965) applies the conservation of potential vorticity and the complex coastal currents to explain forced convergence on the upstream side of capes resulting in divergence on the downstream side. Thus, the cold Peruvian coastal current flowing toward the equator around Punta Santa Ana would enhance upwelling on the downstream side where the colder SST's are observed.

The broad plume of colder SST's agrees well with the location of the V_T-component axis extending westward from its maximum value. Another direct correlation was found in every case studied. As the V_T-component values decreased just north of the Ica River, the SST values became warmer just to the south. The absence of a SST minimum to correspond with the V_T-component maximum located about 18 nm offshore is explained by broadscale downwelling in the area. This downwelling is associated with the changing direction of the wind at the river mouth and to a lesser extent with the prevailing poleward currents flowing slightly downward over the broad continental shelf.

Figure 17a reveals the offshore profiles (a plot of the

averages of grid points equidistant from the coast) of the mean wind components and of the mean SST's for all grid rows and all 12 micro flights. The mean in each case is depicted as a straight line. The significant features of these profiles are very similar to those seen in JOINT II 1976. Watson (1978) offers a good explanation of these observations. Figures 17b, 17c, and 17d are additional offshore profiles averaged over selected rows for all the micro flights. Figure 17b (a profile for the area north of the Ica River valley opening) shows little sea breeze effect owing to the steep coastal terrain along this section. The tangential component maximum at 18 nm from the coast is a feature that was consistently located on all profiles observed. The offshore profiles seen in Fig. 17c are averages over gridrows 7 through 11. The offshore location of the minimum SST and the strong onshore flow are the prominent features of these profiles taken near the mouth of the Ica River. In Figure 17d, a somewhat weaker sea breeze effect is seen in the Rio Grande valley. The V_T-component maximum is located only 7 nm offshore agreeing with the northwest to southeast orientation of the V_T-component axis. The mean alongshore profiles (Fig. 17e) are plots of the averages of each grid row for all 12 flights. Ordinate values are distances measured from the 1976 "C" line (see Fig. 2). Geographical locations are also annotated along the side of the alongshore profiles for additional reference. The

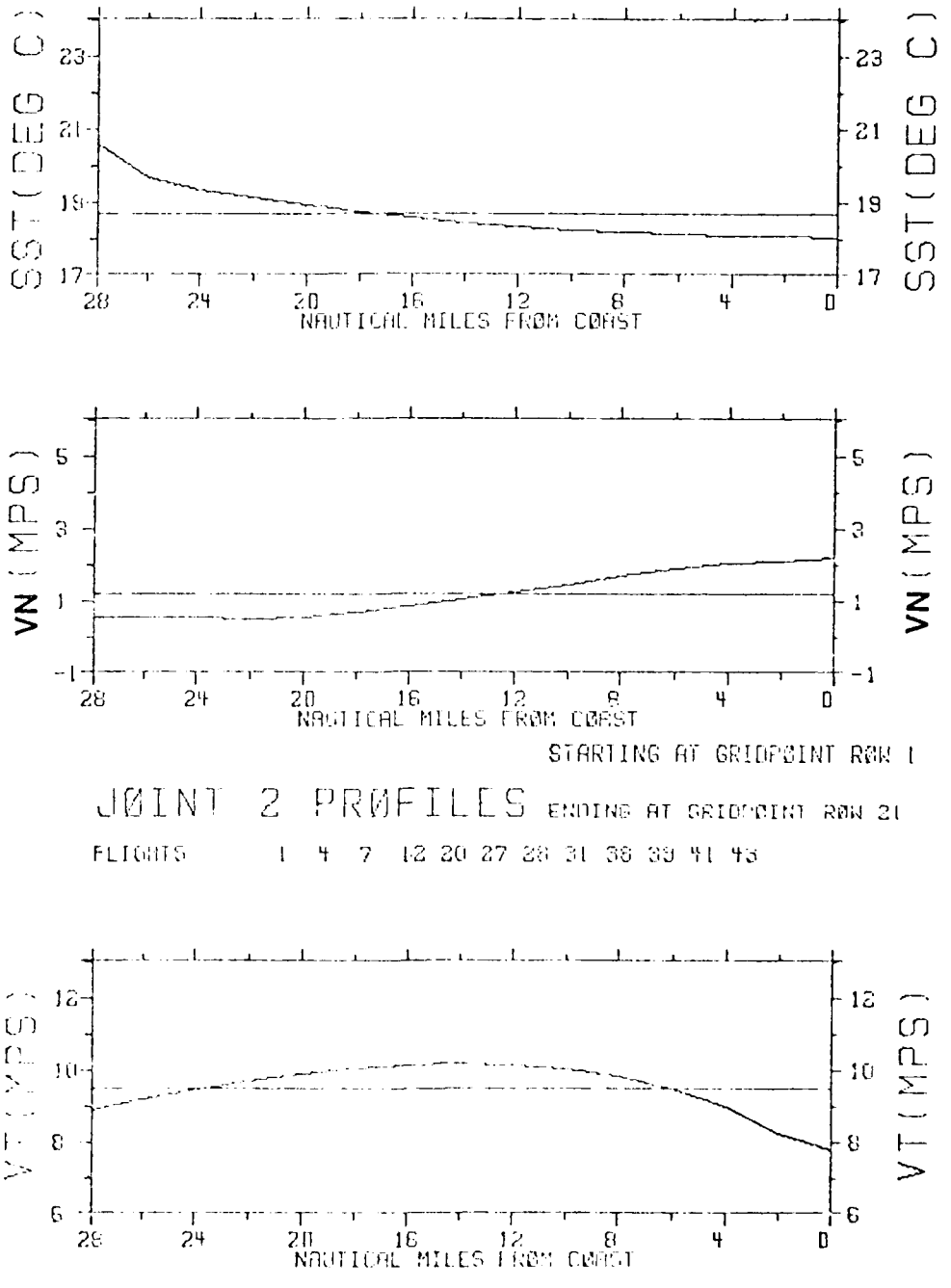

Fig. 17. (a) Offshore profiles of the SST, V_T and V_N-components averaged over all grid rows for the micro-scale flights in 1977.

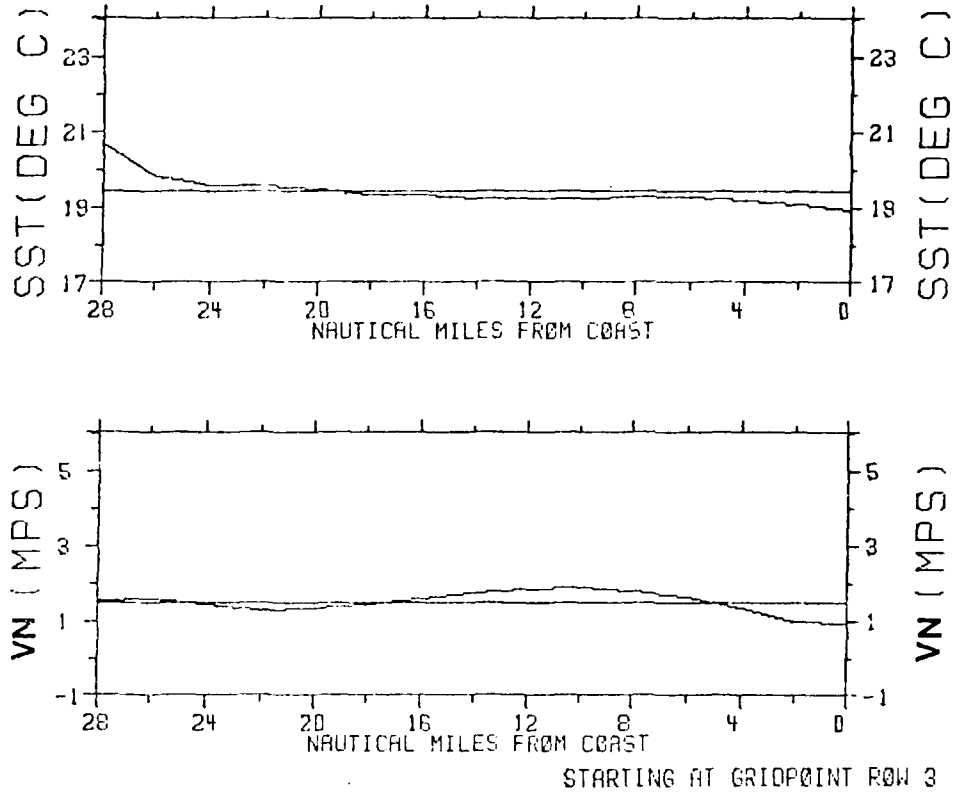

Fig. 17. (b) Offshore profiles of the SST, V_T and V_N-components averaged over grid rows 3 through 7 for the microscale flights in 1977.

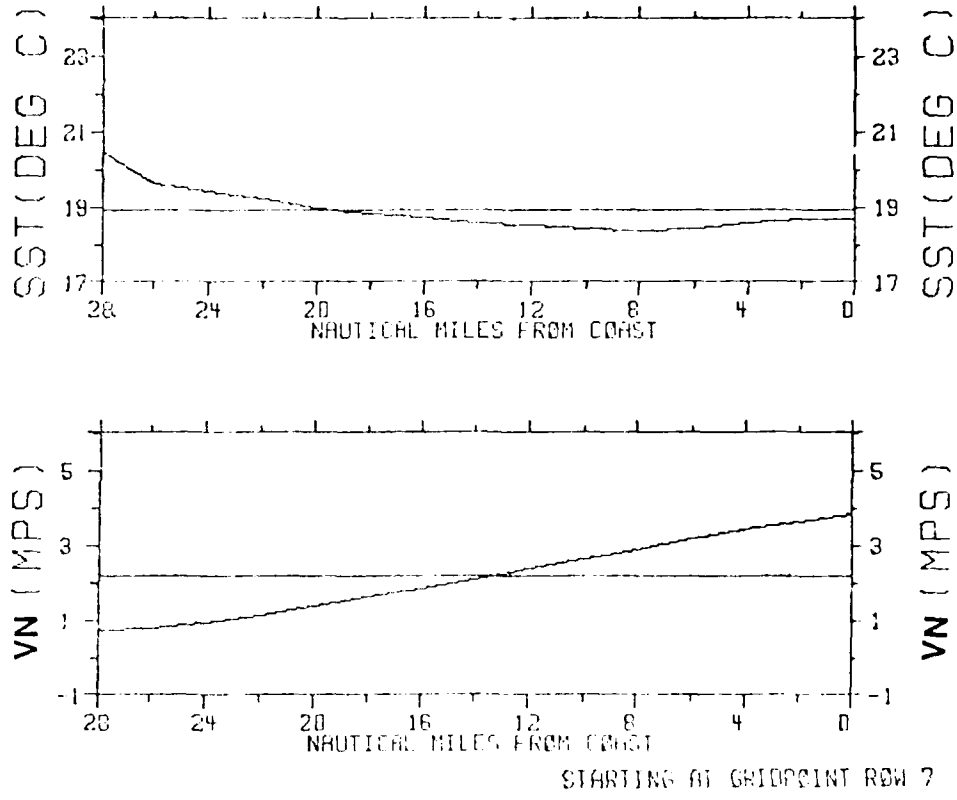

Fig. 17. (c) Offshore profiles of the SST, V_T and V_N-components averaged over grid rows 7 through 11 for the microscale flights in 1977.

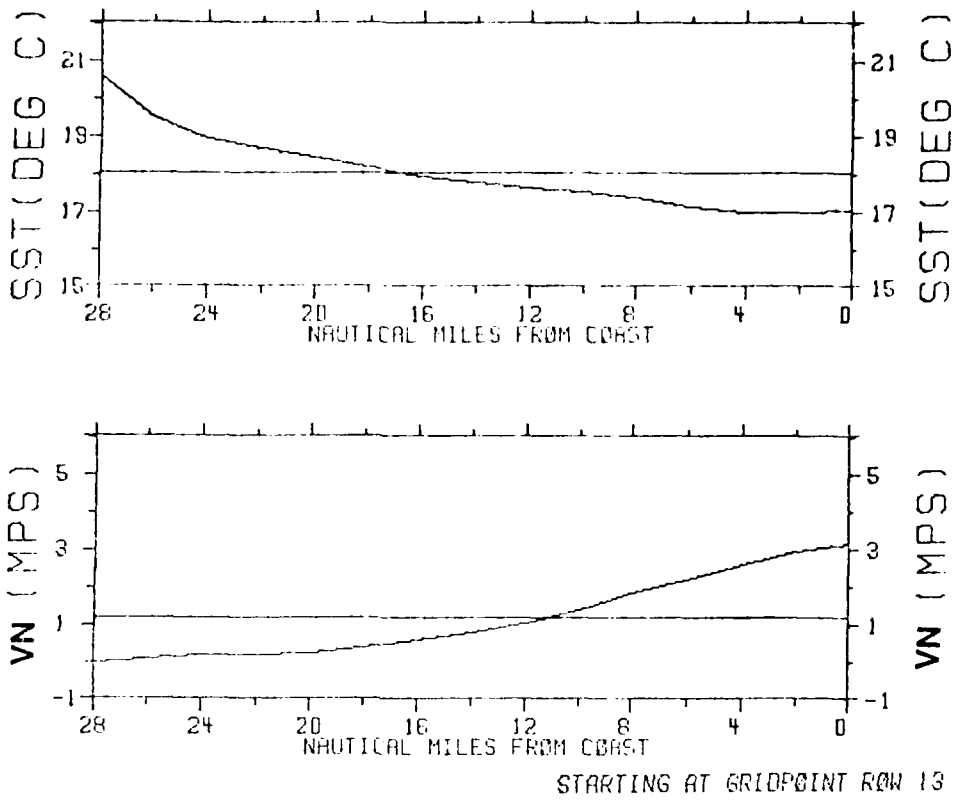

Fig. 17. (d) Offshore profiles of the SST, V_T and V_N-components averaged over grid rows 13 through 17 for the microscale flights in 1977.

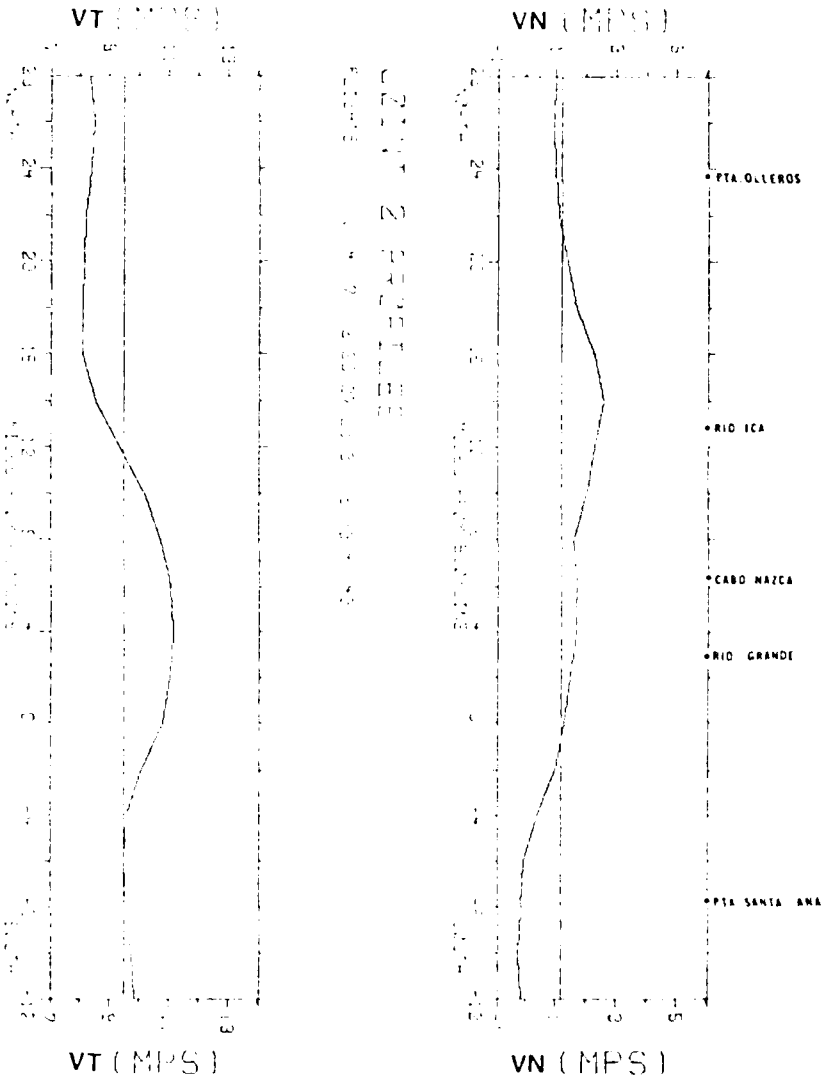

Fig. 17. (e) Alongshore profiles of the V_T and V_N-components averaged over all grid columns for the microscale flights in 1977.

V_N-component profile permits comparison of the stronger onshore flow along the Ica River opening with that near the Rio Grande. The significance of the V_T-component profile is the alongshore variation of this component. This variation (in this case from 8 to 11 m s^{-1}) is important as a forcing mechanism for subsequent upwelling. Only recently has this importance been explored by incorporating the alongshore tangential wind variation into numerical models.

In an effort to study further the correlation of the 500 ft winds with sea surface temperatures, a scattergram of the V_T-component maximum and its associated SST minimum for the 22 individual flights analyzed in 1976 and 1977 was constructed (Fig. 18). The first observation from this figure is that there seems to be a linear relationship, except for 5 flights. A closer study of these five exceptions revealed that numbers 4, 31, 38, and 43 are the flights flown on the weakest wind days in 1977 while number 9 was the one weak wind flight in 1976. Except for numbers 31 and 38, these weaker wind flights display a SST pattern similar to the mean. The interesting feature of this linear relationship is that it seems to be independent of the length of time that the wind has influenced the area, the temperature of the subsurface water, the depth of the thermocline, and the currents. Thus, based on these limited data, there seems to be a linear relationship between the magnitude of the tangential wind maximum at 500 ft and the resultant SST minimum value for values of the V_T-component exceeding

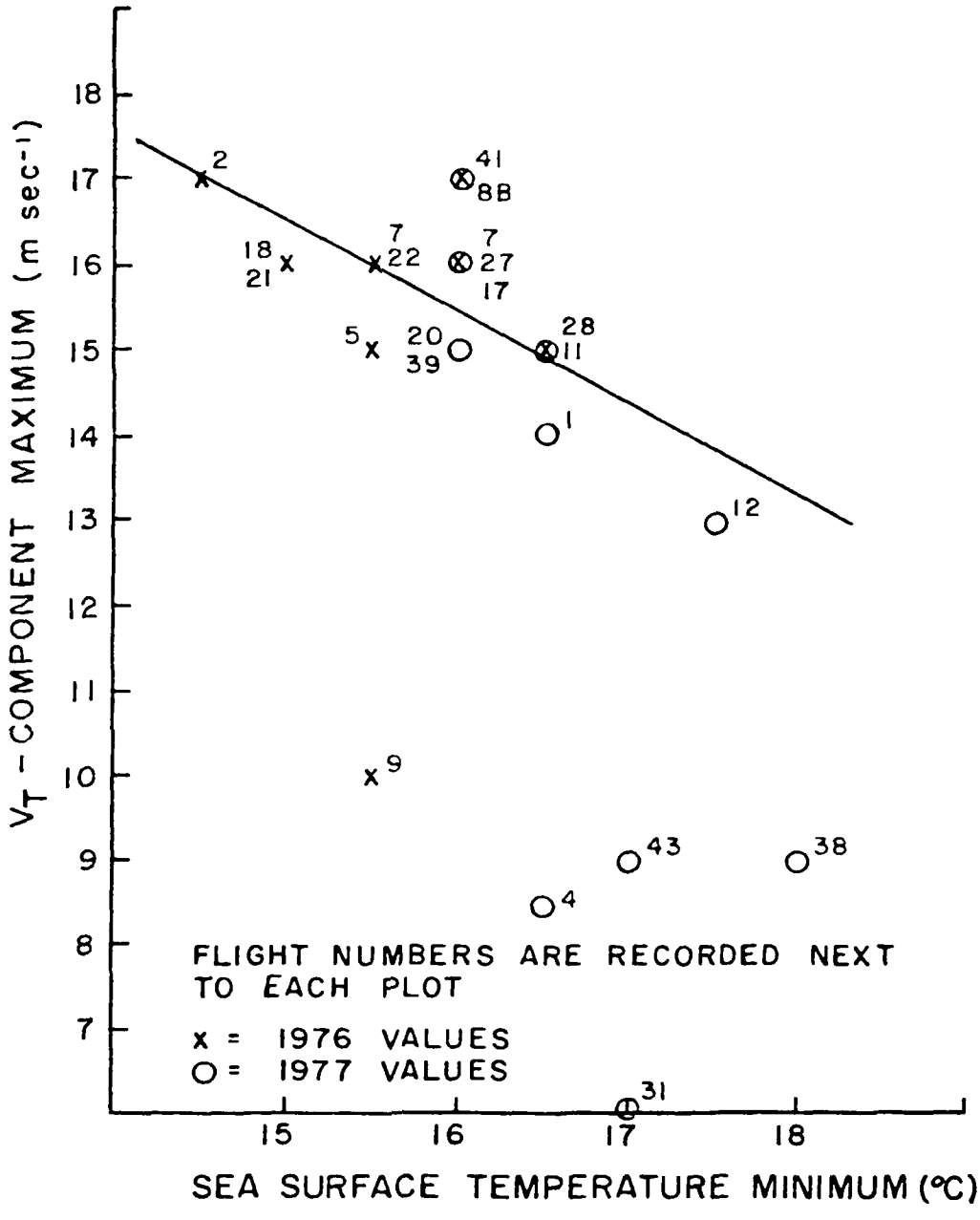

Fig. 18. Scattergram of V_T-component maximum values at 500 ft and associated sea surface temperature (SST) minimum values during 1976 and 1977.

13 m s^{-1}. Unfortunately, this result cannot be investigated further due to the lack of temperature and ocean current data. The accuracy of this correlation is even more remarkable when considering: (1) that the data were taken at different times of the day, (2) the round off error, and (3) that the 500 ft wind may not be representative of the surface wind.

Finally, the result of the observations in this section is that there are direct relationships that appear to exist between the sea surface temperature pattern and the 500 ft wind field over this area off Peru.

3.6 A comparison of the wind and SST fields of 1976 and 1977

A comparison of the mean wind and SST patterns between the two years of the JOINT II experiment reveals remarkable similarities. The most notable difference between the two years is the magnitude of the isotachs and the SST's. The isotachs of the 1976 overall mean wind (Fig. 19a) and the mean V_T-component analysis (Fig. 19b) average about 2 m s^{-1} greater than corresponding 1977 values. To investigate the causes for these differences, discrepancies due to observation time were considered. These data are shown in Table 5.

The 1976 times were always later in the day. Monthly mean diurnal profiles of the surface V_T-component taken nearest these locations revealed a 2.2 m s^{-1} resultant change at the middle location but only 0.5 m s^{-1} and 0.7 m s^{-1} changes at the other two sites. Thus, only a portion

Table 5

Average time differences of aircraft passage over specified locations between 1976 and 1977

Location		Time difference (hours:minutes)
15°10'S	75°22'W	1:43
14°56'S	75°32'W	2:09
14°46'S	75°49'W	2:34

of the magnitude difference can be explained by changes in aircraft sampling times between the two years. The remaining differences are explained by slightly weaker winds on the days of the micro flights in 1977.

Except for a 3 m s^{-1} weaker value for the maximum onshore flow in 1977, the mean V_N-component analyses (Figs. 14 and 19c) are very similar. The mean SST analysis of 1976 (Fig. 19d) averages approximately 1.5°C colder. The cold plume off Cabo Nazca is more rounded in 1977 and less aligned with the bottom contours. Also, the SST in the bay north of Punta San Nicolas was 1.5°C colder in 1976, even though the tangential winds in that area were of the same magnitude. This would seem to imply that a topographical effect (i.e., cape effect) and a greater frequency of poleward currents during the 1977 experiment were dominate factors.

In keeping with the conventions of the 1976 analyses, areas with wind speeds exceeding 16 m s^{-1} are shaded on the

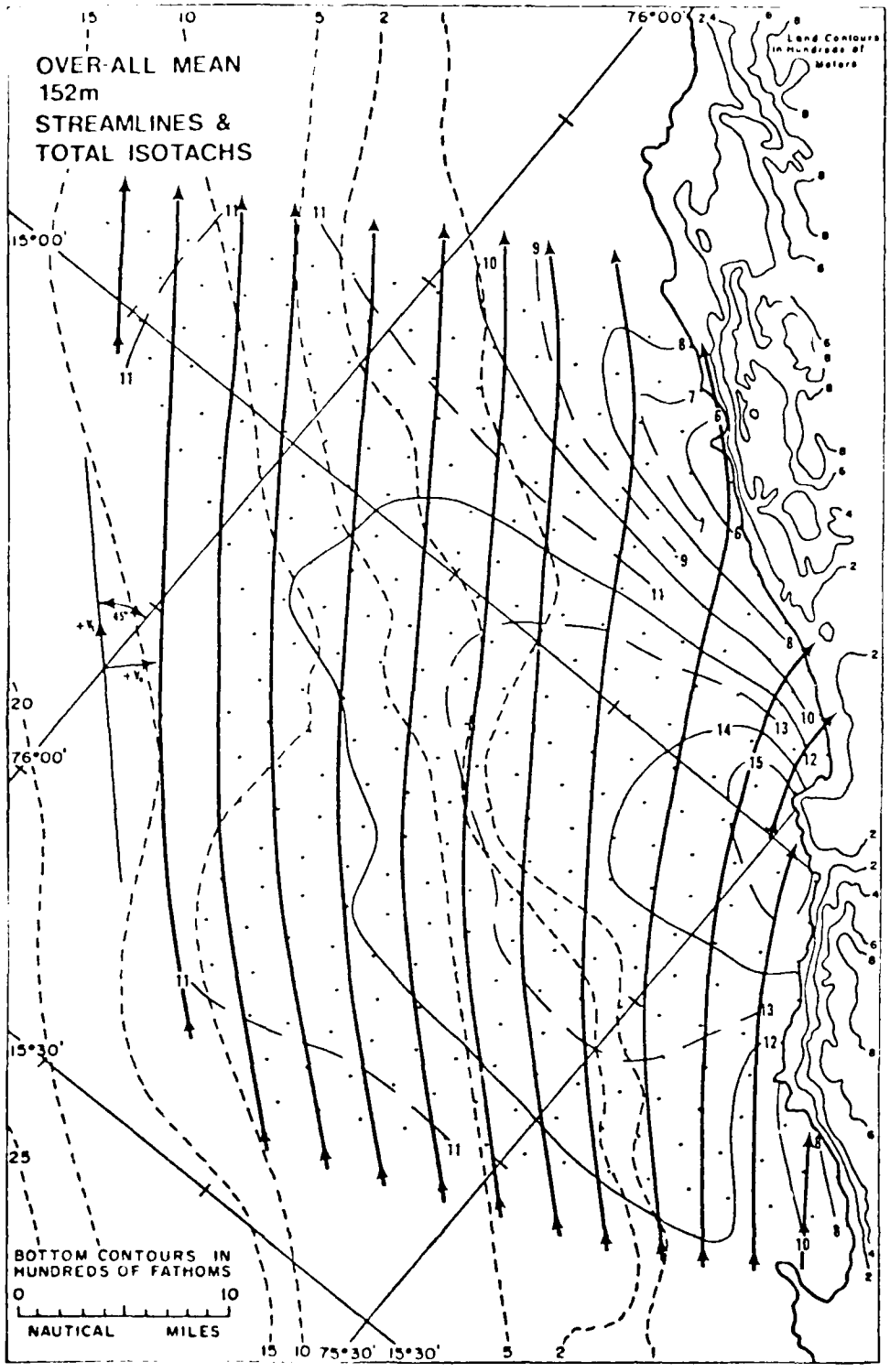

Fig. 19. (a) The mean streamline and total isotach patterns at 500 ft as recorded by an aircraft during March and April 1976.

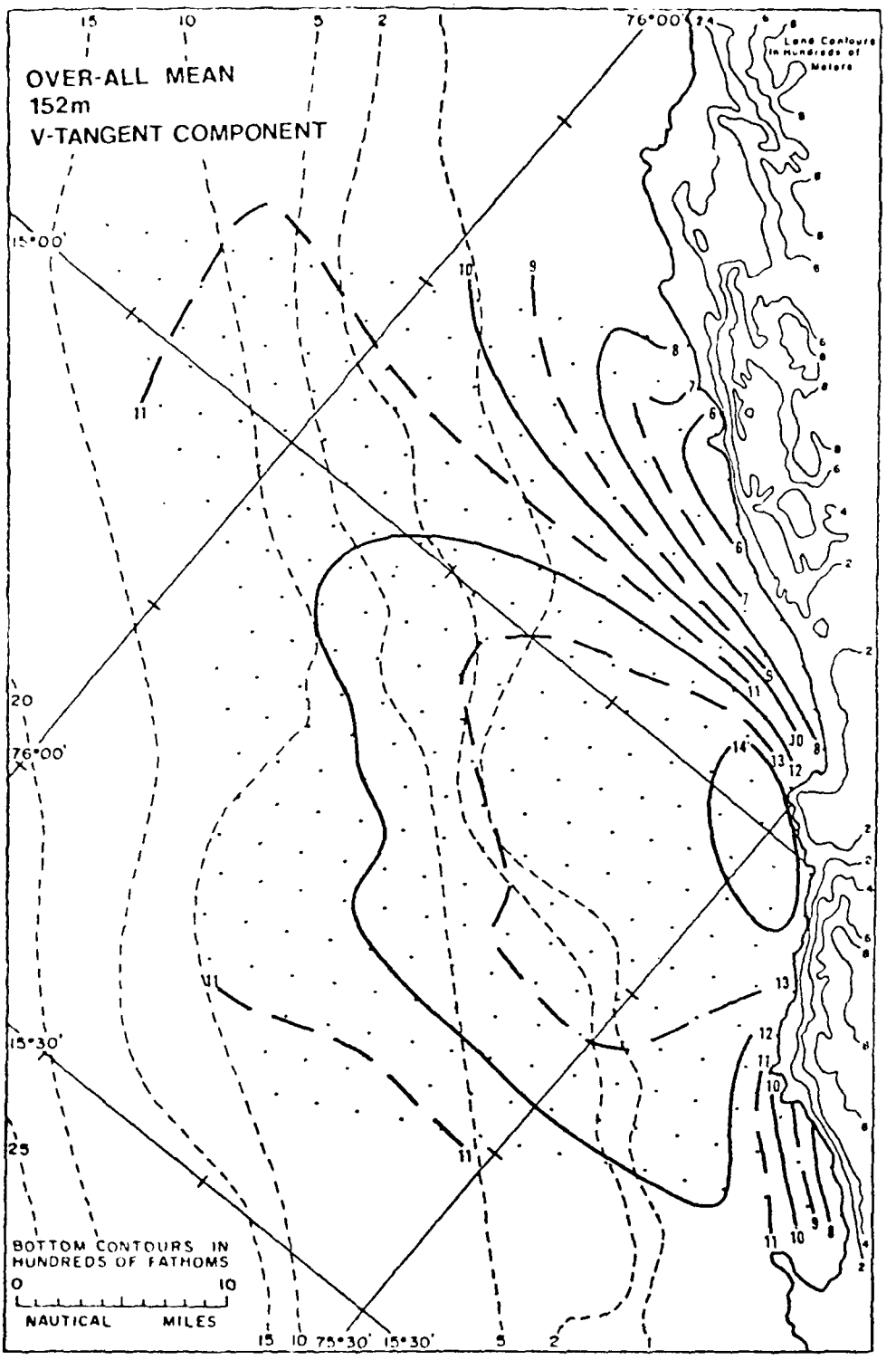

Fig. 19. (b) The mean V_T-component pattern at 500 ft as recorded by an aircraft during March and April 1976.

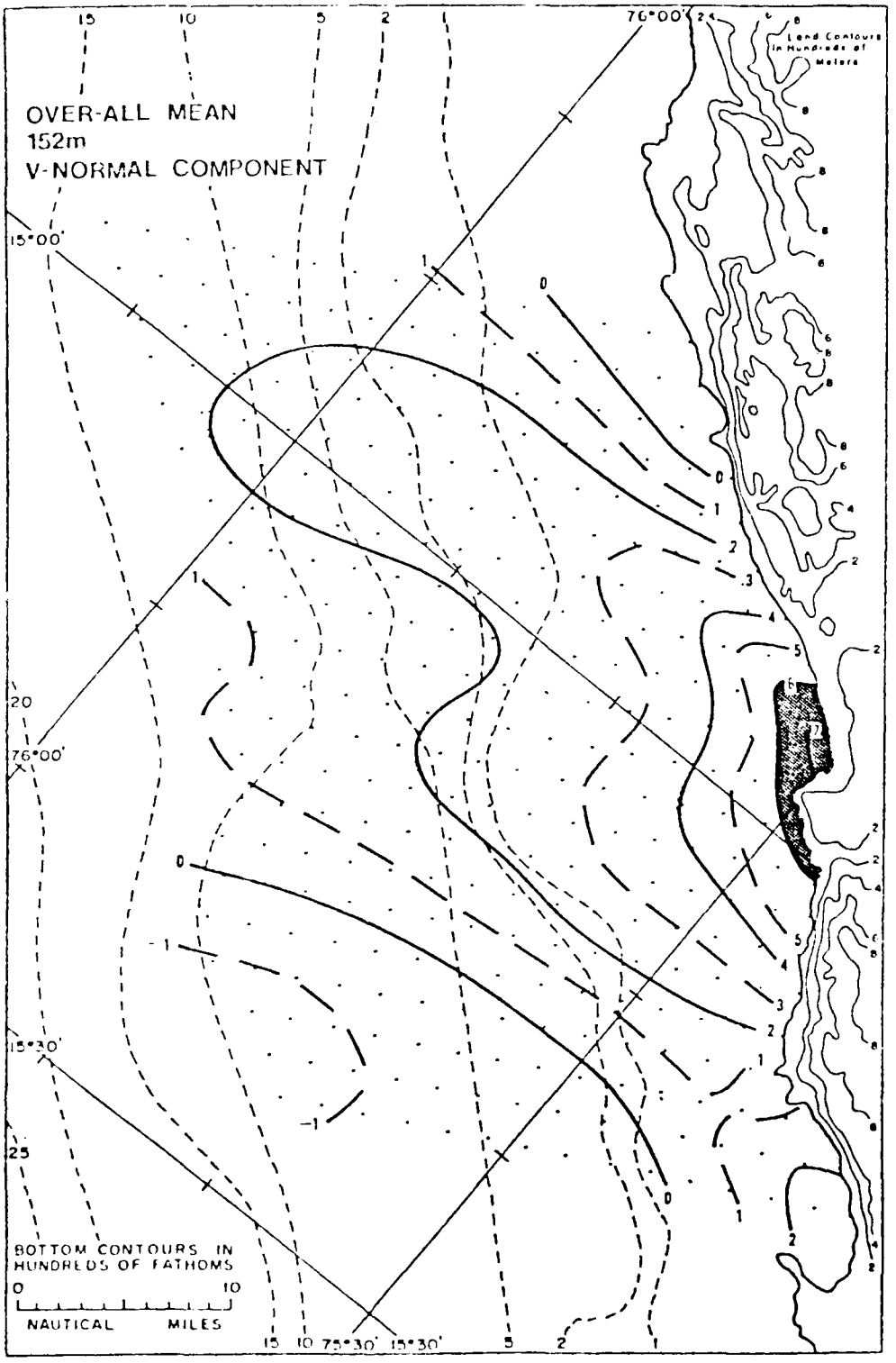

Fig. 19. (c) The mean V_N-component pattern at 500 ft as recorded by an aircraft during March and April 1976.

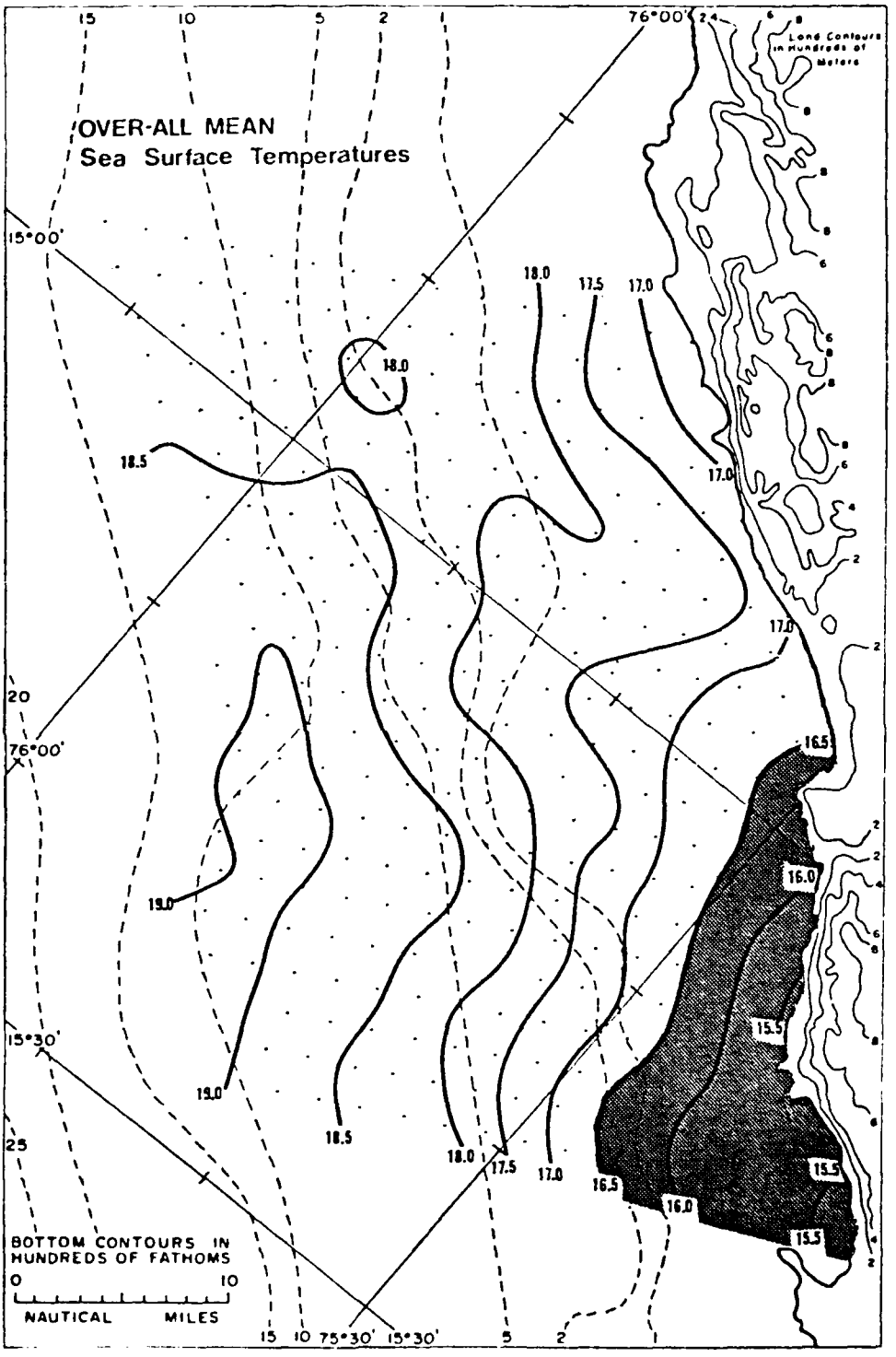

Fig. 19. (d) The mean sea surface temperature (SST) pattern as recorded by an aircraft during March and April 1976.

total wind and V_T-component charts. On the V_N-component analyses, areas of 6 m s^{-1} or greater are shaded.

A comparison of the offshore profiles (1976 profiles appear in Watson, 1978) also shows very good agreement between the two years. The location of the maximum V_T-component in 1977 (Fig. 17a) is 14 nm from the coast, as opposed to 12 nm in 1976. This agrees with the observation made earlier that as the tangential component strengthens, its maximum location moves closer to shore. Further, the onshore flow (sea breeze effect) along the Rio Grande valley is 1.5 m s^{-1} weaker in the 1977 alongshore profile. This could be due to the difference in the daily aircraft passage time over the area or to increased data coverage in 1977.

In general, the observations and results of JOINT II 1977 agree very well with those of 1976 (Watson, 1978 and Nanney, 1978). Considering some of the changes between the two years (flight pattern revisions, use of the flight "L" corrections, different flight times over the survey area, the increased data coverage of 1977, and large scale weather changes) the similarities in the results of this comparison study are surprising.

3.7 A comparison of weaker wind and stronger wind days

A comparison of the four flights with the weakest winds to the four flights with the strongest winds is investigated to emphasize the role of the wind as the forcing mechanism in

coastal upwelling. In 1976 three case studies, each based on a single flight, were done for a strong, weak, and transition regime. The choice of these flights was based on wind data recorded by coastal stations at San Juan and Lomitas. Figure 20 is a plot of the alongshore winds recorded at San Juan (land Station No.2), at the PSS buoy, and at the Parodia buoy (see Fig. 2 for locations) during March, April, and May of 1977 (see Brink, Smith, and Halpern; 1978). The abscissas are days in GMT, which is five hours later than local time. All winds have had high frequency fluctuations filtered out. In 1976 only one flight occurred during a weak wind period; the 1977 plots reveal several flights of each category. Therefore, the author chose to select four flights flown during weaker wind periods (flights 4, 31, 38, and 43) and four flown during stronger wind periods (flights 27, 28, 39, and 41) for comparison. The data from each set of four were then averaged for use in this study. A second method used to determine the selected flights was a comparison of the daily pressure gradients. An average ΔP of 6.9 mb was calculated between San Juan, Peru and a reference point at 25°S, 85°W during the 1977 experiment. The average ΔP for the weak wind flights was 5.2 mb as compared to 7.4 mb for the stronger wind flights. On the days of strong wind flights the subtropical high pressure system was normally located well offshore with a closed low pressure system centered inland and continuing down the South American coast.

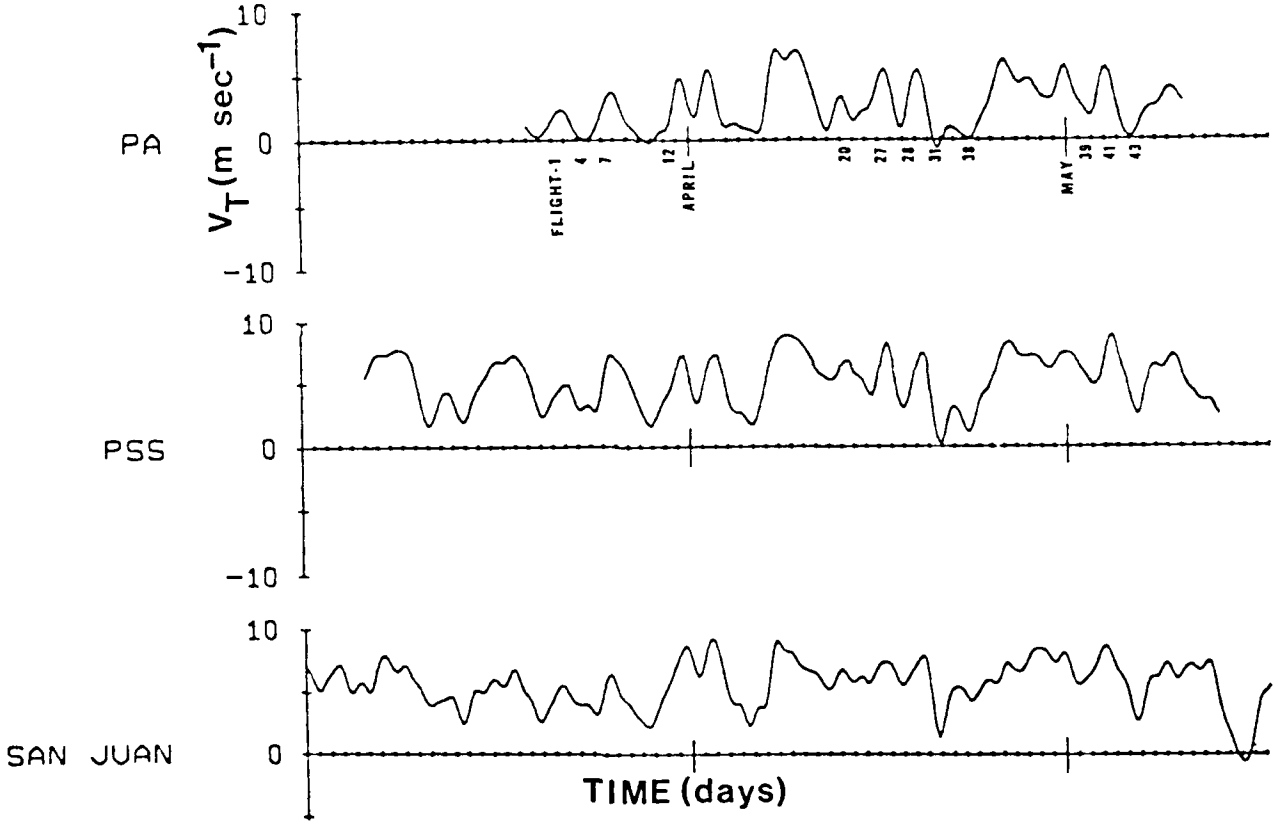

Fig. 20. Line plots of the alongshore wind components for the Parodia buoy (PA), the PSS buoy, and the San Juan coastal station during March, April, and May 1977.

During the weaker wind flights the high pressure had moved much closer to shore and dominated the western portion of the continent.

An examination of the mean charts for the two cases mainly verifies earlier observations. The mean wind and mean V_T-component charts for the strong case (Figs. A1-1 and A1-2) are again very similar in pattern. They show the usual pattern of a wind maximum just off Cabo Nazca with the gradient decreasing to a minimum near Punta de Olleros. The mean V_N-component analysis for the strong case (Fig. A1-3) shows maximum onshore flow up the Ica River valley with lesser positive flow north of Punta San Nicolas. Also, offshore flow is seen off Punta de Olleros and in the southwest part of the grid. The mean SST analysis (Fig. A1-4) shows the expected plume of cold temperatures originating just south of Cabo Nazca. The X's in Figs. A1-4 and A4-4 are where there were fewer than 2 of the 4 values available for analysis.

The importance of sustained strong winds combined with a strong surge of cold equatorward currents to the upwelling process is seen by comparing flight 22 in 1976 (Figs. A2-1 and A2-2) and flight 41 in 1977 (Figs. A3-1 and A3-2). These figures are V_T-component and SST analyses for the two flights. Flight 22 occurred after a sustained period of 16 days of stronger winds averaging 6.3 m s^{-1} at San Juan, Peru with a tangential wind maximum at 500 ft of 17 m s^{-1} on the day of

the flight. Flight 41 was flown after a sustained period of 10 days of stronger winds averaging 6.8 m s^{-1} at San Juan with a tangential wind maximum of 17 m s^{-1} at 500 ft on the day of the flight.

An interesting feature appears in the SST analyses for flights 22 and 41. It is readily apparent that the temperatures on the day of flight 22 are colder especially seaward of the mouth of the Ica River. This is a confusing observation as the V_T-components in this area are greater for flight 41. Since the winds alone do not seem to account for the colder temperatures, a study of the currents was necessary. The best comparison data available for the days of the two flights near the river mouth are given in Table 6. These data are from Enfield, Smith and Huyer (1978). Neglecting the small difference in location (4 nm) of the two buoys and the depth differences, in 1976 the currents were conducive to decreasing the already colder temperatures. Even more important is that Islaya had averaged a 13 cm s^{-1} northward flowing current at 116 m for four days prior to flight 22 while Parodia had averaged a poleward flow of 20 cm s^{-1} at 104 m for five days prior to flight 41. This period of cold northward flowing currents enhanced the results of the upwelling along and on the downstream side of each cape. Consequently, the combination of sustained strong tangential winds combined with an inflow of colder water below can increase the effect of upwelling considerably.

Table 6

Comparison of ocean current data between two sustained strong wind flights during the JOINT II experiment

Buoy	Location	Depth (meters)	Representative temp. (°C)	Representative current (cm s^{-1})
Isalaya I (1976)	15°S-75°39'W	66	14.75	-15
Parodia (1977)	14°56'S-75°40'W	64	15.0	-17
Isalaya I (1976)	15°S-75°39'W	116	14.25	+10
Parodia (1977)	14°56'S-75°40'W	104	14.75	-10

(-) tangential current flowing poleward

(+) tangential current flowing equatorward

The mean streamline and isotach patterns for the four weaker wind flights (Fig. A4-1) are very similar to the overall mean patterns except that the streamlines have less tangential component and the isotach maximum is 19 nm further offshore. The V_T-component analysis for the weak wind case (Fig. A4-2) closely resembles the mean isotach pattern for the weak flights. The normal wind component analysis for the weaker wind case (Fig. A4-3) has two clearly separated belts of weak onshore maxima. There is one just north of the Ica River valley and a second centered just south of the Rio Grande valley. The remainder of the grid shows less than 1 m s^{-1} of coastward flow. The SST pattern for the weak

flights (Fig. A4-4) generally agrees with the overall mean SST pattern. However, the weak flights show a more erratic pattern with approximately 0.5°C warmer surface water.

Selected profiles for these two extremes make possible some notable observations. The offshore V_N-component profiles averaged over various grid rows for the weak flights (Fig. 21) have little or no sea breeze effect. This finding remains true even when averaging over grid rows 7-11 (across the wide Ica River valley opening).

Figure 22, various offshore profiles of the V_N-component for the strong flights, is offered for comparison to Fig. 21. Although there is still no sea breeze effect along the northern rows 3-7 (due to the steep terrain), the other profiles show a well developed effect.

The alongshore profiles averaged over all rows for the two cases are shown in Fig. 23. The stronger wind flights reveal the flow entering from the south with an offshore component then onshore flow increases linearly to a maximum, as expected, at the Ica River. The same profile study for the weaker winds is not so straightforward. The onshore component increases to an initial maximum just south of the narrow Rio Grande valley; then the positive flow subsides until near the Rio Ica valley, where a second stronger onshore maximum is found. The maximum located between the Rio Grande and Punta Santa Ana is surprising due to the steep terrain along that area. Several interpretations could be offered based

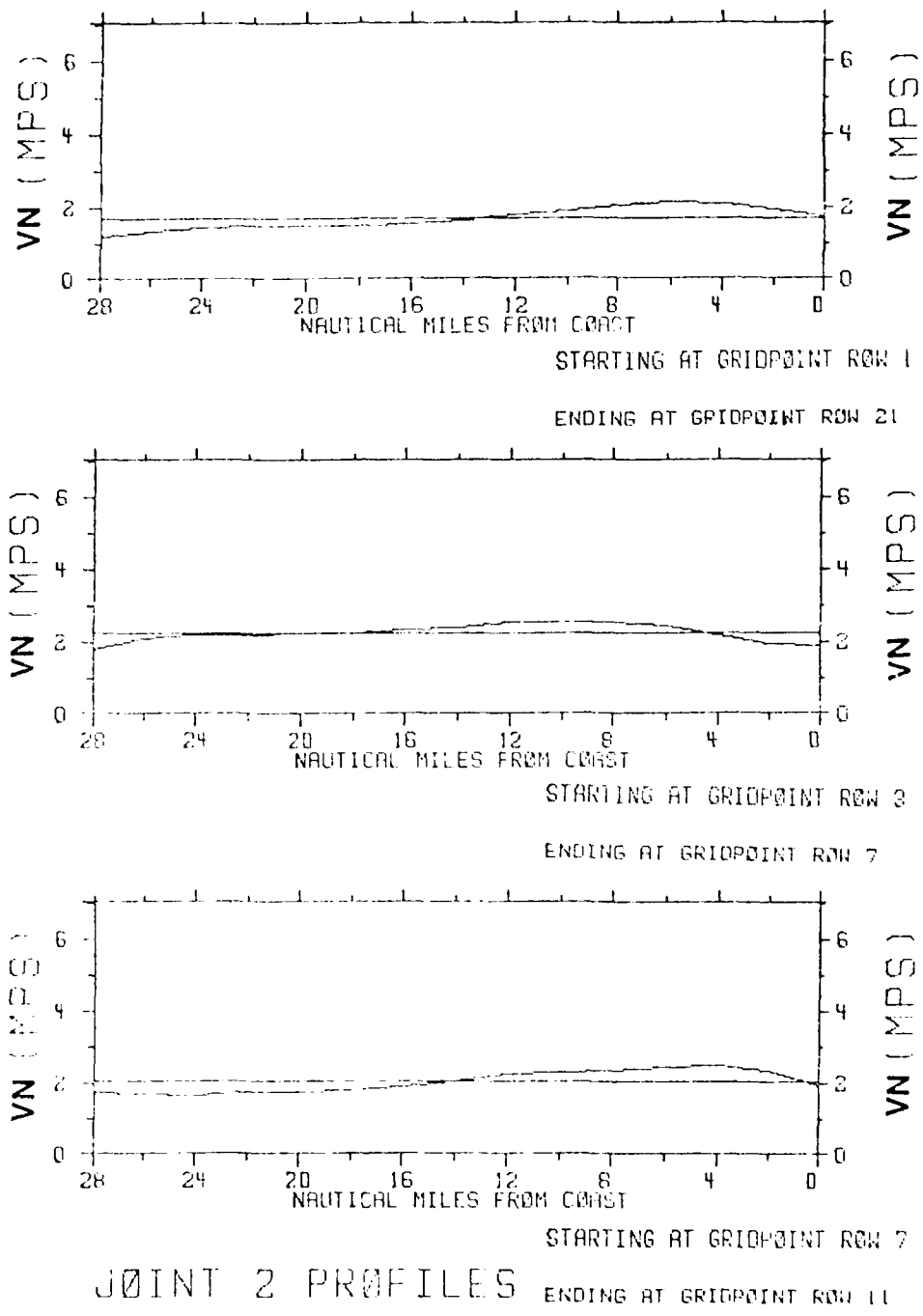

Fig. 21. Offshore profiles of the V_N-components averaged over all grid rows (top), over grid rows 3 through 7 (middle), and over grid rows 7 through 11 (bottom) for the four weakest wind microscale flights of 1977.

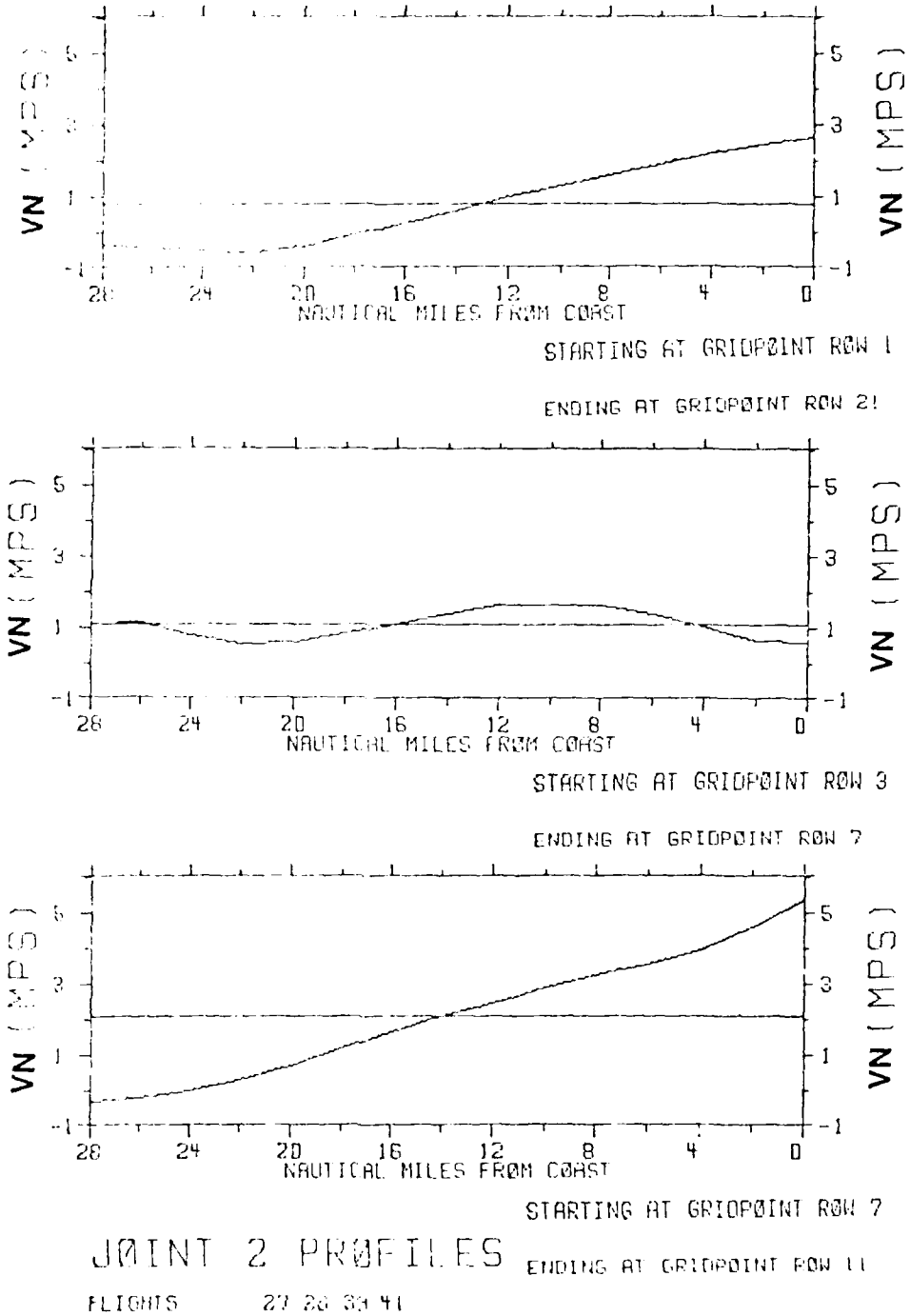

Fig. 22. Offshore profiles of the V_N-components averaged over all grid rows (top), over grid rows 3 through 7 (middle), and over grid rows 7 through 11 (bottom) for the four strongest wind microscale flights of 1977.

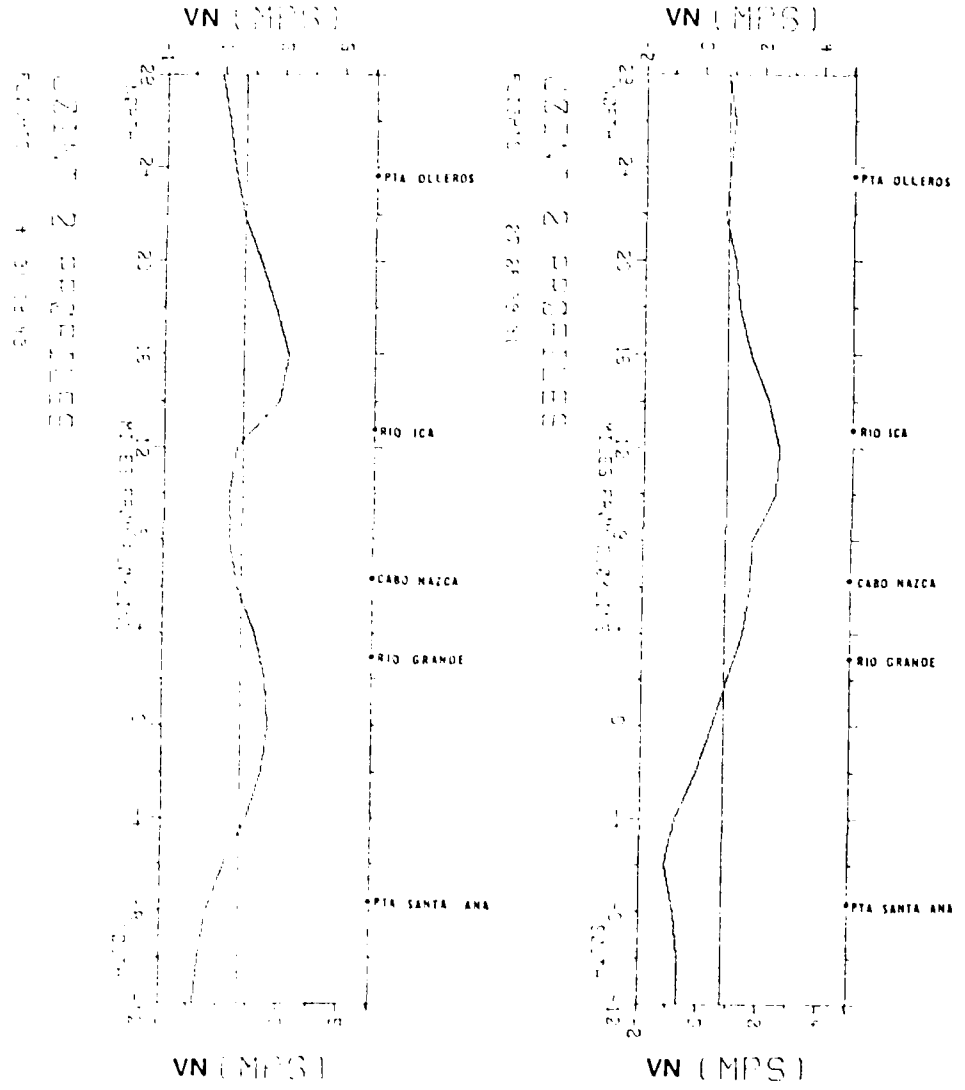

Fig. 23. Alongshore profiles of the V_N components averaged over all grid columns for the four strongest wind microscale flights (right) and four weakest wind microscale flights (left) of 1977.

on an increased dependence of the winds on local thermal effects; however, a satisfactory solution was not found.

It has been seen that a comparison of stronger wind flights with weaker ones revealed some interesting observations. In the next section the author will look specifically at a unique period in 1977 of weaker winds and investigate the sources of the seemingly disordered SST patterns during this period.

3.8 A study of upwelling during a light wind period

In the absence of strong wind forcing, the contribution of other factors to upwelling may be more easily seen. These factors include current flow over various bottom topographies (seamounds, valleys, etc); coastal cape effects; and internal ocean waves. An excellent opportunity to study upwelling during a period of very light winds occurred during JOINT II 1977. The period of this investigation was from 20-23 April 1977 which includes micro flights 31 and 38. Another look at Fig. 20 shows the weaker surface winds at various locations for this period. A similar period in 1976 (April 13-15) could not be used since it lacked SST data over most of the area.

The general synoptic situation (Fig. 24) shows the cause of the decreased winds. An extensive frontal system with associated lower pressures forced the weakened semi-permanent high coastward from its normal position. As the high moved toward the coast, it replaced the lower pressure commonly found inland and down the coast. This series of events led

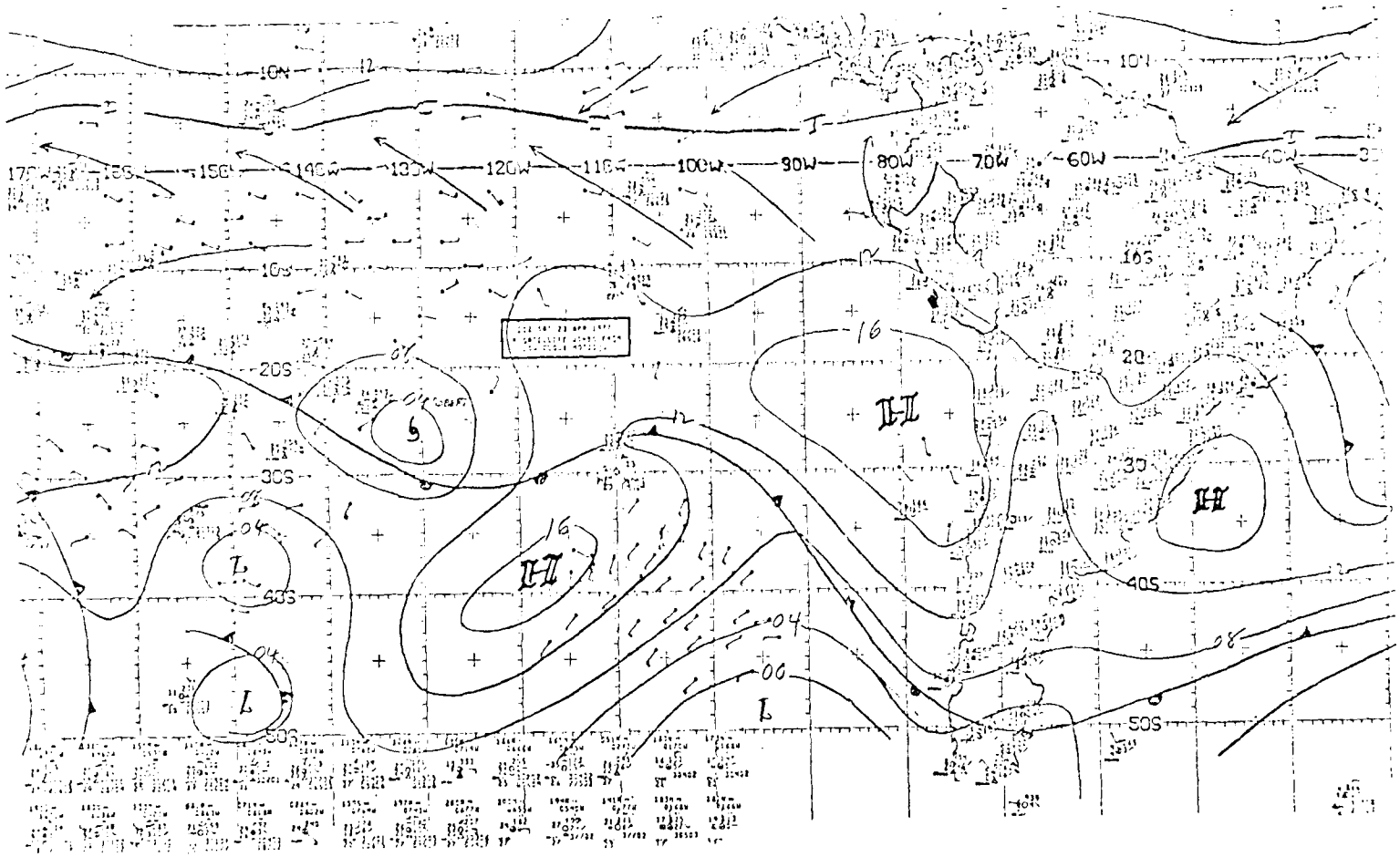

Fig. 24. Sea level pressure analysis via National Weather Service for 0000 GMT 23 April, 1977.

to a reduced pressure gradient over the JOINT II area. The ΔP between San Juan, Peru and 25°S-85°W was approximately 4.0 mb for flight 31 and 3.8 mb for flight 38. These gradients are considerably below the average ΔP of 6.9 mb for the 1977 experiment period. The existing conditions on April 20, 1977 are best summarized by this 1127 LST entry in the JOINT II aircraft observers log: "sea calm, many birds on the surface, water blue color, wind extremely light and variable."

The very light winds seen on flight 31 occurred rapidly following a week of reasonably strong winds averaging 6 m s^{-1} at Punta San Juan. The streamlines (Fig. A5-1) are very erratic with tight cyclonic curvature noted near Punta Santa Ana and across the Ica River mouth. The isotachs of both the total wind and the V_T-component analyses (Fig. A5-2) have relatively small maxima located well offshore to the southwest of Cabo Nazca and along a narrow east-west belt from the Ica River mouth out to 15°S-76°W. Negative tangential wind components are surprisingly present off Punta de Olleros and in the bay north of Punta San Nicolas. The V_N-component pattern (Fig. A5-3) displays a well-defined east-west orientation. There is quite strong onshore flow just north of the Ica River that quickly reverses to a maximum of offshore flow only 6 nm further south.

The streamlines of flight 38 (Fig. A6-1) are nearly tangential to the coast exhibiting only small variations. The isotach values of the total wind and of the tangential component (Fig. A6-2) are slightly less than the overall mean

values. The location of these maxima is considerably further offshore and to the north of the normal location. The V_N-component wind analysis (Fig. A6-3) is similar to the overall mean pattern, except slightly weaker in magnitude. The unexplained second maximum of onshore flow, characteristic of the weaker wind cases, is again seen between the Rio Grande and Punta Santa Ana. Thus, the analyzed 500 ft winds were weaker than normal during the period of interest.

To study the effect of this reduced wind forcing, the SST patterns for the two flights are examined. An initial inspection of the SST analyses of flights 31 (Fig. 25a) and 38 (Fig. 25b) shows considerably different patterns on the two days. Noticeably absent is the characteristic cold plume off Cabo Nazca. These differences are due to several factors; the most important of which is the ocean currents. Included in Figs. 25a and 25b are vector arrows pointing in the direction of current flow at various depths (the depth is given in meters at the head of each arrow) for the given day. These values were daily averages taken from filtered time series buoy data contained in Brink, Smith, and Halpern (1978). Due to the limited amount of available ocean current observations, several assumed current directions must be made. Also the newer bottom contours, discussed earlier in this report, are a valuable aid in this discussion.

An important factor in the analysis of the SST pattern for flight 31 is that the observations were taken less than

12-15 hours after the winds subsided. Accordingly, this increases the importance of advective processes in explaining the pattern. Advected distances can only be estimated, again owing to the lack of ocean current data. Flight 28 was flown two days prior to flight 31, and the SST analysis on that mission (Fig. 26) resembled the overall mean pattern. It is assumed that a similar pattern existed at the time that the winds abated. Referring to Fig. 25a, horizontal advection by the prevailing poleward currents along with some overall warming would account for the strength and arrangement of most of the northern half of the analysis. The colder area enclosed by the 18°C isotherm along the coast off Punta de Olleros and the 19.5°C warm pocket north of Cabo Nazca are most likely due to both a cape effect and advection. The cold minimum seaward of the Ica River valley is primarily a result of equatorward movement of the cold plume that was just to the south. A second contributing factor is the poleward currents flowing up a slight rise, depicted as a small seaward curvature in the 100 m contour. Also, the warm center just to the west of this rise is due to downwelling. Finally, the cold minimum offshore of Punta Santa Ana is a good example of the northward flowing currents swirling around and over the steep seamound. A prominent feature of flight 28 is the cold (16.5°C) plume along the coast. The disappearance of this plume (Fig. 25a) and the warmer temperatures in the northwest portion of the area demonstrate how quickly the surface values increase when the winds

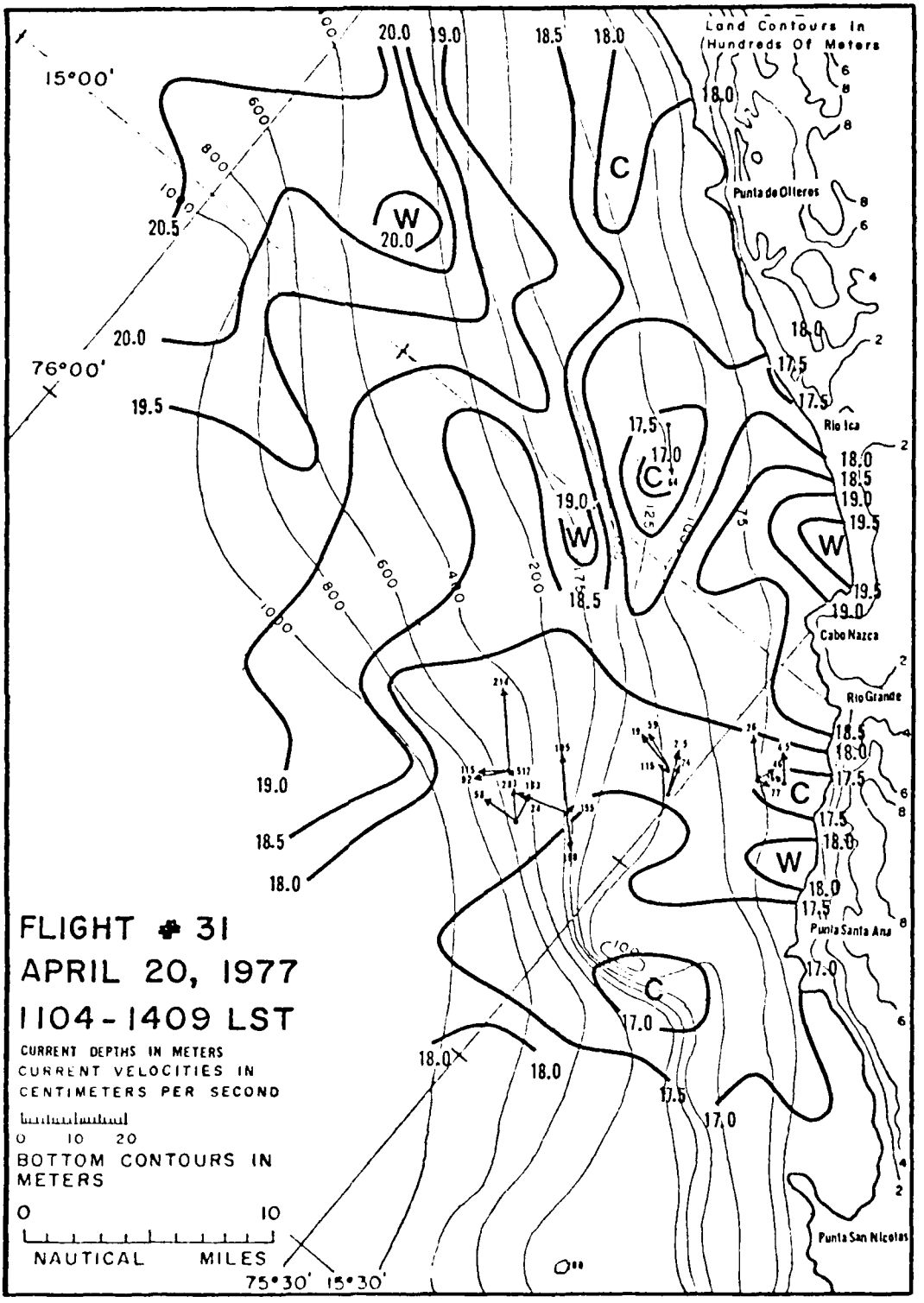

Fig. 25. (a) SST analysis for flight 31 and ocean current vectors for April 20, 1977.

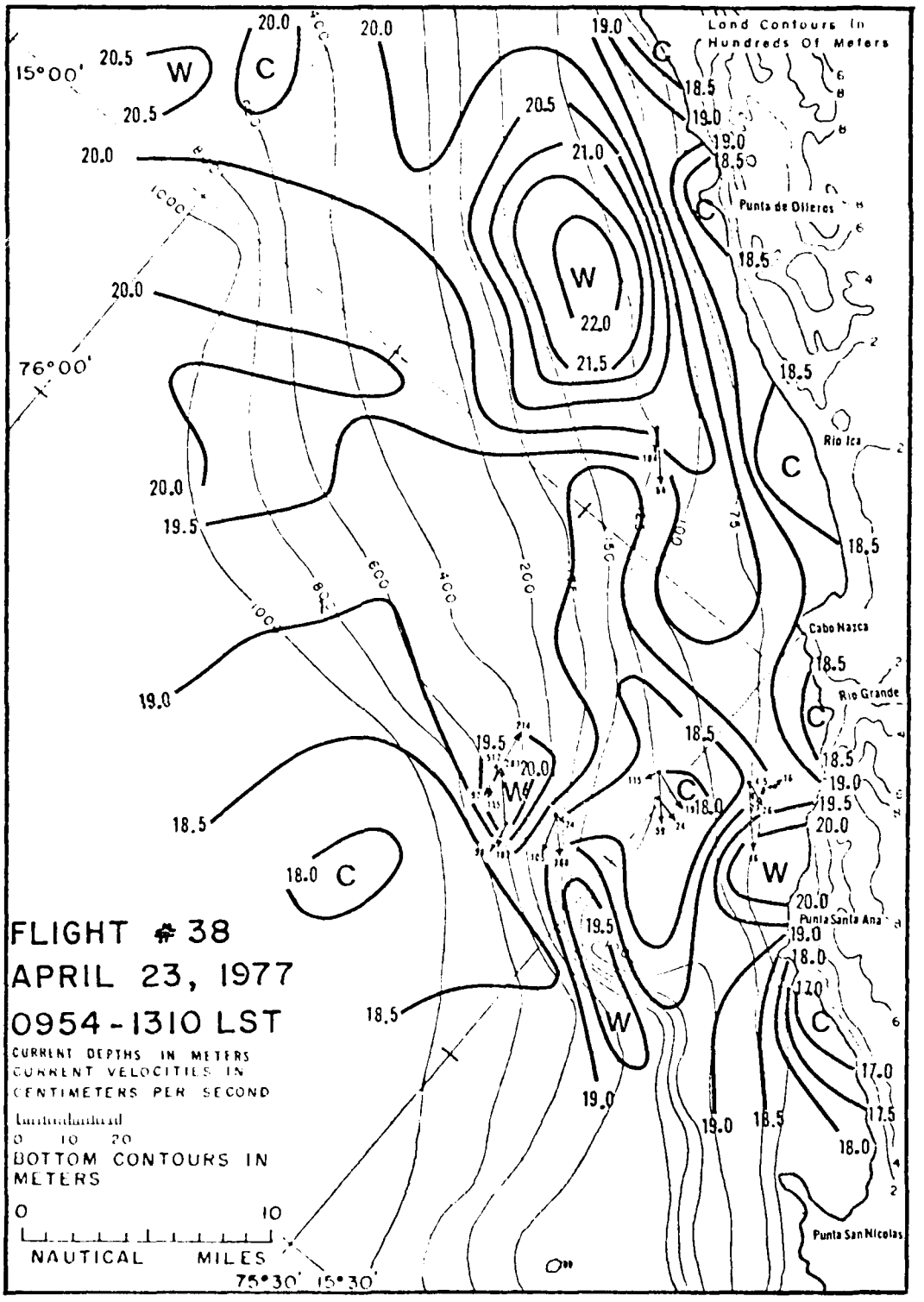

Fig. 25. (b) SST analysis for flight 38 and ocean current vectors for April 23, 1977.

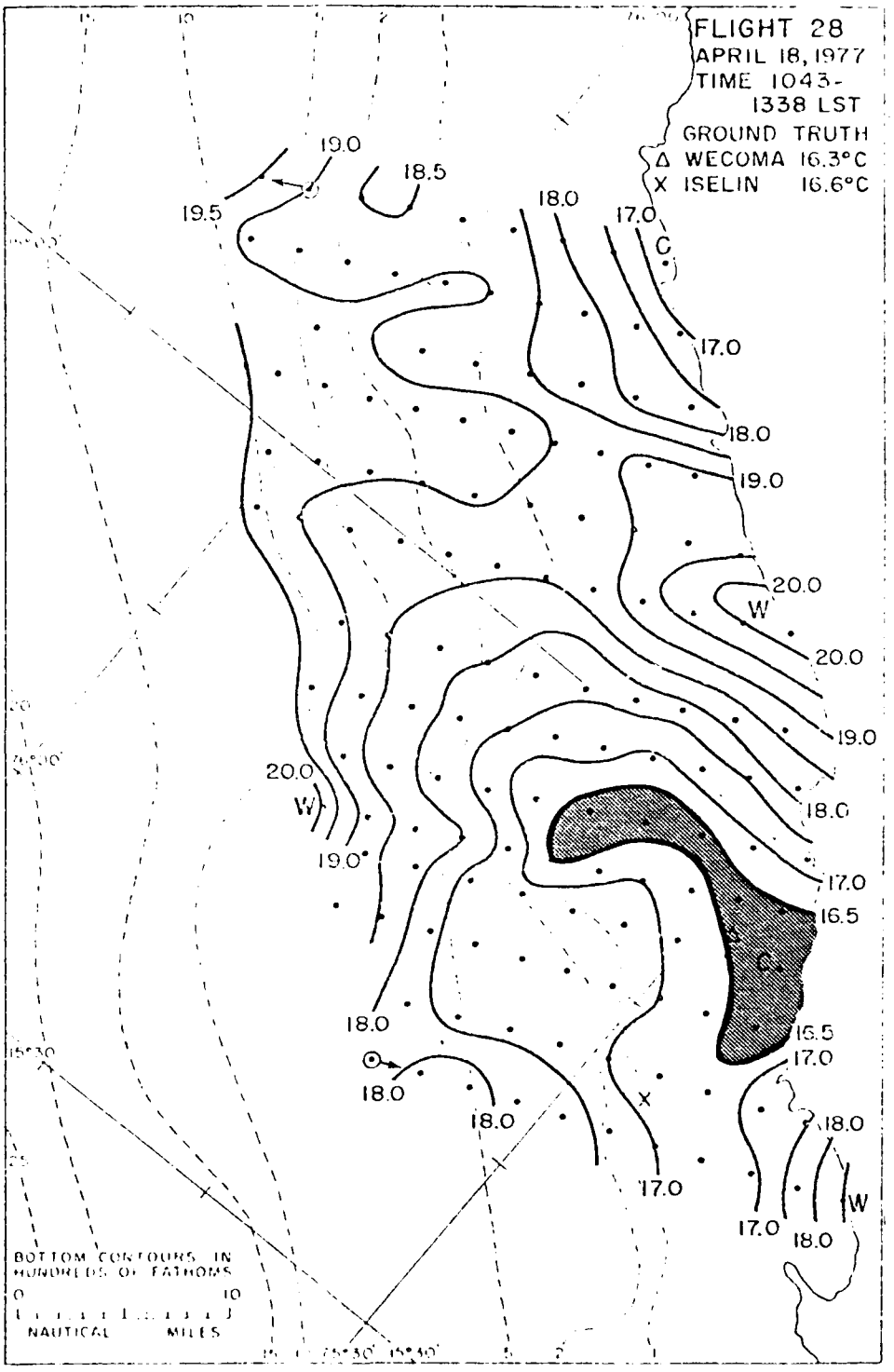

Fig. 26. SST analysis for flight 28 (from Stuart and Bates, 1977).

slacken and mixing is reduced.

The effect of a prolonged period of light winds is evident when considering that the warm center (22°C) in the top of Fig. 25b is the warmest value recorded for any flight in either 1976 or 1977. Several possible causes for this SST can be eliminated. Advection is not the primary factor since such warm water was not seen near there in Fig. 25a. The center is too far offshore to be a result of some coastal effect. Since the current flow parallels the bottom contours of the broad continental shelf and there are no nearby bottom irregularities, it is unlikely that downwelling due to botton topography is the principal cause. The best explanation is based on the realization that there still exists a wind stress factor at the surface. A review of the overall mean SST pattern will show that the warmest center is typically located near the warm maximum of flight 38. Also, a look at Fig. A6-1 shows that this warm maximum is located in the area of the weakest 500 ft winds. Thus, the surface wind stress is at a minimum reducing the upwelling in that location.

Each of the numerous SST maxima and minima within 5 nm of the coast are readily explained by the cape effect. An excellent example of this effect is seen off Punta Santa Ana. The poleward current flowing along the coast converges north of the cape with resultant downwelling. The opposite is true on the downstream of the cape where the concept of mass continuity requires that divergence occurring in the surface layer results in upwelling. The intensity of the cape effect

is evidenced by the fact that the cold (17°C) upwelled water south of the cape is the coldest observed over the analysis.

The southern part of the analysis area reveals a good example of flow over a seamound. Numerical models have shown that bottom features such as seamounds and valleys can induce upwelling with or without forcing at the surface (Preller, 1979). In this case the predominately poleward currents rise up over the 100 meter seamound causing the cold SST minimum. They also flow downward into the valleys to the south and the west of the peak causing downwelling and warmer surface temperatures at these two locations.

Unfortunately, there was an insufficient number of surface measured temperatures to check the validity of the aircraft measured SST's These analyzed sea surface temperatures were sensed by a PRT-5 (Barnes Precision Radiation Thermometer) carried aboard the aircraft. In comparing these values with corresponding ground truth data, the discrepancies averaged 0.5°C. The PRT-5 temperatures were consistently higher due to differences in the depth of the sampling. This value is in good agreement with a previous comparison by Nanney (1978) and is within the published instrument error tolerance of $\pm$0.5°C.

The increased emphasis during JOINT II 1977 on more complete aircraft data coverage on the micro flights increased the accuracy of this light wind comparison. This increased data network enabled the small scale features to be more

readily observed and more accurately interpreted.

A closer look at flights 31 and 38 in the absence of the usual strong wind forcing has revealed how other factors may play a role in the upwelling process. The wind, even when light, is the dominating factor. The noticeable absence of the cold plume in the SST analyses during this period is an example of the relevance of the wind to the upwelling process. The direction of the current flow, causing a resultant change in the water temperature, must be considered; especially during sustained periods of weaker winds. Advection becomes more of a factor, especially when winds have abated quickly. The current flow around bottom and coastal features is an ever present factor in coastal upwelling. The most important of these topographical effects seems to be flow around capes and over seamounds. The cape effect usually only extends 4-5 nm from the coast, while a seamound can be a factor at greater distances. A more accurate understanding of the upwelling phenomenon will require more extensive current data.

It has been proposed that internal Kelvin waves propagate poleward and can serve to enhance upwelling along the Peruvian coast (Smith, 1978). These waves are thought to influence only the alongshore component of the ocean currents and to have about a two day period. Some evidence of this is present in the JOINT II data of 1977 and could have been a strong factor in this lighter wind period. Numerical models using a variable tangential wind component and more

accurate topographical features are showing good prognostic results. Continuing advancements are possible with more inclusive numerical models and through intensive studies of internal waves.

CHAPTER IV

SUMMARY AND CONCLUSIONS

The two-dimensional, horizontal analyses of low-level (500 ft) mesoscale winds and SST's for the JOINT II 1977 experiment generally confirm the results of a similar experiment in 1976. In 1977 the wind speeds were slightly less and the SST's warmer than those of the previous year. This was found to be partly due to an average two-hour earlier flight time and to ligher winds on the days of the micro flights in 1977. The consistency of the prevailing southeasterly winds along the Peruvian coast reduces the effect of such temporal changes. This consistency is due to the character of the South Pacific Anticyclone. The strength and permanency of this large-scale feature reduces the number of synoptic changes that have complicated experiments in other areas.

A direct relationship between the low-level wind and the SST was observed when the wind at 500 ft exceeded 13 m s^{-1} during the JOINT II experiment. Such a relationship was not seen in previous studies by Elliott (1974) off Oregon or by Duval (1977) off northwest Africa. The continually changing synoptic situation in these other areas made observation of any direct relationship difficult. Such clear

evidence of such a relationship is surprising since many factors could influence or change the result. These include the response time of the SST's to the wind, the ocean currents, the thermocline depth, the synoptic situation, and the use of the 500 ft wind to represent surface forcing throughout the area. In spite of these limitations, a reasonably good relationship was found between the maximum V_T-component and the minimum (coldest) SST values. A similar finding was that as the tangential wind components decreased north of the Ica River, the SST's of that area became warmer. It was also seen that as the wind speeds increased (decreased), the location of the isotach maximum and the SST minimum moved closer to (further from) the coast. This is an expected result, since increased winds would overcome more of the orographic frictional force and the maximum value would relocate nearer the shore. Since the alongshore wind component has also increased, this component acting over a smaller area would increase the Ekman transport and cause stronger upwelling. Accompanying the coastward displacement of the isotach maximum the vertical profiles of wind data showed a more intense jet at a lower level for the buoy location nearer the coast. Further evidence of a relationship between the winds and the SST's is found by observing comparable line plots of alongshore wind velocity and of SST for various locations in the JOINT II area (see Brink, Smith, and Halpern; 1978). All of these observations verify that the wind is the dominate factor in upwelling off Peru.

Profiles of the wind and SST data show several interesting features. The coldest SST's were consistently located at or near the coast. An unexplained area of strong onshore flow was repeatedly seen between the Rio Grande and Punta Santa Ana on the days of weaker wind flights. There is an organized alongshore variability in the magnitude of the tangential wind component over this area. The SST's rise sharply in the western edge of the survey area. This would seem to indicate that most of the stronger upwelling is taking place in the 28 nm area nearest the coast.

The accuracy of the analyses over the gridded area was increased in 1977 by expanding the density of aircraft coverage, analyzing data from all legs of the flight track, and applying corrections to the data. These corrections came from flight patterns at the beginning and end of each micro flight. This resulted in the reduction of systematic errors in the resultant winds. On the inbound (outbound) legs, the INS computed wind directions were too large (small), and the speeds too small (large). These errors were found to occur when the TAS was sensed as lower than the actual value, and the discrepancies were larger when the winds were weaker than normal.

A period of reduced wind forcing due to lighter winds allowed an investigation of other upwelling causes. The weaker winds were a result of the coastward movement of the semipermanent high from its usual location thus reducing the

pressure gradient over the area. This gradient gives an indication of the overall wind strength, but the smaller scale thermal effect must also be considered. An SST pattern much changed from the mean was observed only 12 to 15 hours after the winds dropped off. The entire resultant analysis can be explained by factors other than the wind, which seems to indicate that the response time required for the cessation of upwelling due to the wind is less than 15 hours. This value is much less than the one-day response time indicated by Nanney (1978).

Although coastal upwelling is primarily driven by the wind, several other factors are seen to play important roles. Within 4 to 5 nm of the coast, the divergence and convergence caused by ocean currents flowing past coastal irregularities (cape effect) lead to warmer and colder SST's. Flow of the currents over ocean bottom features (up a seamound or down a valley) contribute to upwelling in some locations and downwelling in others. Horizontal advection of surface water is a factor in the varying SST patterns. Another cause that has been proposed is the enhancement of upwelling by poleward moving internal ocean waves (Kelvin waves). These waves could cause a sustained surge of cold water resulting in expanded areas of colder upwelled water in the surface layer. Existence of such a case was seen in the SST's of flight 22 in 1976 (see Section 3.7). Finally, the disappearance during the weaker wind period of the cold plume of SST's normally

AD-A090 634 AIR FORCE INST OF TECH WRIGHT-PATTERSON AFB OH F/G 8/3
AIRCRAFT DERIVED LOW LEVEL WINDS AND UPWELLING OFF THE PERUVIAN--ETC(U)
AUG 79 G L MOODY
UNCLASSIFIED AFIT-CI-79-195T NL

found seaward of Cabo Nazca, is evidence of the influence of the wind on the upwelling phenomenon.

Numerical modeling is only one area of research that could lead to more accurate forecasting of coastal upwelling events. Such models need to include the alongshore variability of the V_T-component of the wind, accurate bottom and coastal features, and thermodynamic considerations. Extensive ocean current data observations are required, if an accurate study of the contribution of these currents to upwelling is to be successful. Several days of continual observations are required to examine the response time of upwelling to daily changes in the wind forcing, possible nocturnal katabatic flow, and other diurnal effects. All of these suggested areas of research will assist the study of the importance of internal ocean waves to upwelling. Omega low frequency navigational systems could be utilized to increase the accuracy of aircraft data observations. These ideas and others will lead to a better understanding of the upwelling process and may someday lead to its successful prognostication.

APPENDIX

APPENDIX

The 500 ft (152 m) mean wind and SST analyses are presented for the strongest (Figs. A1-1,4) wind case and for the weakest (Figs. A4-1,4) wind case during 1977. Both cases contain maps of streamlines and total isotachs, V_T-component, V_N-component, and SST.

Selected 500 ft analyses are presented for two strong wind flights; flight 22 in 1976 (Figs. A2-1,3) and flight 41 in 1977 (Figs. A3-1,3). Both flights contain maps of V_T-component, SST, and total aircraft track.

Also, the 500 ft wind analyses are presented for two weak wind flights during JOINT II 1977; flight 31 (Figs. A5-1,4) and flight 38 (Figs. A6-1,4). Both flights contain maps of streamlines and total isotachs, V_T-component, V_N-component, and total aircraft track.

On the total aircraft track maps, dots represent each whole minute while times are printed every 15 minutes in local standard time (LST) along the track. The surface data are plotted on the mean maps when there were two or more observations available.

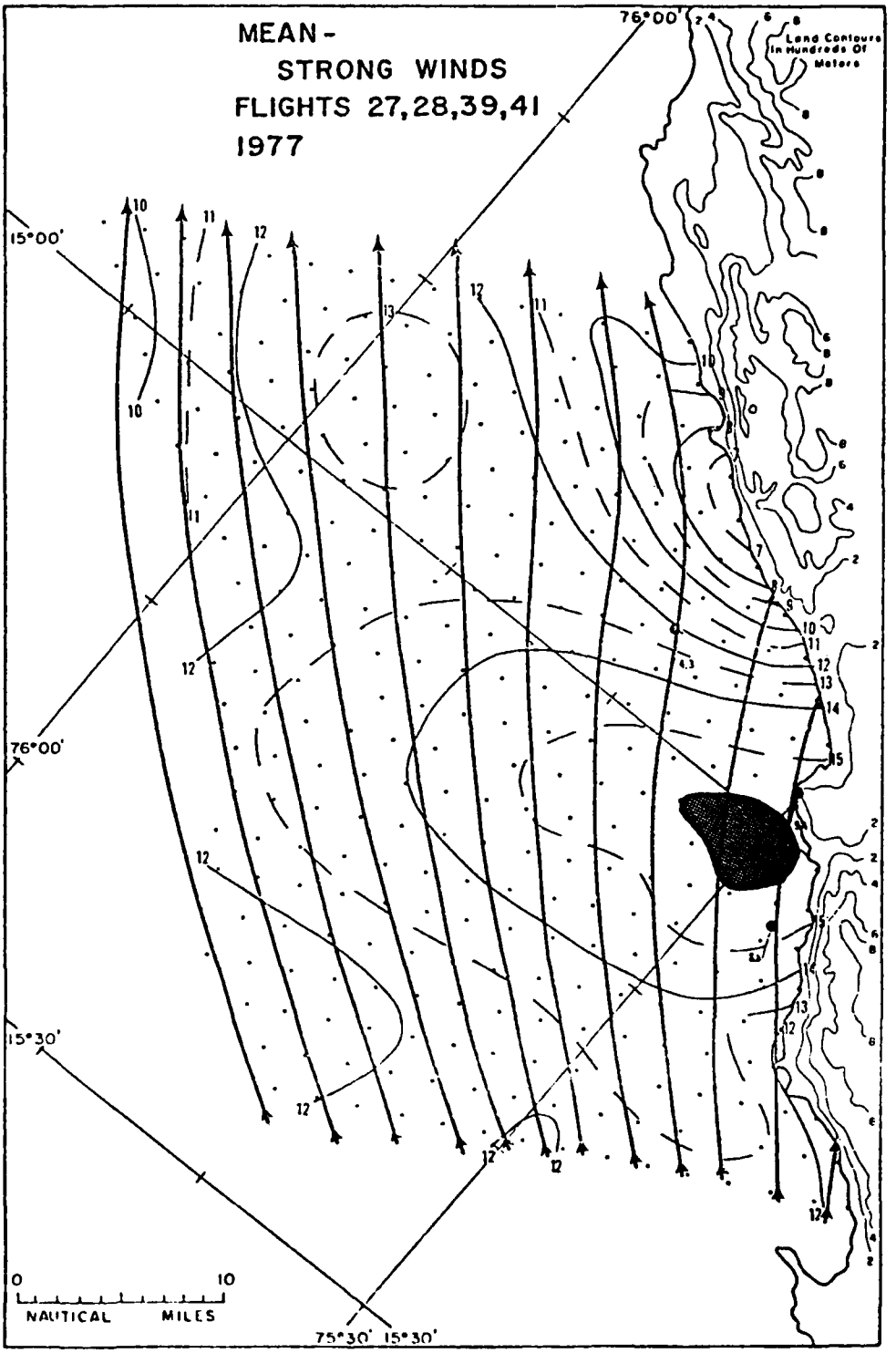

Fig. A1-1. The mean streamline and total isotach patterns at 500 ft for the strongest wind flights during March, April, and May 1977.

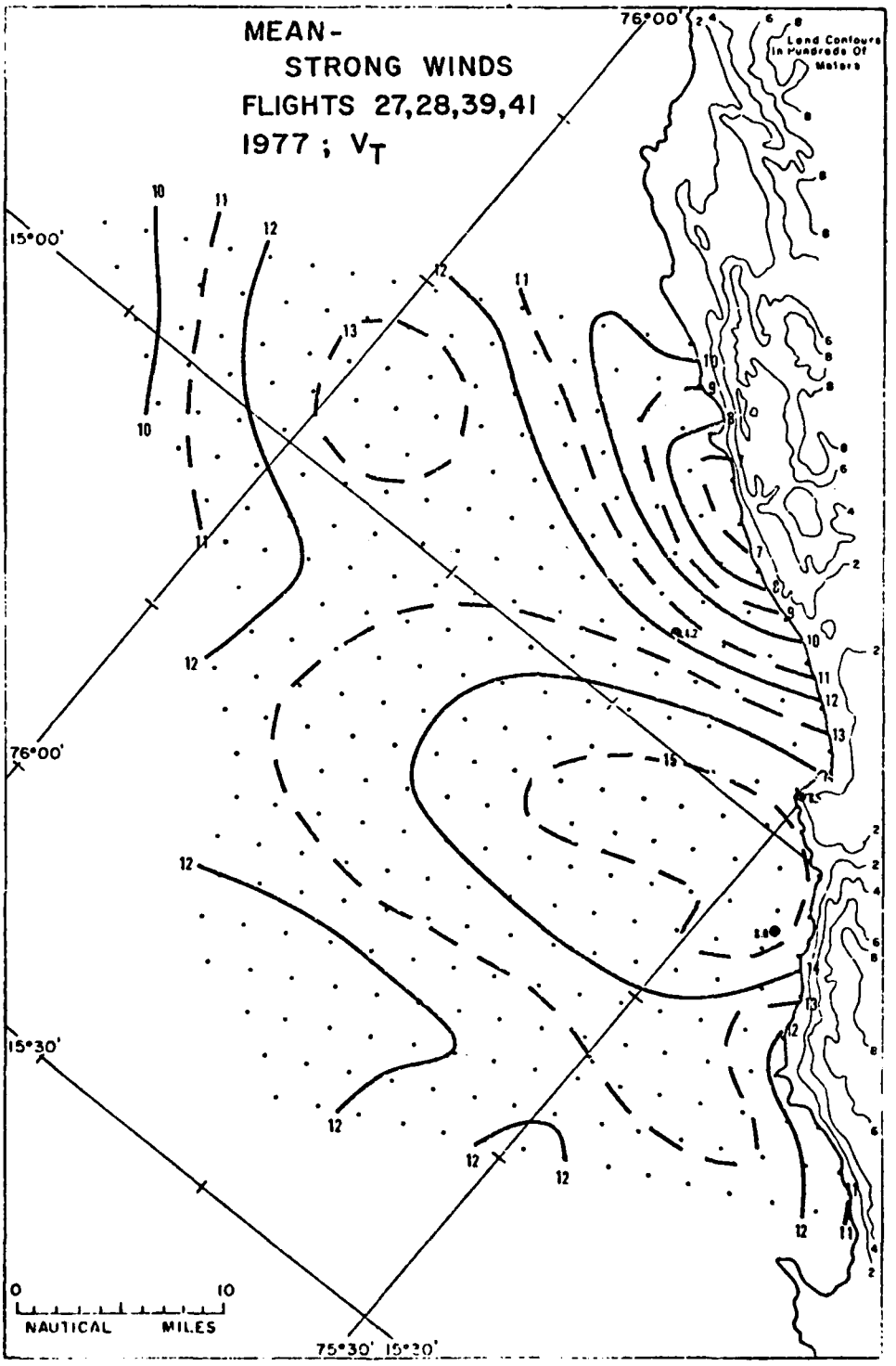

Fig. A1-2. The mean V_T-component pattern at 500 ft for the strongest wind flights during March, April, and May 1977.

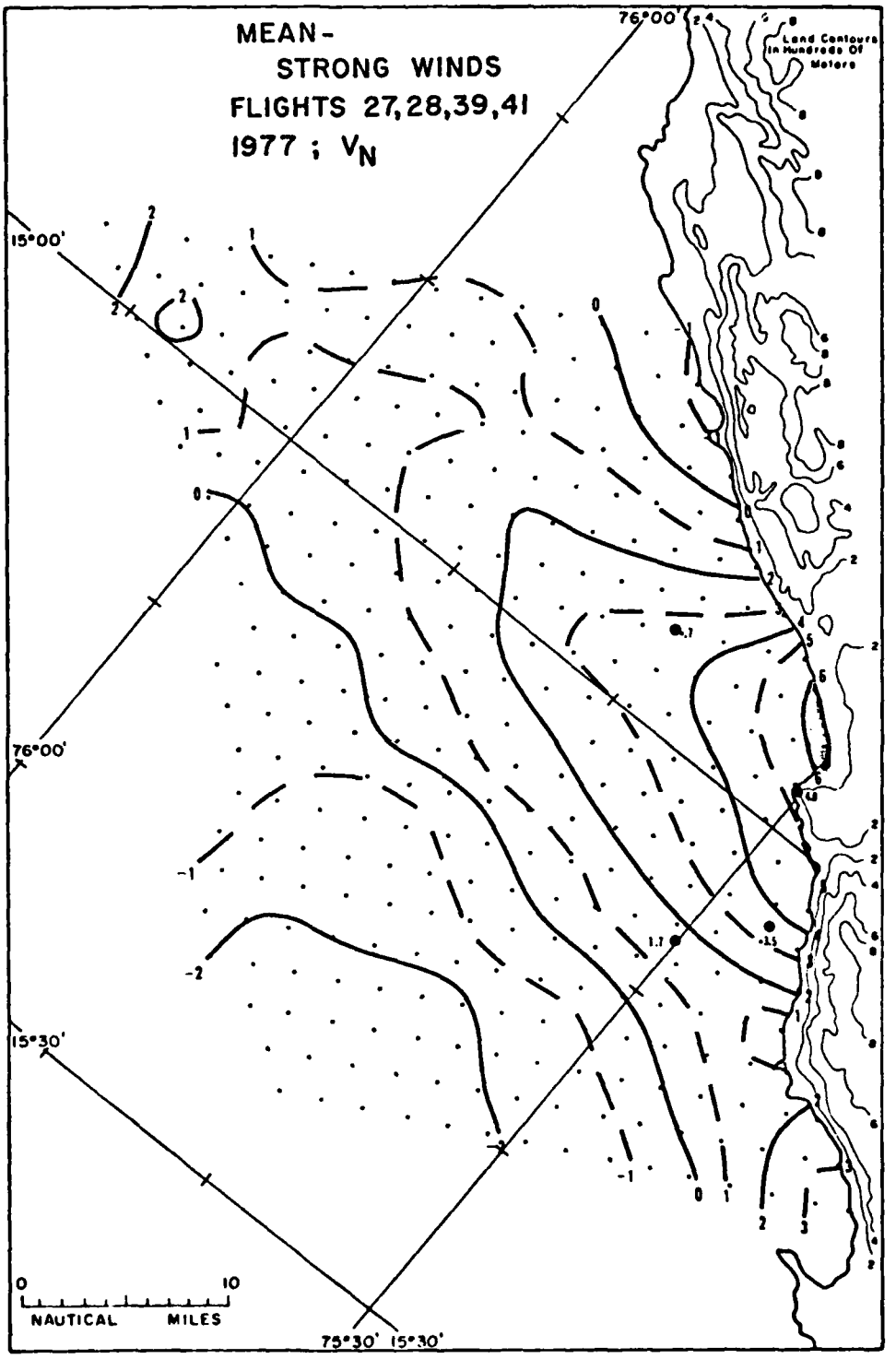

Fig. A1-3. The mean V_N-component pattern at 500 ft for the strongest wind flights during March, April, and May 1977.

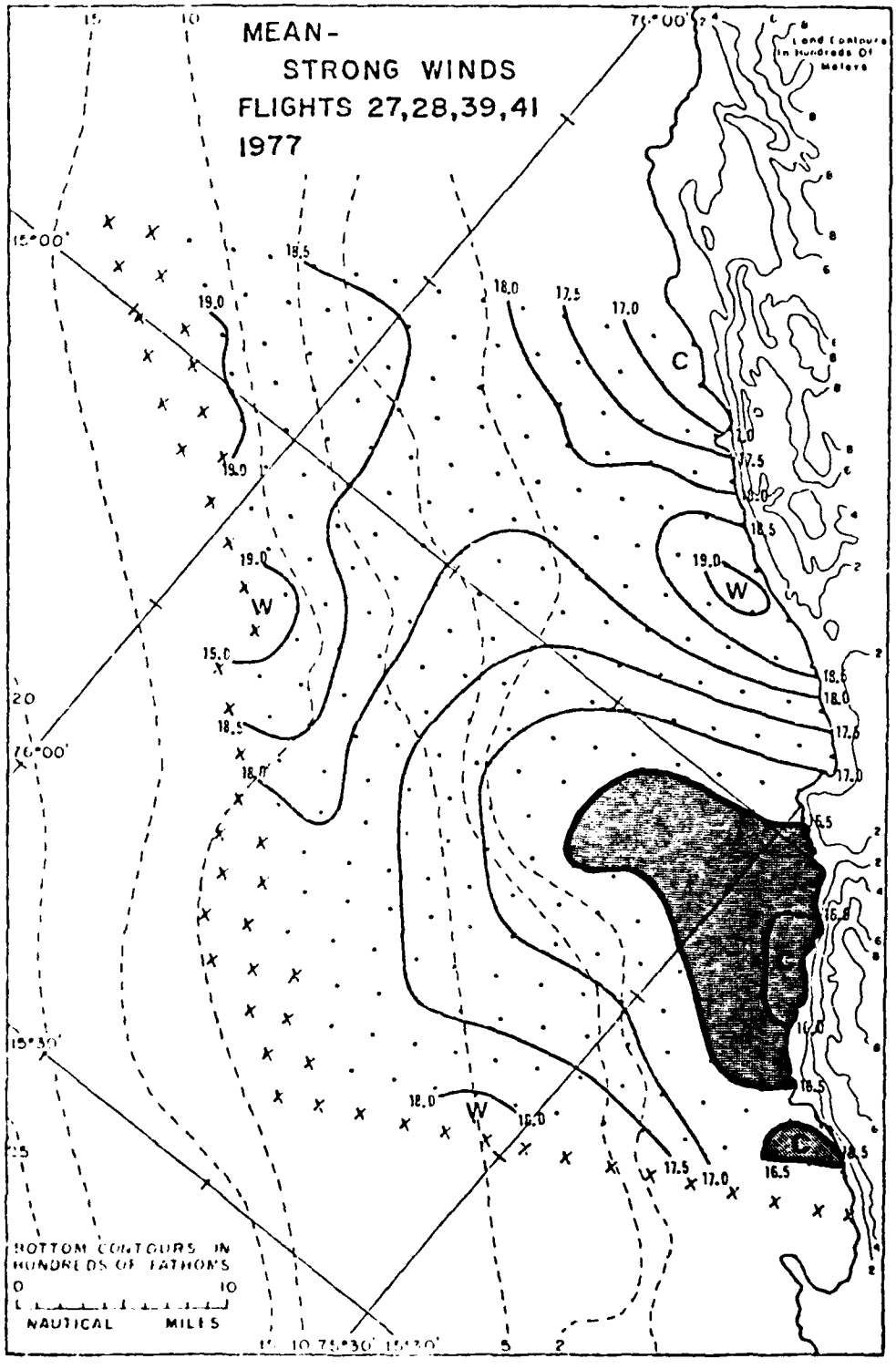

Fig. A1-4. The mean SST pattern for the strongest wind flights during March, April, and May 1977.

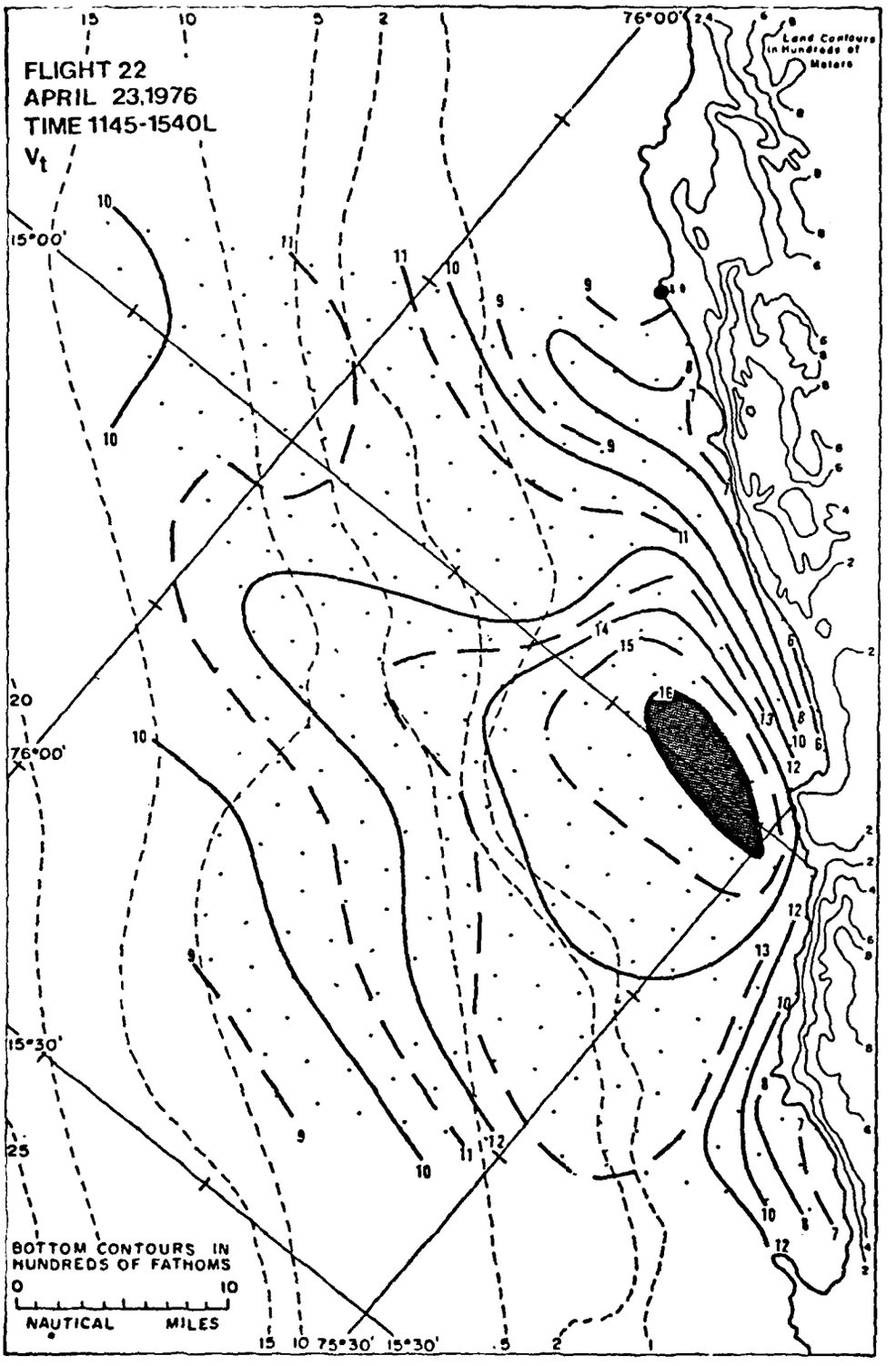

Fig. A2-1. The V_T-component pattern at 500 ft for flight 22 in 1976.

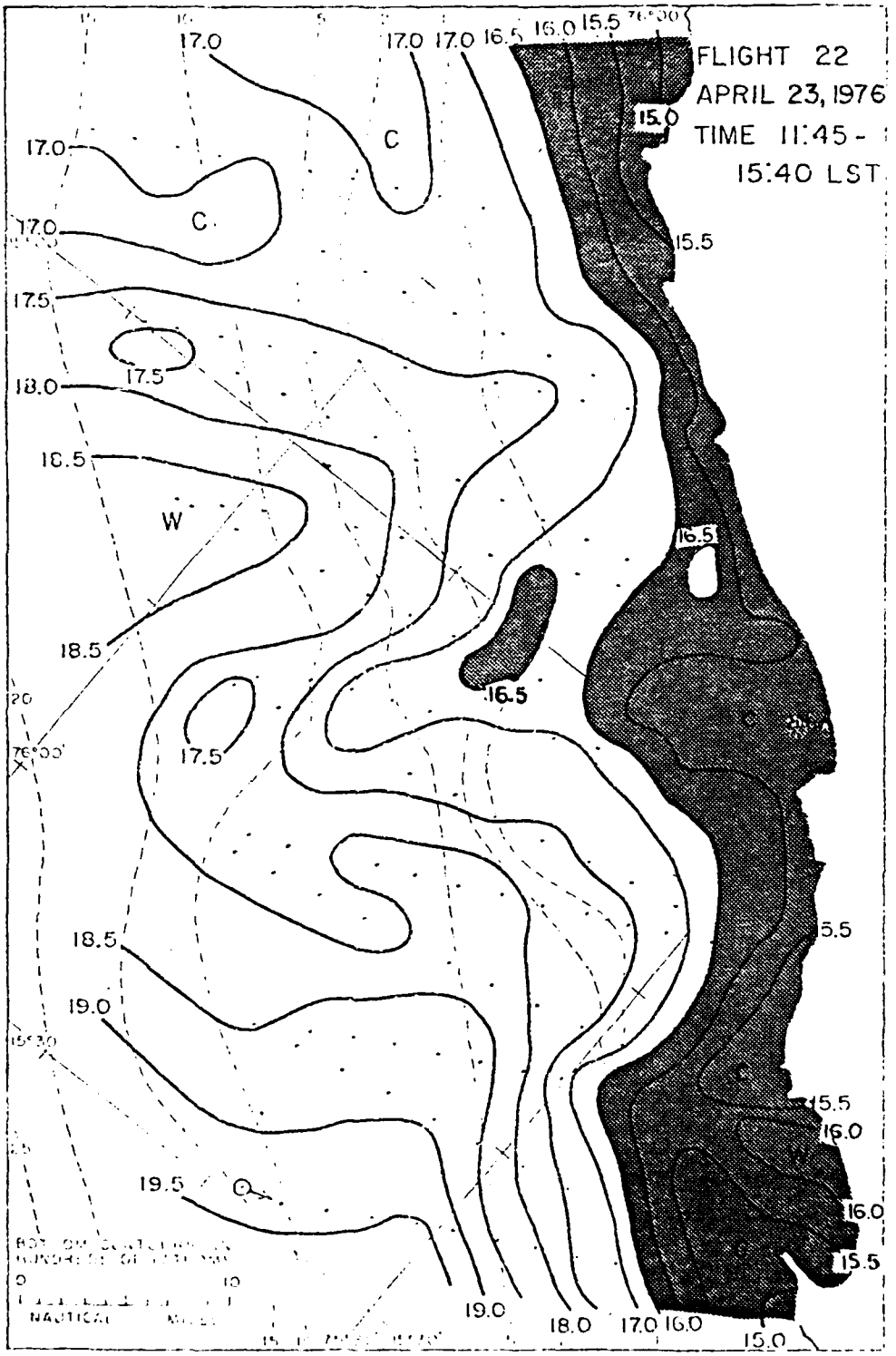

Fig. A2-2. The SST pattern for flight 22 in 1976.

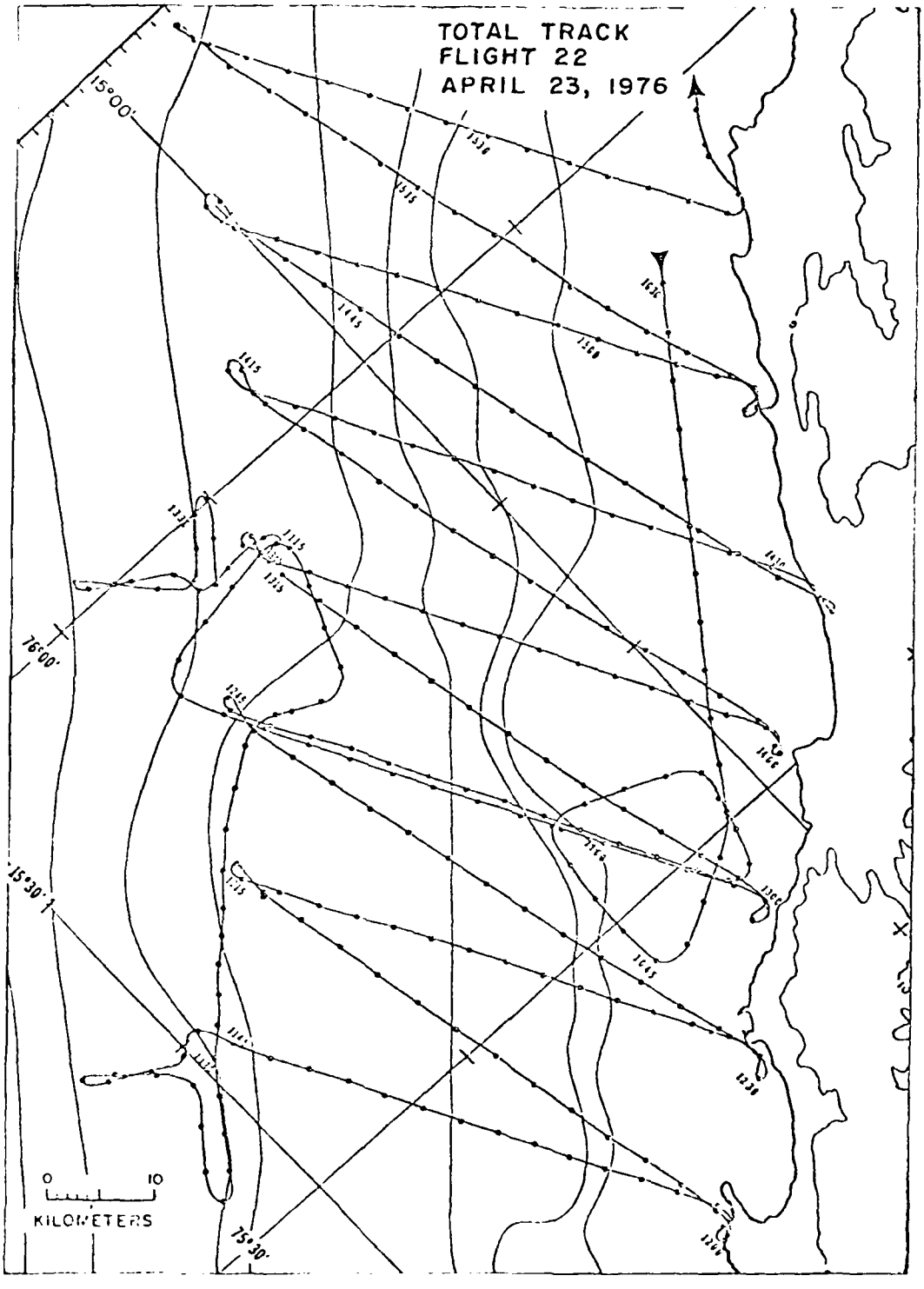

Fig. A2-3. The total aircraft track for flight 22 in 1976.

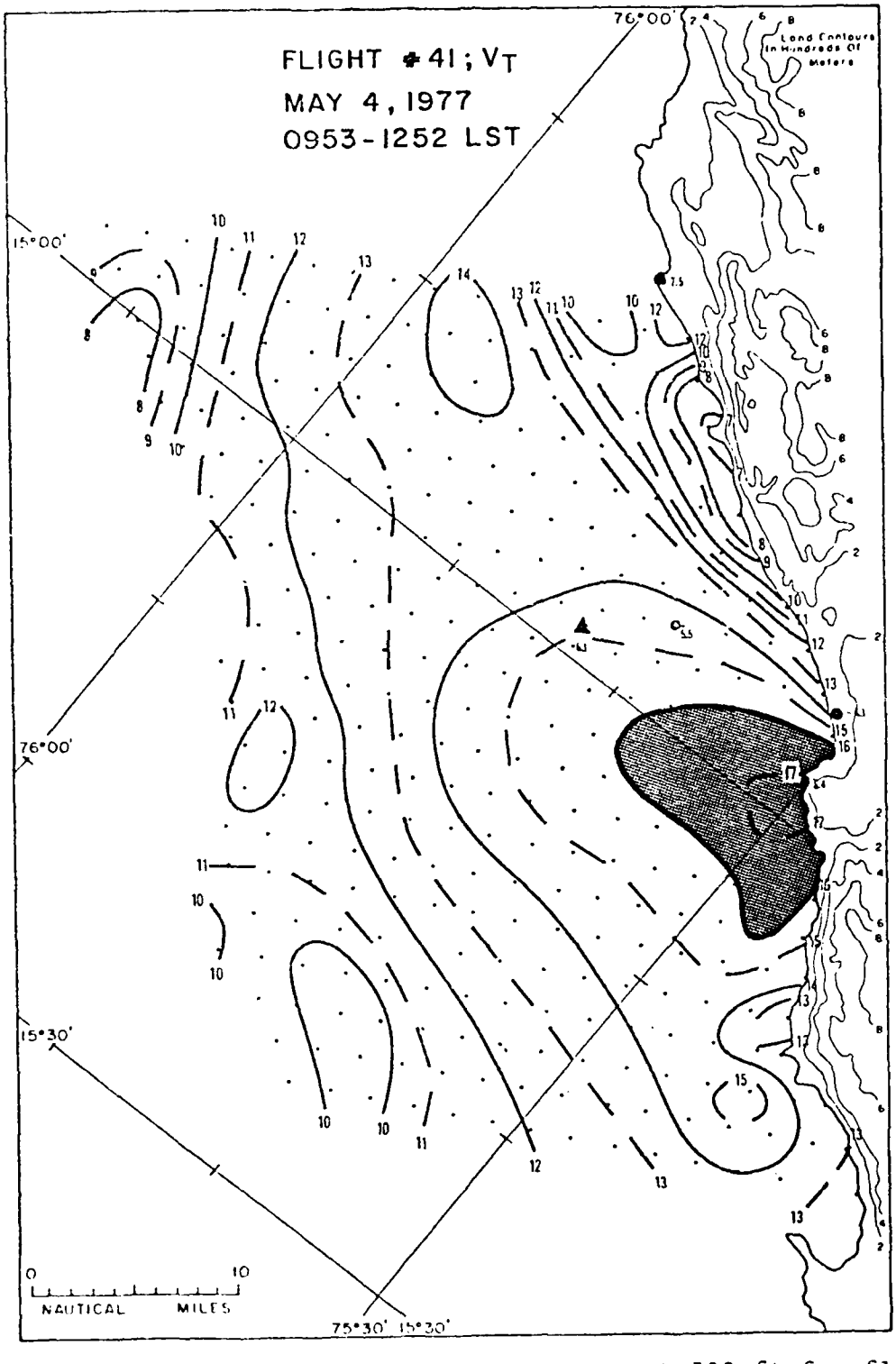

Fig. A3-1. The V_T-component pattern at 500 ft for flight 41 in 1977.

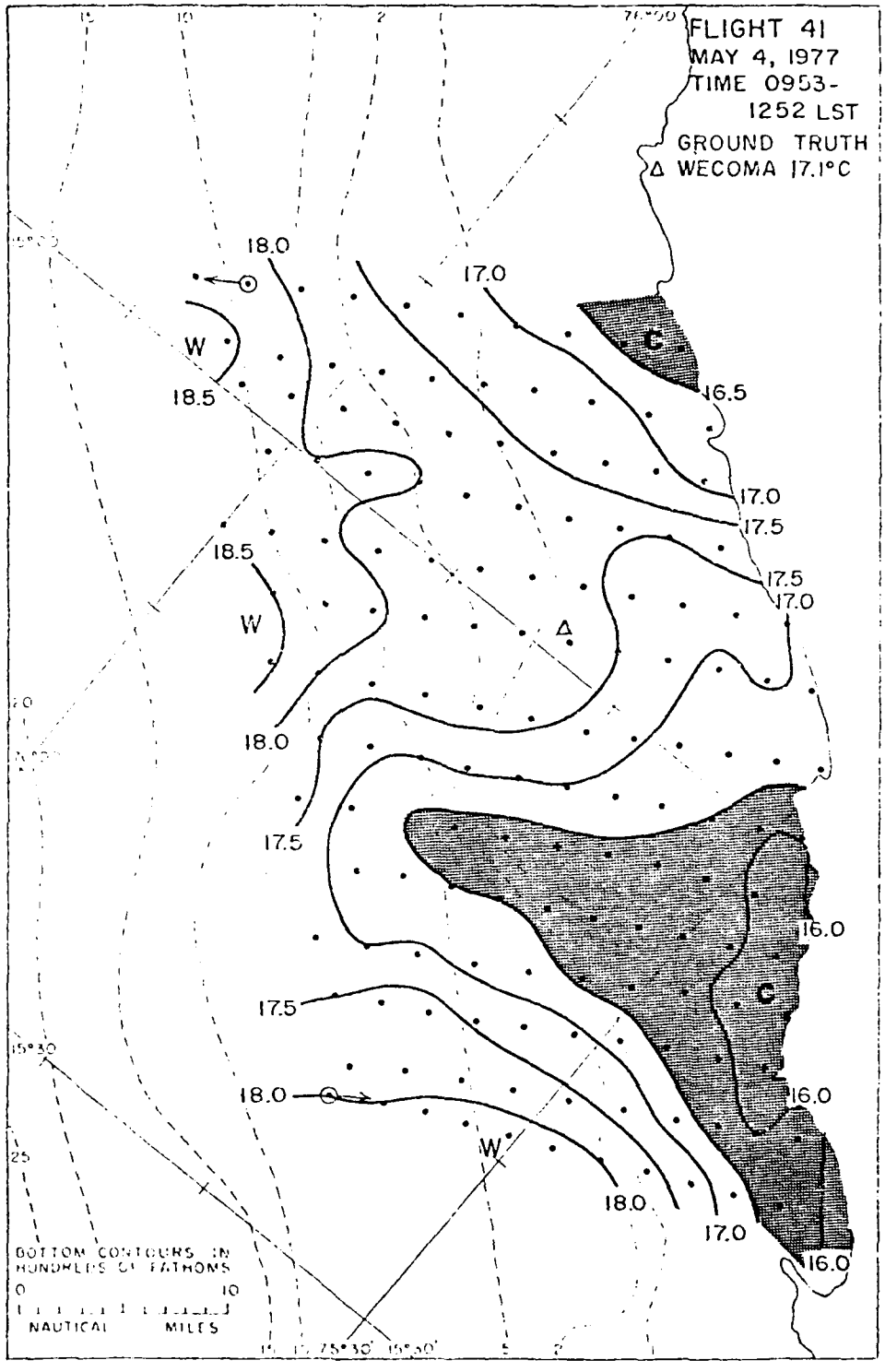

Fig. A3-2. The SST pattern for flight 41 in 1977.

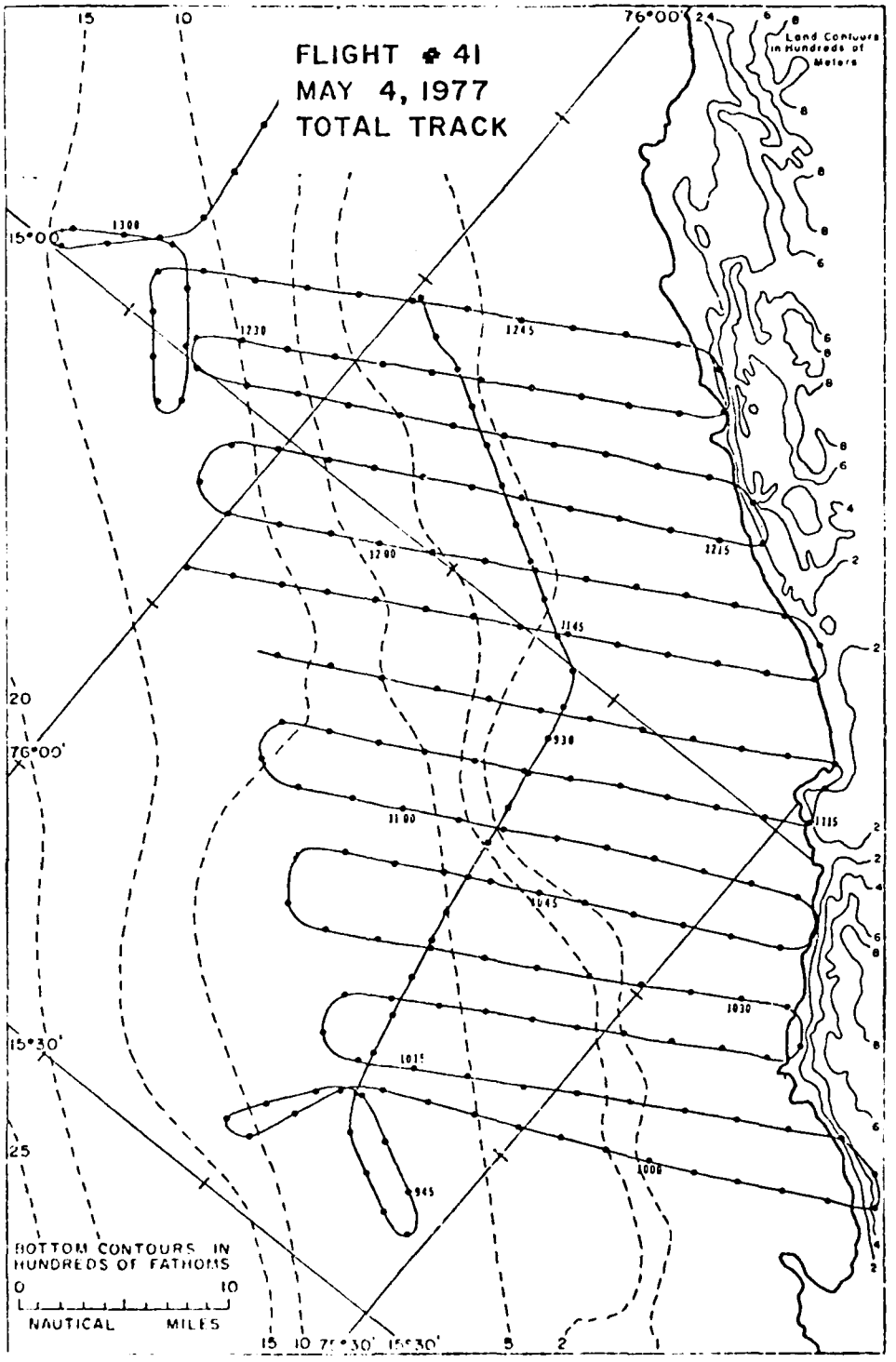

Fig. A3-3. The total aircraft track for flight 41 in 1977.

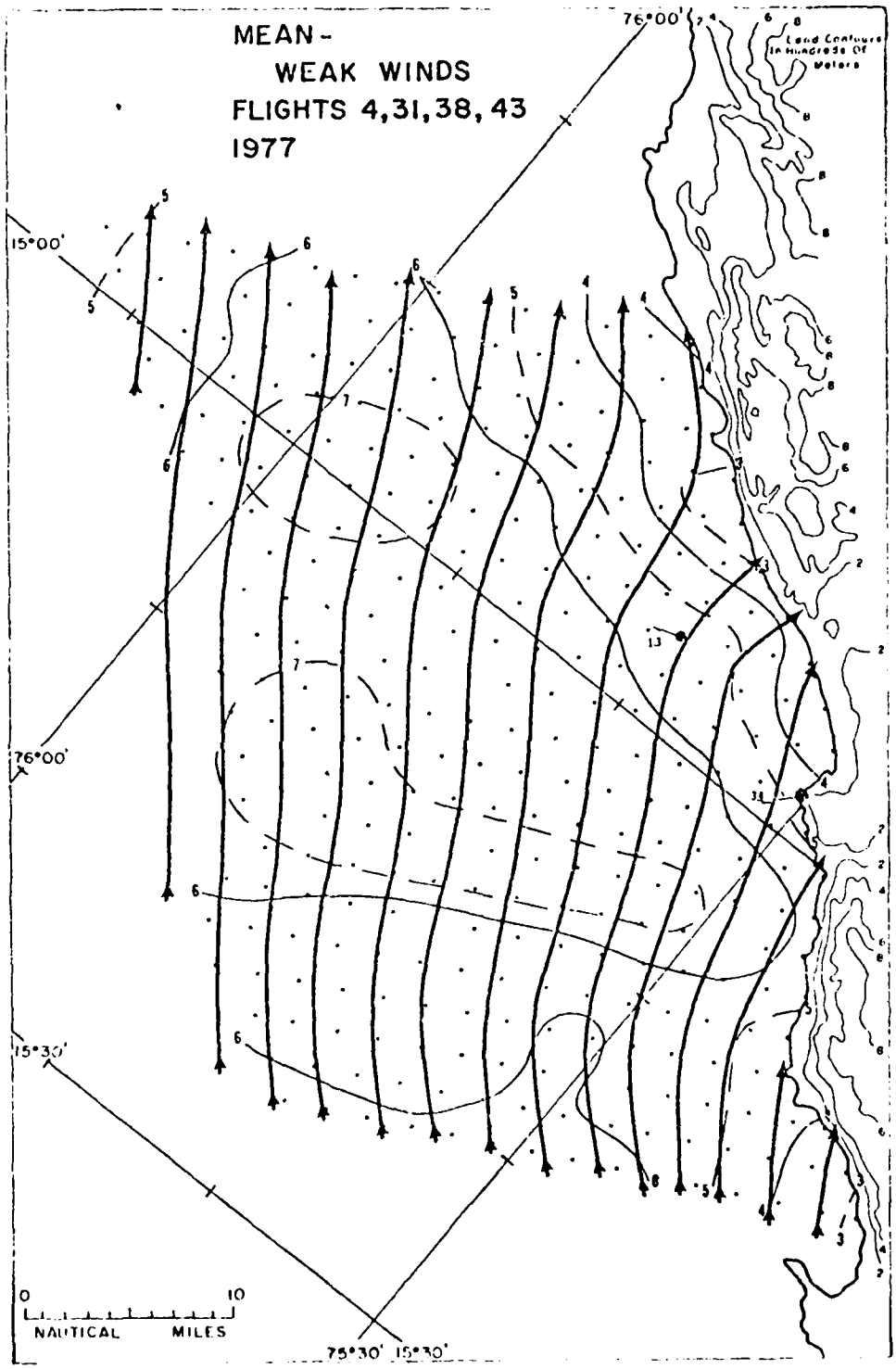

Fig. A4-1. The mean streamline and total isotach patterns at 500 ft for the weakest wind flights during March, April, and May 1977.

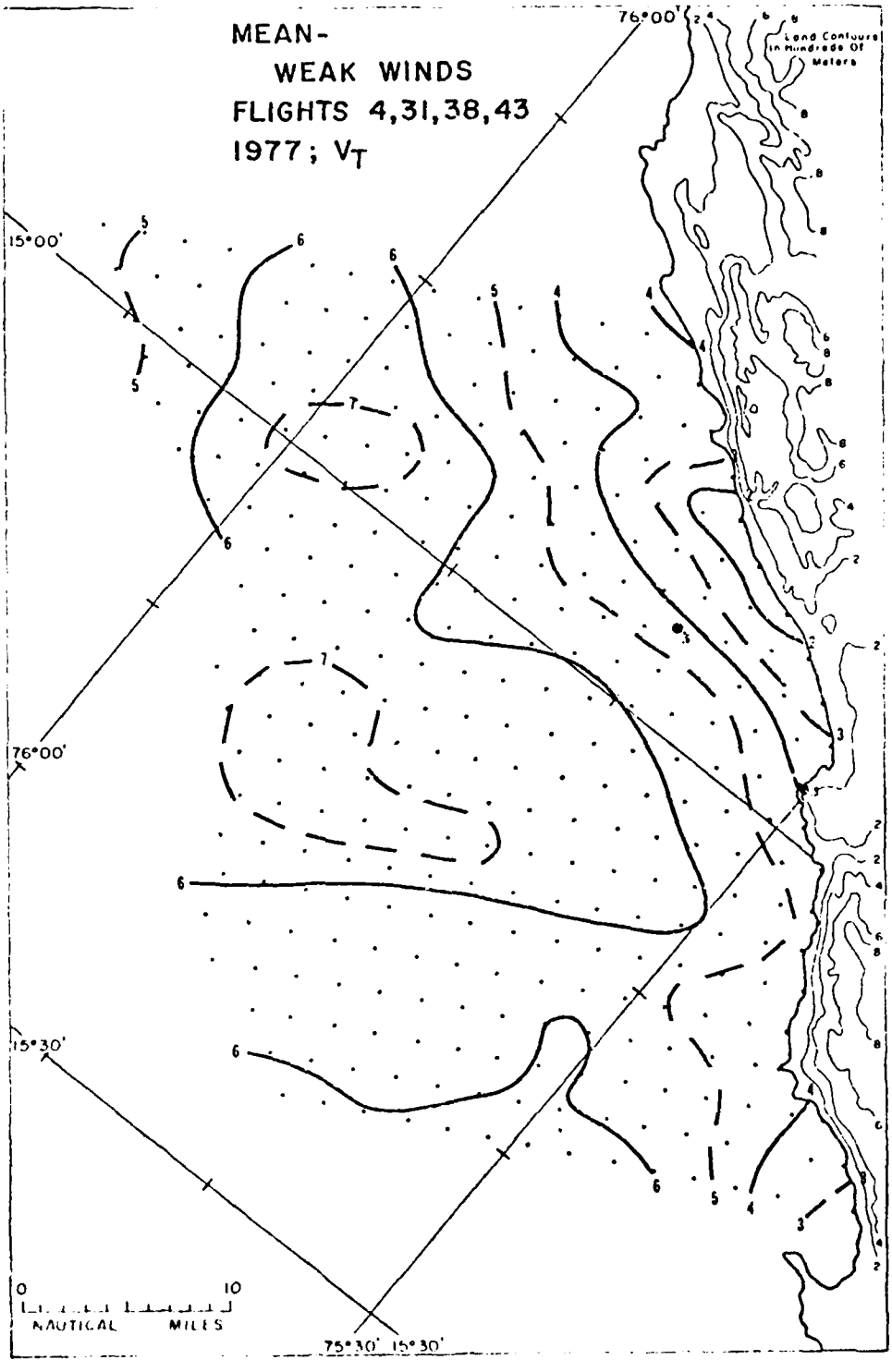

Fig. A4-2. The mean V_T-component pattern at 500 ft for the weakest wind flights during March, April, and May 1977.

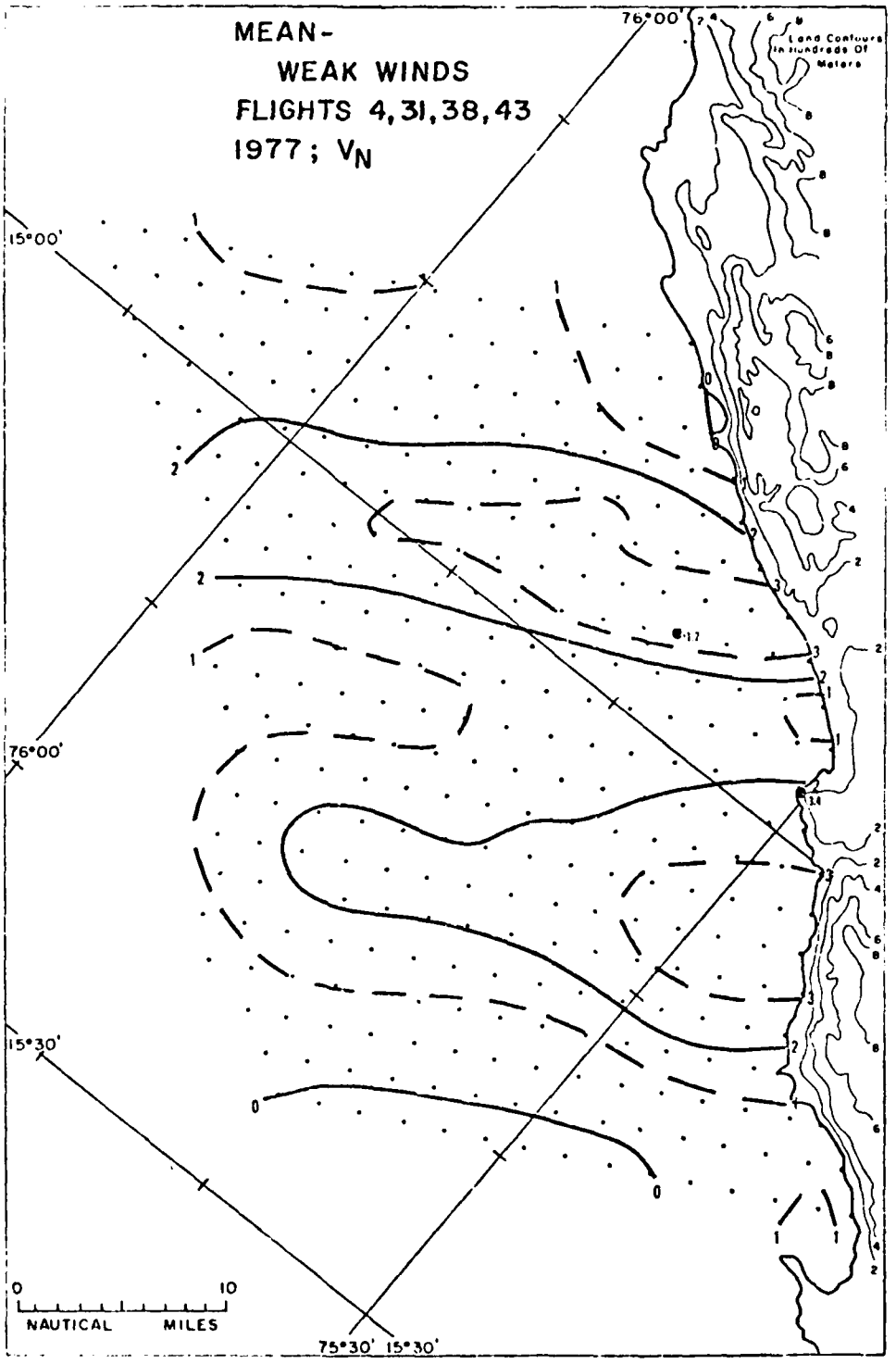

Fig. A4-3. The mean V_N-component pattern at 500 ft for the weakest wind flights during March, April, and May 1977.

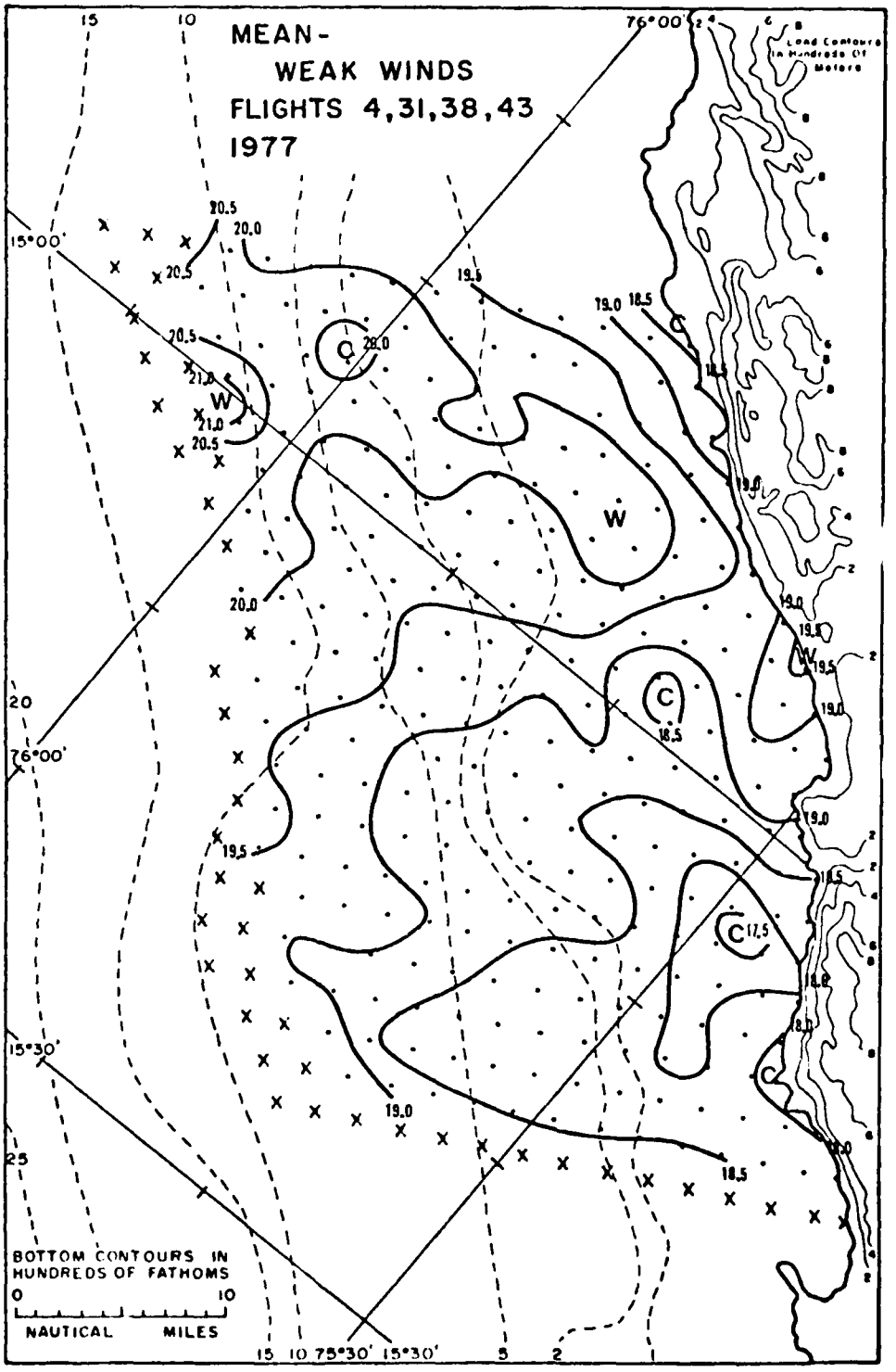

Fig. A4-4. The mean SST pattern for the weakest wind flights during March, April, and May 1977.

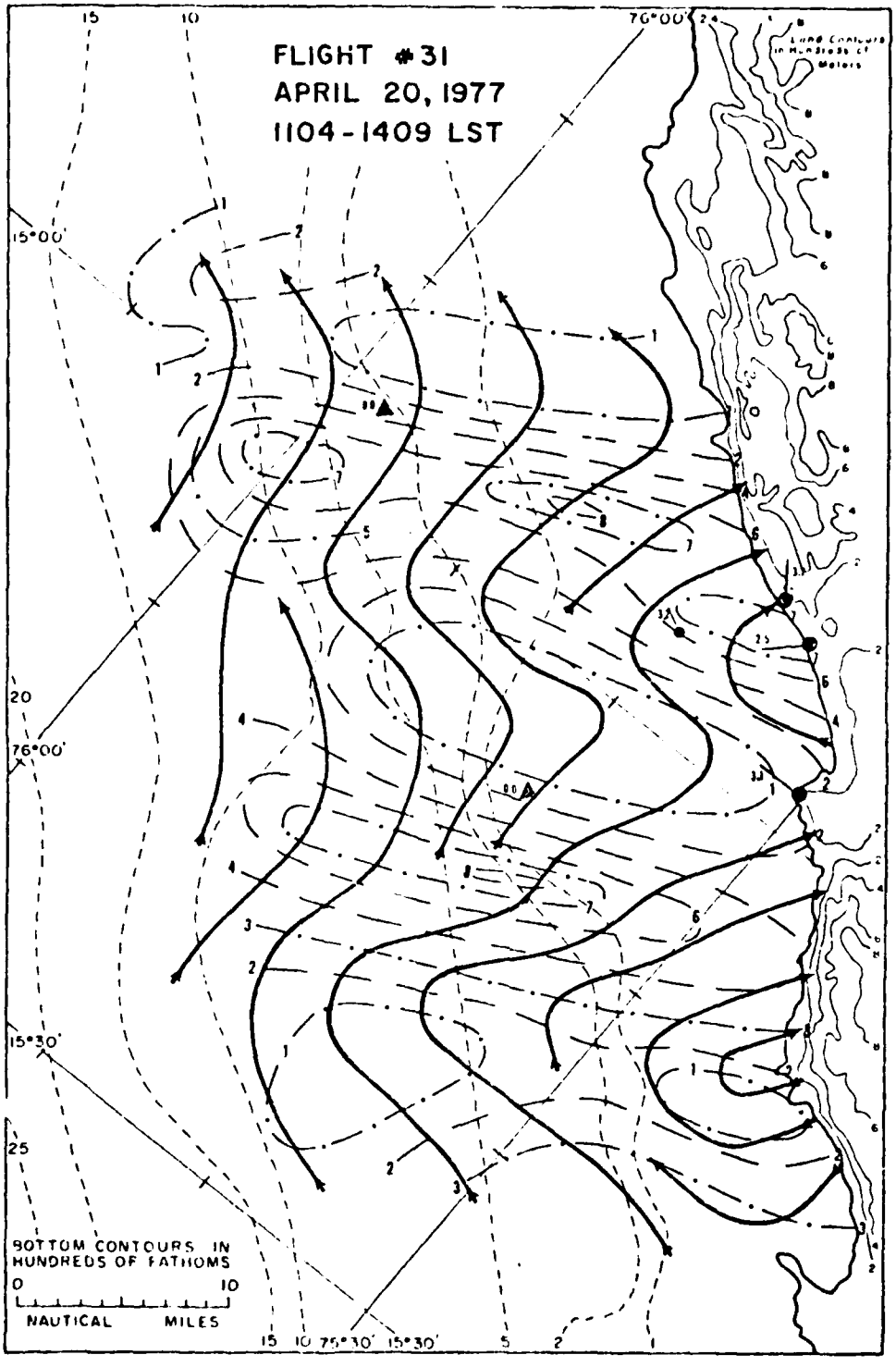

Fig. A5-1. The streamline and total isotach patterns at 500 ft for flight 31 in 1977.

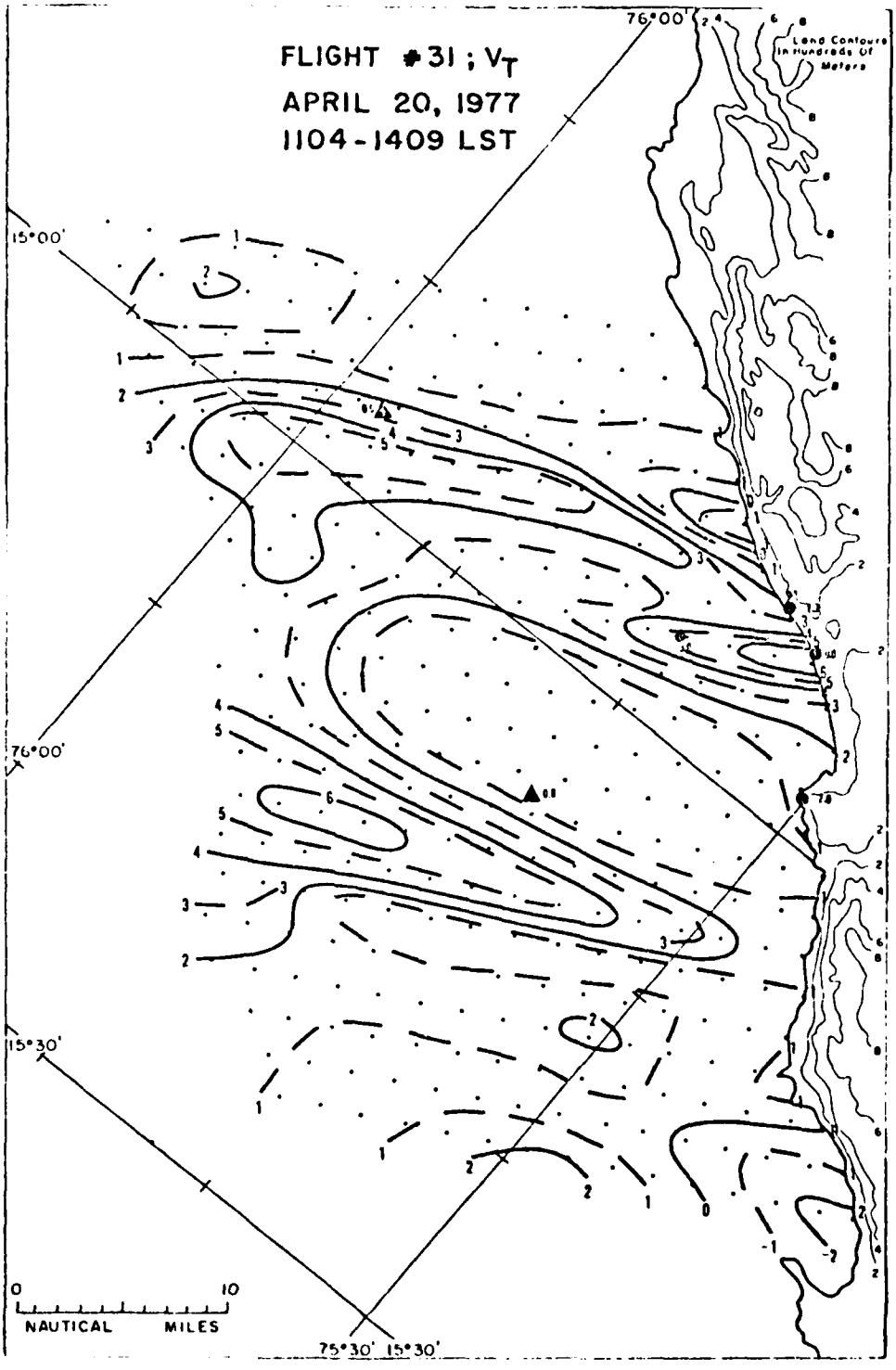

Fig. 5-2. The V_T-component pattern at 500 ft for flight 31 in 1977.

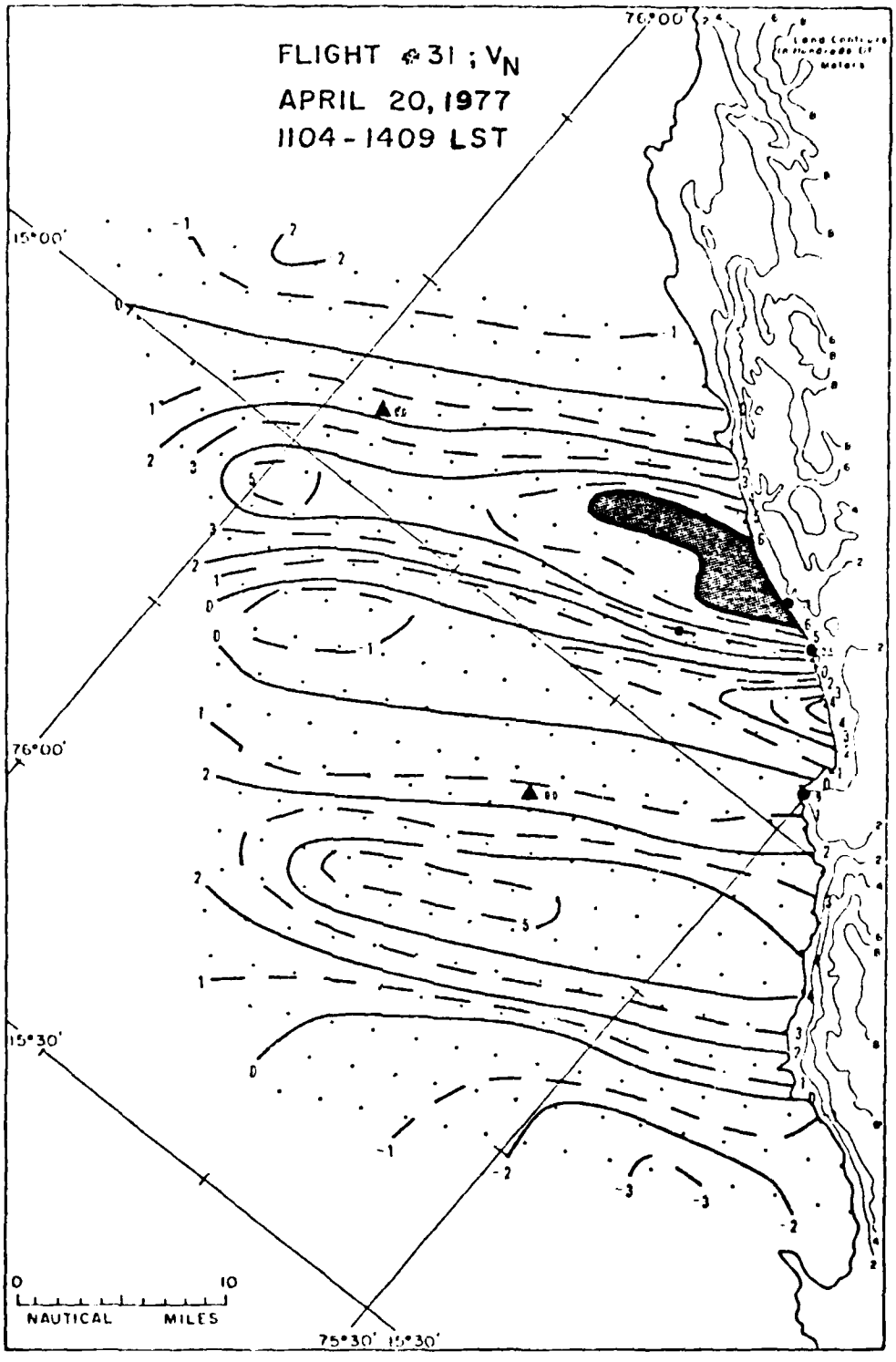

Fig. A5-3. The V_N-component pattern at 500 ft for flight 31 in 1977.

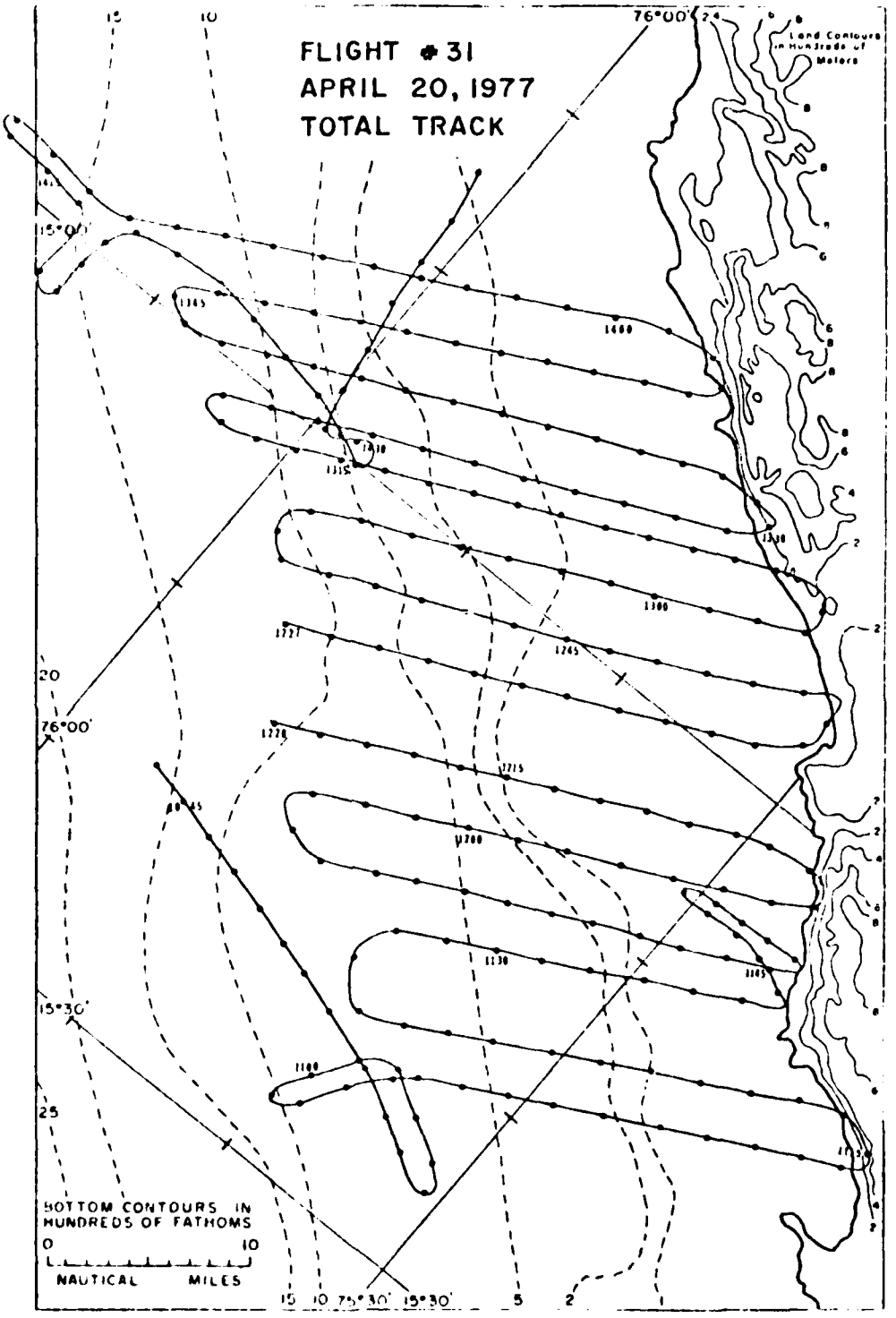

Fig. AS-4. The total aircraft track for flight 31 in 1977.

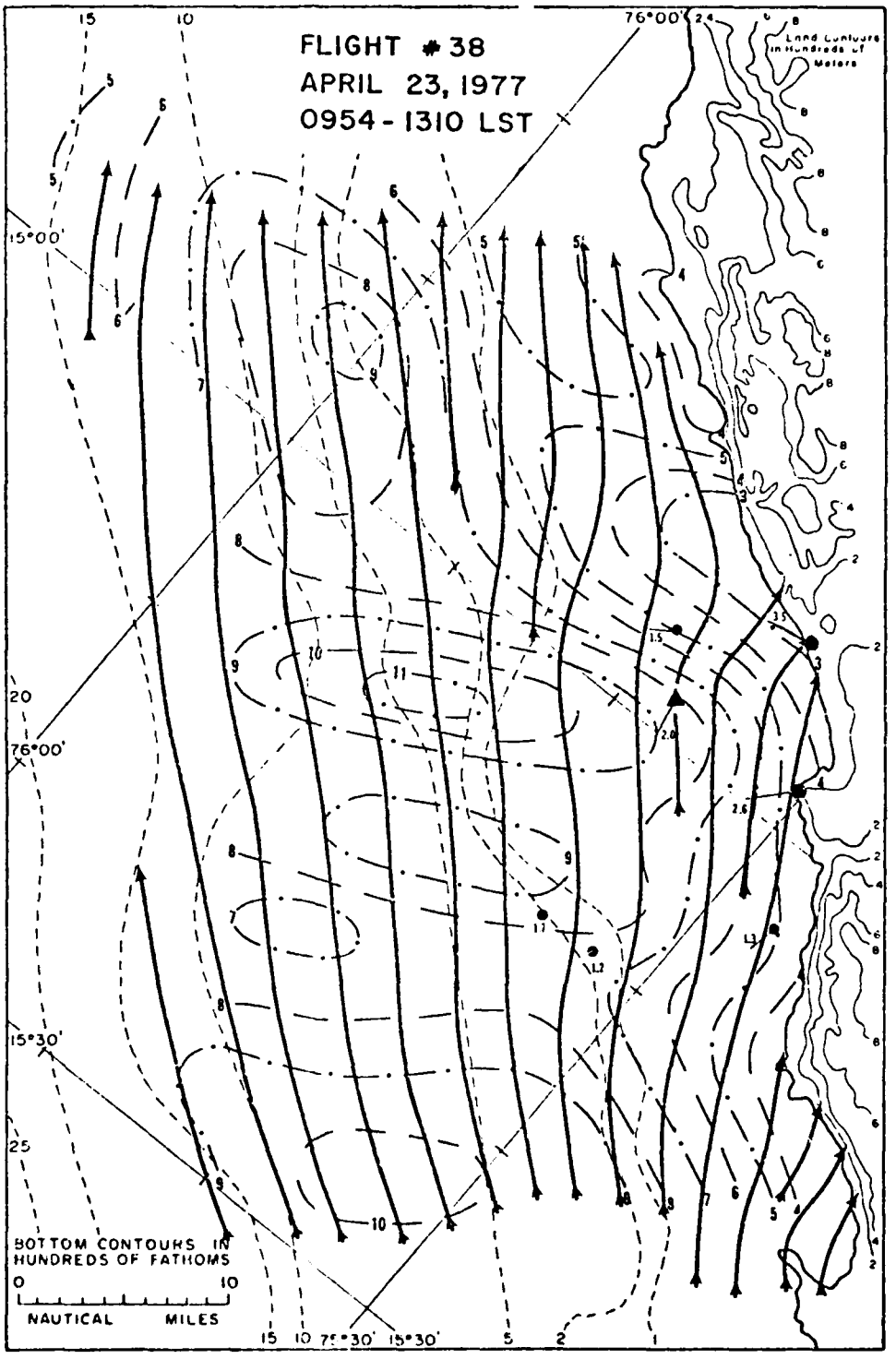

Fig. A6-1. The streamline and total isotach patterns at 500 ft for flight 38 in 1977.

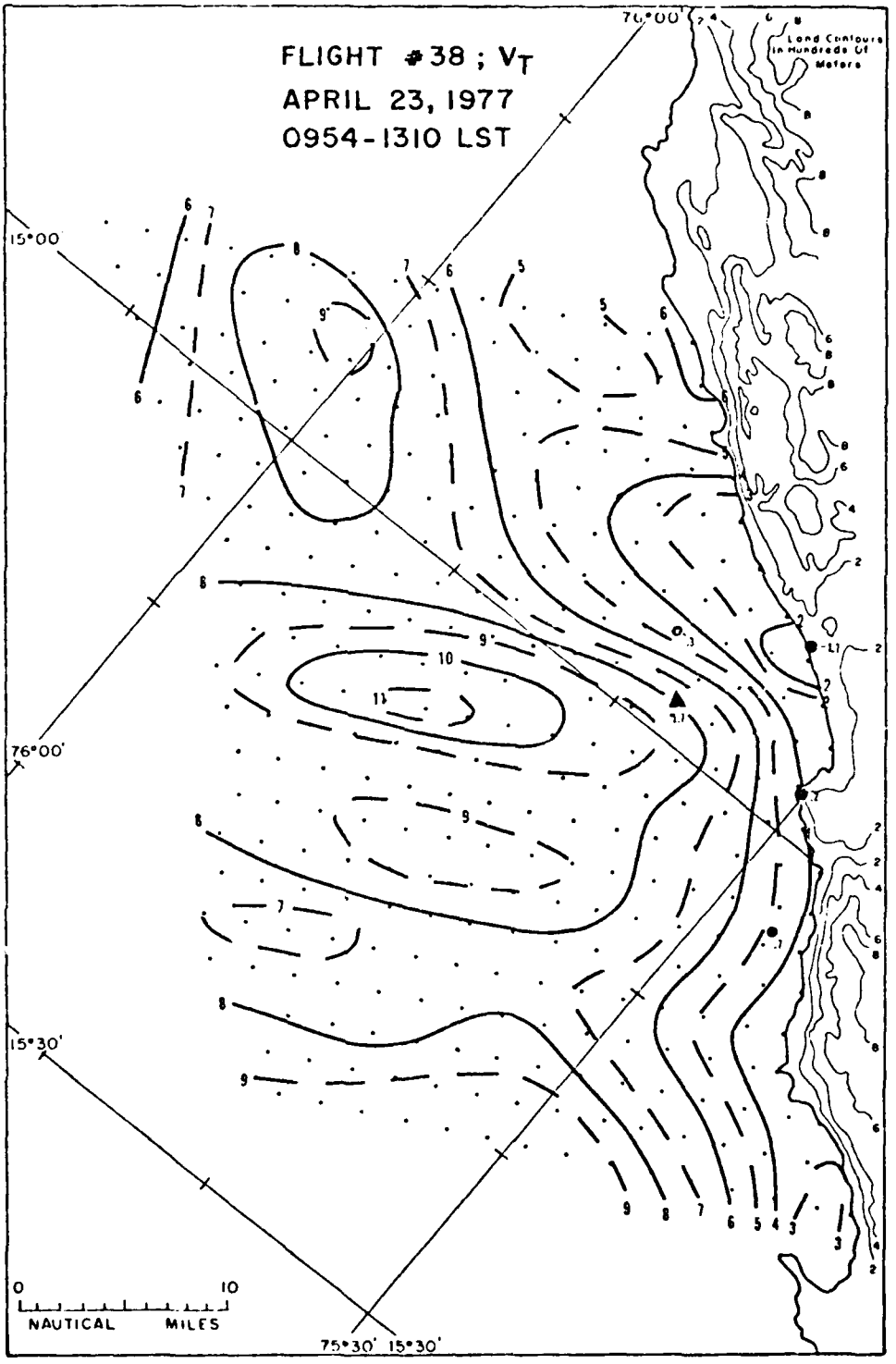

Fig. A6-2. The V_T-component patterns at 500 ft for flight 38 in 1977.

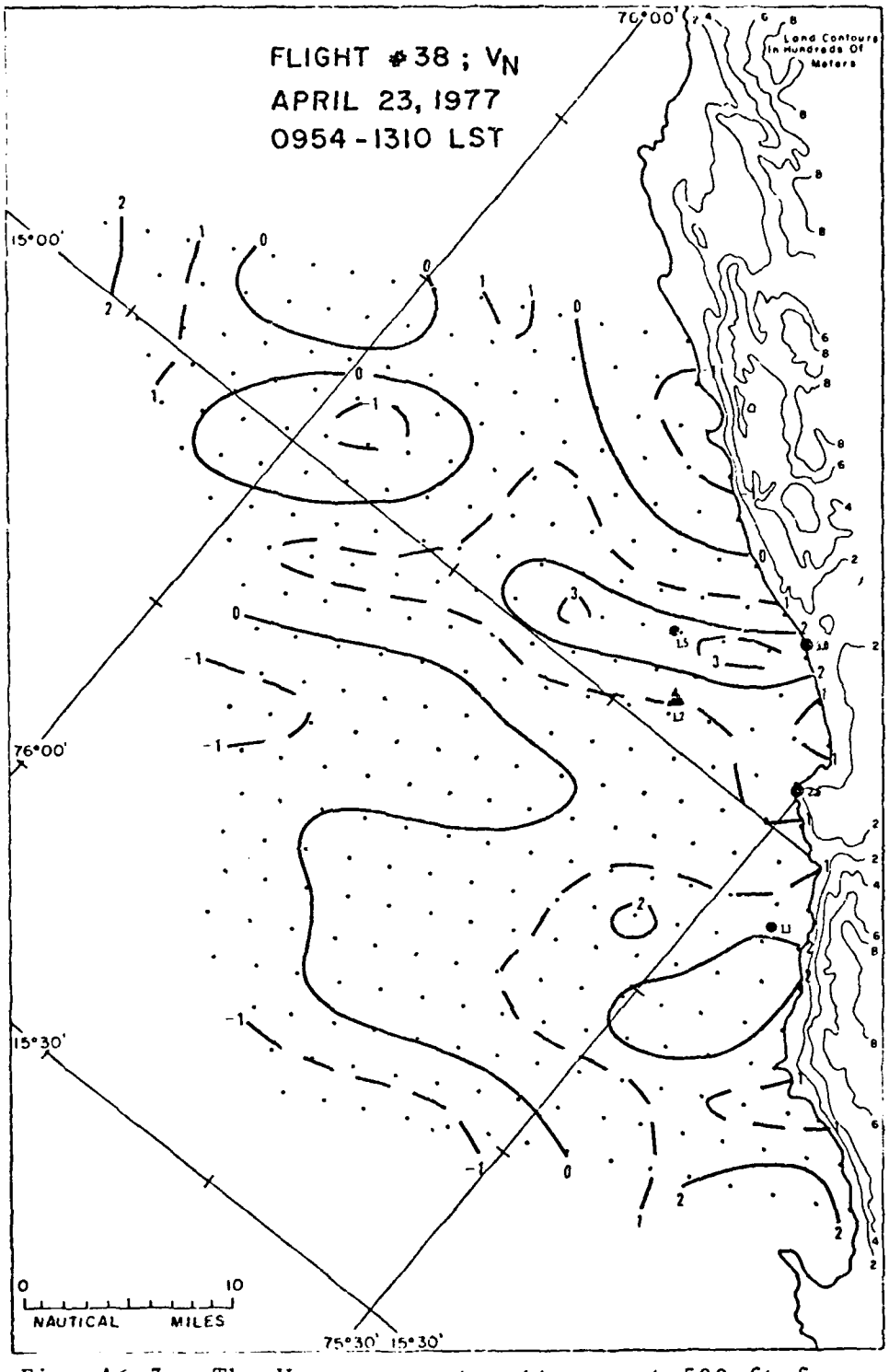

Fig. A6-3. The V_N-component patterns at 500 ft for flight 38 in 1977.

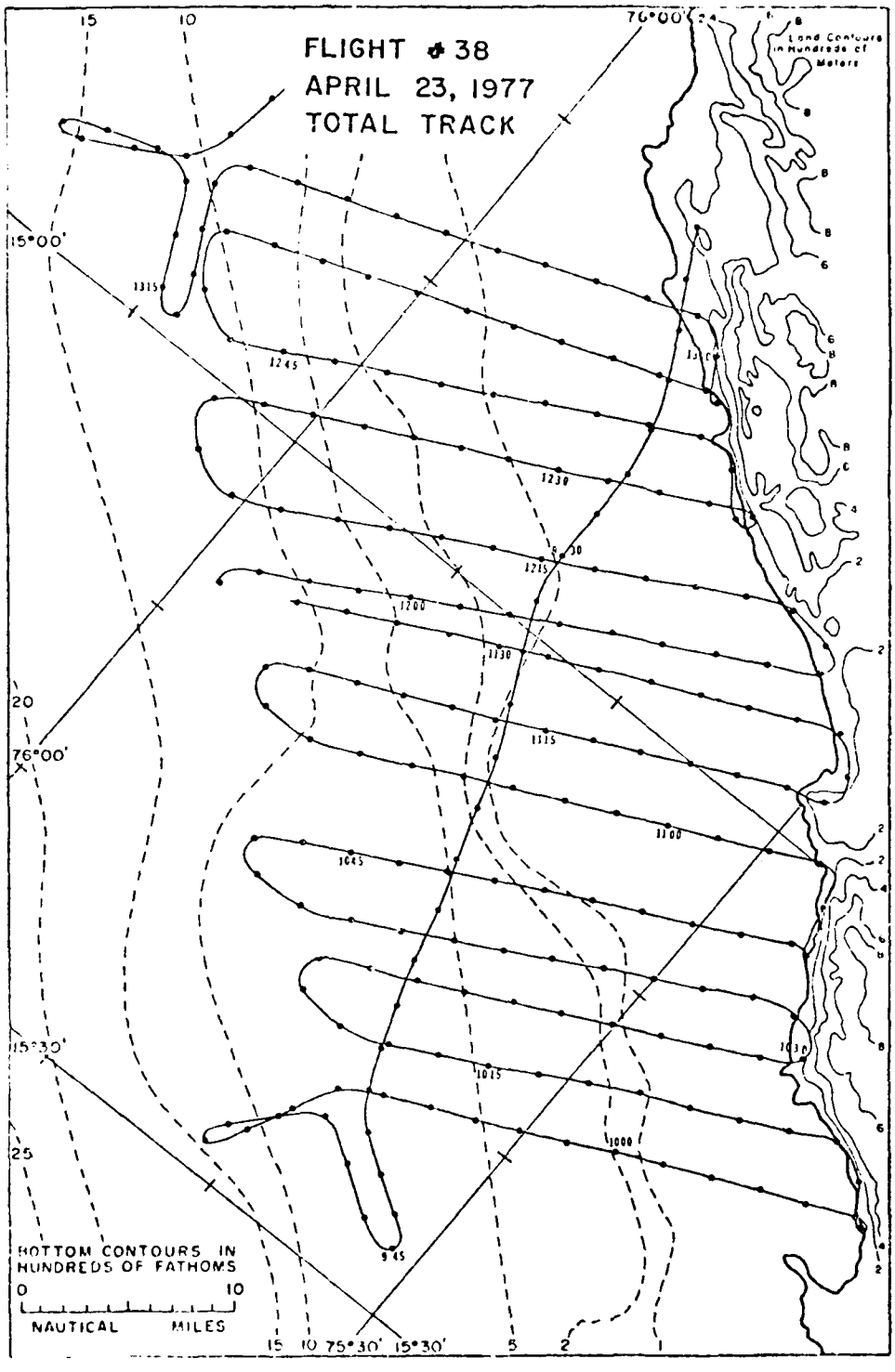

Fig. A6-4. The total aircraft track for flight 38 in 1977.

REFERENCES

Arthur, R. S., 1965: On the calculation of vertical motion in eastern boundary currents from determinations of horizontal motion. J. Geophys. Res., 70, 2794-2803.

Brink, K. H., R. L. Smith, and D. Halpern, 1978: A compendium of time series measurements from moored instrumentation during the MAM '77 phase of JOINT-II. CUEA Technical Report 45, School of Oceanography, Oregon State University, Corvallis, 72 pp.

Duval, W. P., 1977: Aircraft-observed winds over a coastal upwelling region. CUEA Technical Report 29, Dept. of Meteorology, Florida State University, Tallahassee, 120 pp.

Elliott, D. L., and J. J. O'Brien, 1977: Observational studies of the marine boundary layer over an upwelling region. Mon. Wea. Rev., 105, 86-98.

Ekman, V. W., 1905: On the influence of the earth's rotation on ocean currents. Ark. f. Mat. Astr. och Fysik, K. Sv. Vet. AK., Stockholm, 2, 11.

Enfield, D. B., R. L. Smith, and A. Huyer, 1978: A compilation of observations from moored current meters. CUEA Data Report 70, School of Oceanography, Oregon State University, Corvallis, 343 pp.

Goodwin, J. A., 1979: A study of surface winds off the coast of Peru. Master's Thesis in progress, Dept. of Meteorology, Florida State University, Tallahassee.

Gunther, E. R., 1936: A report on oceanographical investigations in the Peru coastal current. Discovery Reports, 13, 107-276.

Holladay, C. G., and J. J. O'Brien, 1975: Mesoscale variability of sea surface temperature. J. Phys. Oceanogr., 5, 761-772.

Idyll, C. P., 1973: The anchovy crisis. Scientific American, 228, 22-29.

Nanney, M. M., 1978: The variability of sea surface temperatures off the coast of Peru during March and April 1976. CUEA Technical Report 42, Florida State University, Dept. of Meteorology, Tallahassee, 99 pp.

Preller, R., 1979: The influence of bottom topography on upwelling off Peru. Master's Thesis, Depts. of Meteorology and Oceanography, Florida State University, Tallahassee, 80 pp.

Smith, R. L., 1978: Poleward propagating perturbations in currents and sea level along the Peru coast. J. Geophys. Res., 83., 6083-6092.

Stuart, D. W., 1975: Meteorological conditions in the JOINT II region. CUEA Data Report 75-4, Dept. of Meteorology, Florida State University, Tallahassee, 41 pp.

_____, 1977: JOINT II field report March-April-May 1977 meteorology-aircraft operations. CUEA Newsletter, Vol. 6, No. 4, 39-45. (Available from Duke University Marine Lab., Beaufort, North Carolina.)

_____, and J. J. Bates, 1977: Aircraft sea surface temperature data - JOINT II 1977. CUEA Data Report 42, Dept. of Meteorology, Florida State University, Tallahassee, 39 pp.

_____, and G. L. Moody, 1979: Atlas of the JOINT II 1977 aircraft winds for the 500 foot level. To appear as a CUEA Technical Report, Dept. of Meteorology, Florida State University, Tallahassee.

Watson, A. I., 1978: A study of the low-level mesoscale winds observed off the Peruvian coast during March and April 1976. CUEA Technical Report 41, Dept. of Meteorology, Florida State University, Tallahassee, 121 pp.

Wirfel, W. P., 1979: A study of the atmospheric structure off the coast of Peru. Master's Thesis in progress. Dept. of Meteorology, Florida State University, Tallahassee.

Wyrtki, K., 1966: Oceanography of the eastern equatorial Pacific Ocean. Oceanogr. Mar. Biol. Ann. Rev., 4,33-68.

Yoshida, K., 1967: Circulation in the eastern tropical oceans with special references to upwelling and undercurrents. Japanese Journal of Geophysics, 4, 1-75.

Zuta, S., and W. Urquizo, 1972: Temperatura promedio de la superficie del mar frente a la costa peruana, periodo 1928-1969. Instituto Del Mar Del Peru Boletin, Vol. 2, No. 8, 500-501. (Available from Biblioteca, Instituto del Mar del Peru, Apartado 3734, Lima, Peru.)

VITA

Glenn LeRoy Moody was born in Lawrenceville, Illinois on October 26, 1942. He graduated magna cum laude with a B.S. degree in meteorology from the University of Utah in June, 1968. He began his graduate study in the Department of Meteorology at the Florida State University in September, 1977. He has spent the last fifteen years serving in the U.S. Air Force as a forecaster and as a navigator with the 53rd Weather Reconnaissance Squadron.